Spring 2021

RNA Methylation and Ythdf Readers in Posttranscriptional Regulation and Development

Cassandra Kontur

Yale University Graduate School of Arts and Sciences, cassandra.n.kontur@gmail.com

Abstract

RNA Methylation and Ythdf Readers in Posttranscriptional Regulation and Development

Cassandra Kontur

2021

Development in animals requires precise and coordinated changes in gene expression. This genetic remodeling is achieved through extensive regulatory networks of proteins and RNAs that function together to specify new cell fates and patterns. One developmental event heavily reliant on these regulatory networks is the maternal-to-zygotic transition (MZT), a universal step in metazoan embryogenesis in which a fertilized oocyte is reprogrammed into a pluripotent embryo. The earliest stages of the MZT are governed by maternally inherited gene products, which are required for cellular functions in the initially transcriptionally silent embryo. To shift developmental control to the zygote, these maternal mRNAs are massively degraded through multiple posttranscriptional mechanisms. The RNA modification, N^6-methyladenosine (m^6A) has been proposed as a master regulator of mRNA decay during developmental transitions, but the direct effects of this pathway on maternal transcript clearance remain unclear. To determine whether m^6A facilitates gene expression changes during the MZT, I employed zebrafish embryos as a model system to dissect the contributions of RNA methylation and its reader proteins to maternal transcript fate.

Through transcriptome analysis and reporter assays, I found that m^6A controls maternal mRNA degradation by promoting deadenylation. To understand how RNA methylation fits into the framework of known decay pathways, I compared transcripts co-targeted by m^6A and miR-430, a microRNA that controls mRNA clearance in zebrafish. This revealed that these mechanisms

function independently but additively to promote mRNA degradation, reflecting that methylation modulates transcript abundance in concert with known regulators.

To disentangle the roles of the Ythdf proteins that mediate the effects of m⁶A on mRNA, I generated zebrafish genetic mutants of Ythdf1, Ythdf2, and Ythdf3. Through transcriptomic and phenotypic analysis of these mutants, I determined that global maternal mRNA clearance, zygotic genome activation, and development proceed normally in the absence of any one reader. This revealed that individual Ythdf proteins have limited effects on the removal of methylated maternal mRNAs during the MZT. To test if this limited impact of single Ythdf loss stems from functional redundancy between the readers, I produced double mutants of Ythdf2 and Ythdf3. Double Ythdf deletion prevents female gonad development, indicating that these factors exert overlapping activities during oogenesis. Finally, to fully establish functionally redundancy, I created triple Ythdf mutants, which are larval lethal. I observed this same phenotype in zebrafish lacking the methylases that add m⁶A to mRNA, indicating that RNA methylation is essential for developmental viability.

Together, this work provides insight into the contributions of the m⁶A modification and its Ythdf effectors to maternal mRNA clearance, and establishes how these key regulators coordinate the gene expression changes that underlie embryonic reprogramming.

RNA Methylation and Ythdf Readers in Posttranscriptional Regulation and Development

A Dissertation
Presented to the Faculty of the Graduate School
of
Yale University
in Candidacy for the Degree of
Doctor of Philosophy

by
Cassandra Kontur

Dissertation Director: Antonio Giraldez, Ph.D.

June, 2021

Table of Contents

List of Tables and Figures

Acknowledgements

First, I would like to acknowledge my advisor, Dr. Antonio J. Giraldez. During my time in his lab, he afforded me every opportunity to grow as a scientist and as an individual. He created a space for me to work and explore science independently, while offering continuous support and guidance. He is as committed to and excited about mentoring as he is science, and has taught me not only how to ask and answer big questions but how to communicate my ideas and follow through on my goals. His selfless commitment to his lab and to my own journey has been inspiring and I am incredibly grateful to be his student.

I am also grateful to Dr. Aaron Turkewitz, Dr. Joseph Briguglio, and Dr. Santosh Kumar for being my first scientific mentors, and for creating the most kind, generous, and patient learning environment that I have ever experienced. I would like to thank my committee members Dr. Jun Lu, Dr. Matthew Simon, and Dr. Karla Neugebauer for their encouragement, insight, and ideas that always advanced my science. I thank Dr. Jeff Gruen, Dr. Megan King, and Dr. Karla Neugebauer for joining my qualifying committee and inspiring my early scientific interests. I am also grateful for the RNA and developmental biology communities at Yale, where I had the opportunity to learn about both great science and great presentations.

I would like to thank all members of the Giraldez lab for making research exciting, enjoyable, and impactful. I would especially like to thank Dr. Charles Vejnar for his help, patience, and endless explanations to my repeated questions. I am grateful for your mentorship and most importantly for your friendship, and for encouraging me to take on the challenges of computational biology. I would also like to thank Dr. Jean-Denis Beaudoin, who taught me everything about RNA biology and provided constant support and insight in my research. I would like to thank Dr. Liyun Miao for always helping and listening to me, and for making long nights in the lab more

CHAPTER 1: RNA methylation regulates gene expression during development

Global changes in gene expression underlie all cellular transitions. To ensure that this massive genetic remodeling is executed precisely and efficiently, a complex web of regulatory mechanisms coordinate their functions to specify new cell fates and patterns. While transcription is integral to the modulation of gene expression, multiple posttranscriptional maneuvers also contribute to reprogramming. By finetuning the genetic output from already synthesized mRNAs, these posttranscriptional mechanisms offer rapid and responsive transcriptome manipulations without necessitating largescale transcriptional adjustments.

One transition heavily reliant on posttranscriptional regulation is the maternal-to-zygotic transition (MZT), a process universal to all metazoans. The MZT is the hallmark first step in embryogenesis, in which a fertilized oocyte undergoes developmental reprogramming into a pluripotent embryo. This transition is an ideal situation to study the effects of posttranscriptional processes, as the zygote is initially transcriptionally silent and development is sustained by maternally inherited gene products. This means that posttranscriptional pathways dominate the early MZT, and a vast network of regulatory factors remodels the maternal transcriptome and proteome to facilitate proper developmental progression.

The posttranscriptional mechanisms controlling gene expression changes during the MZT are extensive, interwoven, and often universal across organisms. The embryo employs multiple regulatory pathways simultaneously, including those involving RNA-binding proteins (RBPs) and microRNAs, which rely on sequence elements embedded in target mRNAs for their activity. Other pathways engage features inherent to the mRNA transcript, such as RNA secondary structures or codon identity. Ubiquitous RNA modifications such as the 5'end cap and the 3'end poly(A) tail

also play a crucial regulatory role, through interactions with translation and decay machinery. Recently, internal mRNA modifications have been identified as mediators of mRNA fate, where deposition of chemical groups on the canonical A, C, G, and U nucleotides confers an additional layer of regulatory information. As the most abundant internal mRNA modification, N^6-methyladenosine (m^{6}A, also termed methylation) has the capacity to mark thousands of transcripts for simultaneous, specific changes in RNA regulation, making it an especially promising mechanism to control maternal transcriptome remodeling.

RNA methylation has already been implicated in numerous developmental transitions that require extensive genetic reprogramming, suggesting that it may be a global mechanism to control development. m^{6}A has been linked to stem cell differentiation, gametogenesis, and embryogenesis, where the function of m^{6}A as a posttranscriptional regulator is central to its facilitation of these transitions (**Fig. 1.1.**). To direct cell state switching, RNA methylation tags transcripts encoding developmental regulators and relies on its effectors to mediate their degradation or translation. The enzymes responsible for m^{6}A metabolism are often essential to development across organisms, reflecting that this pathway plays a critical role in reprogramming. Given that m^{6}A is a master mediator of posttranscriptional remodeling during developmental transitions, its impact on the maternal transcriptome during the MZT is likely to be significant.

non-m^{6}A

mRNA

m^{6}A

time

gene expression changes

pluripotency
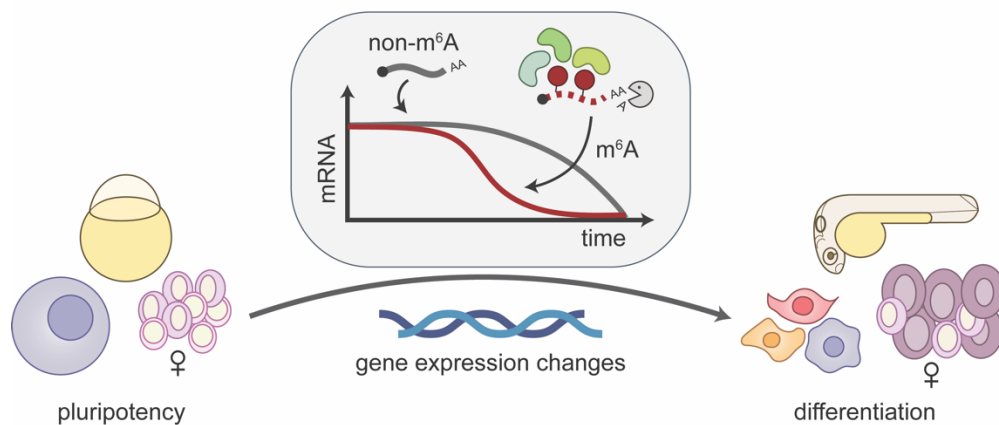
differentiation

Figure 1.1. m⁶A facilitates developmental transitions by modulating mRNA decay
RNA methylation contributes to the transition from a pluripotent to a differentiated state in multiple developmental contexts, including in stem cells, oogenesis, and zebrafish embryogenesis. Transcripts marked by m⁶A are more rapidly degraded than unmarked mRNAs, allowing for global changes in gene expression. These effects of m⁶A on mRNA fate are frequently mediated by the YTHDF readers (green).

In this dissertation, I aim to address how the m⁶A modification serves as a central determinant of gene expression changes during key developmental transitions. First, I review foundational literature in the field of maternal mRNA clearance during the maternal-to-zygotic transition (**Chapter 1.1.**). I then focus on the posttranscriptional mechanisms through which m⁶A controls mRNA decay and translation, with an emphasis on the factors involved in adding and interpreting the modification (**Chapter 1.2.**). I address how RNA methylation contributes to both embryogenesis and parallel transcriptome reprogramming events, including in stem cells and gametogenesis (**Chapter 1.3.**)

I then explore whether these roles of RNA methylation on mRNA decay and translation extend into control of gene expression during the maternal-to-zygotic transition in zebrafish. In **Chapter 2**, I investigate the behavior of endogenously methylated maternal mRNAs to gain insight into how this mark specifies maternal transcript fate. I combine mRNA-sequencing and poly(A) tail analysis to reveal that m⁶A modification is associated with enhanced deadenylation, clarifying the mechanistic underpinnings of m⁶A regulation of maternal mRNA clearance (**Chapter 2.1**). I validate the impact of m⁶A on poly(A) tail shortening through methylated reporters, and demonstrate the reliance of this pathway on zygotic transcription (**Chapter 2.2.**). I explore the interplay between methylation and microRNAs, revealing that these pathways coordinate their functions to co-target specific mRNAs for enhanced clearance (**Chapter 2.3.**), and that the microRNA miR-430 controls Ythdf3 downregulation at the mRNA level. Finally, I analyze ribosome profiling data to show that m⁶A also promotes maternal mRNA translation (**Chapter**

2.4.). Together, these analyses demonstrate how RNA methylation contributes to the posttranscriptional regulatory landscape guiding transcriptome turnover during the MZT.

To understand which m^{6}A writers and readers impart the significance of methylation onto maternal transcripts, I analyze their expression during the MZT (**Chapter 3.1.**) To dissect the contributions of each YTHDF reader to maternal mRNA clearance, I generate single mutants of YTHDF1, YTHDF2, and YTHDF3, and use RNA-sequencing analysis to establish the consequences of reader deletion on the maternal transcriptome. I reveal that loss of any one reader is not sufficient to fully stabilize methylated maternal messages, suggesting that these factors redundantly control degradation (**Chapter 3.2.**). Further, I carefully address the role of YTHDF2 on maternal mRNA clearance versus zygotic genome activation, uncovering that YTHDF2 is not required for progression of either event, thus overturning the view that YTHDF2 alone dictates timing of decay and transcription during the MZT (**Chapter 3.2., Chapter 3.3.**).

Finally, I examine the possibility of redundancy of YTHDF function through single, double, and triple zebrafish mutants. I demonstrate that deletion of any single YTHDF or even double YTHDFs does not impact embryogenesis (**Chapter 4.1.**). Yet, I discover that the YTHDFs exhibit dosage dependency to control oogenesis and larval viability, as double mutants cannot establish ovaries, and triple mutants are lethal (**Chapter 4.2., Chapter 4.3.**). Together, this reveals that the YTHDFs exert overlapping functions to control gene expression changes, and that these m^{6}A readers are essential for multiple stages of development.

Lastly, I summarize the results obtained and explain their implications relative to the field of RNA methylation as a whole in **Chapter 5**. I suggest routes of further exploration, and explore outstanding questions (**Chapter 5**). Finally, I describe the methodologies employed (**Chapter 6**).

1.1. Posttranscriptional control of maternal mRNA clearance

Early embryonic development is initially sustained by maternal mRNAs and proteins pre-loaded into the oocyte (Vastenhouw et al., 2019). As developmental control shifts towards the zygote, these maternally inherited products are systematically degraded through multiple, interconnected clearance pathways (Despic and Neugebauer, 2018; Tadros and Lipshitz, 2009; Vastenhouw et al., 2019; Yartseva and Giraldez, 2015). While the extent and timing of maternal clearance vary across eukaryotes, several core posttranscriptional mechanisms are found to contribute to mRNA removal in most species (**Fig. 1.2.**) (Vastenhouw et al., 2019). These factors and elements can be both maternally derived or zygotically produced, and frequently target the same mRNAs simultaneously (Yartseva and Giraldez, 2015).
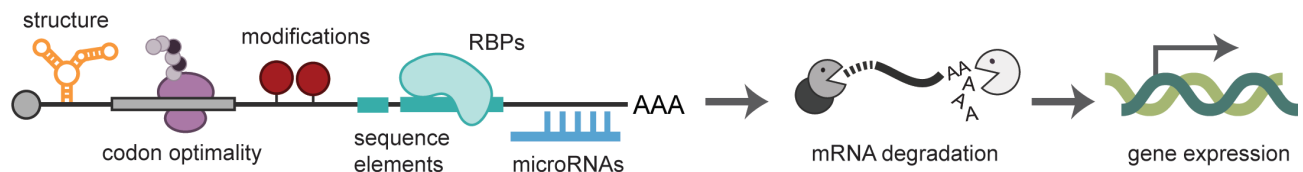
Figure 1.2. Mechanisms of maternal mRNA clearance
Multiple pathways and features contribute to maternal mRNA degradation in zebrafish embryos, and thus enable changes in gene expression. These mechanisms include RNA secondary structure, codon optimality, RNA modifications, sequence elements, RNA-binding proteins (RBPs), and microRNAs.

The first major mechanism facilitating maternal mRNA clearance is RNA binding proteins (RBPs), which bind to sequence elements in transcripts and recruit effectors to enable deadenylation and decay. For example, in *Drosophila*, binding of the Smaug RBP to specific hairpin structures results in transcript deadenylation or translational repression, through interactions with downstream factors (Chen et al., 2014a; Newton et al., 2015; Semotok et al., 2005; Tadros et al., 2007; Temme et al., 2010). Pumilio and BRAT also function in flies, and

recognize unique motifs to promote deadenylation (Gerber et al., 2006; Laver et al., 2015; Thomsen et al., 2010; Weidmann et al., 2014), thus ensuring specific sets of mRNAs are cleared by different trans-acting factors. Similarly, AU-rich-element binding proteins help degrade transcripts in zebrafish (Despic et al., 2017; Rabani et al., 2017; Vejnar et al., 2019), *C. elegans* (D'Agostino et al., 2006; Gallo et al., 2008; Schubert et al., 2000), and *Xenopus laevis* (Graindorge et al., 2008; Moraes et al., 2006; Paillard et al., 1998; Voeltz and Steitz, 1998), and the factor BTG4 in mice mediates deadenylation (Yu et al., 2016).

A second major player degrading maternal transcripts is small non-coding RNA, which includes microRNAs (miRNAs), PIWI-interacting RNAs (piRNAs), and endogenous small interfering RNAs (endo-siRNAs) (Vastenhouw et al., 2019). For instance, the miRNA miR-430 in zebrafish induces translational repression and deadenylation of hundreds of maternal transcripts (Bazzini et al., 2012; Giraldez et al., 2006), and miR-427 in *Xenopus* (Lund et al., 2009) and miR-309 in *Drosophila* (Bushati et al., 2008) function similarly. In *Drosophila*, maternal transcripts are also cleared by piRNAs (Barckmann et al., 2015; Dufourt et al., 2017; Rouget et al., 2010), and in *C. elegans*, endo-siRNAs are required for transcript elimination (Stoeckius et al., 2014). Both RBPs and these non-coding RNAs rely on *cis* elements embedded in the transcript for their function, such as specific sequences or structures (Rabani et al., 2017; Vejnar et al., 2019).

A third recently uncovered pathway is codon optimality, in which the ratio of stabilizing to destabilizing codons influences maternal mRNA translation and half-life in zebrafish, *Drosophila*, *Xenopus*, and mouse (Bazzini et al., 2016; Medina-Muñoz et al., 2021; Mishima and Tomari, 2016). Codon optimality relies on the abundance of cognate tRNAs for each codon, where the search for scarce tRNAs slows ribosome decoding, enabling interactions with deadenylase machinery (Boël et al., 2016; Presnyak et al., 2015; Wu et al., 2019a). Several factors have been

proposed to sense codon-dependent slowing and modulate downstream decay, including the RNA helicase Dhh1p (Radhakrishnan et al., 2016), the RBP FMRP (Shu et al., 2020), and CCR4-NOT itself (Buschauer et al., 2020), although which of these are required for codon-mediated mRNA degradation in the MZT remains unclear.

Finally, chemical modifications of the mRNA have emerged as another regulatory layer in maternal mRNA clearance. For example, the m^{6}A reader YTHDF2 controls maternal transcript abundance in early mouse oocytes and in zebrafish embryos (Ivanova et al., 2017; Zhao et al., 2017). Similarly, the reader of 5-methylcytosine, Ybx1 promotes mRNA stabilization and translational repression in zebrafish, potentially via interaction with poly(A) tail binding proteins ((Sun et al., 2018; Yang et al., 2019). Terminal uridylation of maternal transcripts in mice, zebrafish, and *Xenopus* helps rapidly degrade transcripts with short poly(A) tails during the MZT and oocyte-to-embryo transition (Chang et al., 2018; Morgan et al., 2017). Finally, loss of the deadenylase component CNOT6L in mice reduces inosine modifications in maternal mRNAs, although whether this accounts for defective translation and decay in these mutants is unclear (Brachova et al., 2021). While these examples illustrate the importance of these marks in specific contexts, the universality, extent of activity, and mechanisms employed by RNA modifications to remove messages during the MZT are yet to be defined.

Together, this multitude of pathways orchestrates maternal mRNA clearance across organisms. These pathways frequently intersect, with the fate of a single transcript simultaneously dictated by multiple modes of clearance, potentially to ensure robust and timely degradation. Yet, as known mechanisms cannot account for the full breadth of clearance (Yartseva and Giraldez, 2015), additional pathways or interactions governing maternal mRNA decay are likely to be revealed through future research.

1.2. RNA methylation and posttranscriptional control of gene expression

1.2.1. Characteristics of the m⁶A modification

m⁶A was initially discovered through several landmark studies in the 1970s, which revealed not only the presence of this modification on mRNA molecules, but also its function in transcript destabilization (Adams and Cory, 1975; Camper et al., 1984; Desrosiers et al., 1974; Dubin and Taylor, 1975; Perry and Kelley, 1974; Perry et al., 1975; Sommer et al., 1978). The m⁶A modification is conserved across eukaryotes, from plants to yeast to vertebrates, and can also be found in bacteria and viruses (Beemon and Keith, 1977; Bodi et al., 2010; Canaani et al., 1979; Deng et al., 2015; Furuichi et al., 1975; Garcias Morales and Reyes, 2021; Horowitz et al., 1984; Nichols, 1979; Sommer et al., 1978; Zhong et al., 2008). Although m⁶A on mRNA is the focus here, this mark is also found in other classes of RNA, including tRNAs, rRNAs, lncRNAs, snRNAs, and microRNAs, each with unique processing machinery (Lence et al., 2019). Since the early demonstrations that m⁶A is functionally significant to the cell (Camper et al., 1984; Sommer et al., 1978), RNA methylation is now understood to contribute to almost every aspect of the mRNA lifestyle, including processing, splicing, polyadenylation, nuclear export, localization, stability, and translation (Heck and Wilusz, 2019; Roundtree et al., 2017a; Zaccara et al., 2019). The mark itself appears to be regulatorily neutral, and its functional outcome is instead dictated by its context and interactors. Characterization of the enzymes and proteins that control m⁶A homeostasis, termed the writers, readers, and erasers, have demonstrated that the modification is highly regulated and required for specific cellular and developmental processes (Heck and Wilusz, 2019). Similarly, high throughput m⁶A-sequencing (Dominissini et al., 2012; Meyer et al., 2012) uncovered specific features of m⁶A topology throughout the transcriptome that suggest its

incorporation is intentional and meant to confer specific instructions for gene expression (Zaccara et al., 2019). These mapping studies also uncovered the abundance of m^{6}A throughout the transcriptome, where 25% of transcripts are estimated to harbor at least one modification in mammals (Balacco and Soller, 2019; Dominissini et al., 2012; Meyer et al., 2012; Wei et al., 1975, 1976), further strengthening the view that methylation functionally regulates mRNA and cell fates.

1.2.2. Transcriptome topography of the m^{6}A modification

While m^{6}A is highly abundant, its presence is also selective, and only some transcripts are enriched in the modification (Linder et al., 2015; Schwartz et al., 2014). Precisely how this specificity is achieved remains unclear, but it likely stems from the selectivity of its writer proteins and their cofactors, as well as the underlying structural and sequence contexts of the mRNA (Lence et al., 2019). Several specific features are known to define the m^{6}A modification landscape, many of which were established through early high-throughput sequencing studies of methylated mRNAs (Dominissini et al., 2012; Meyer et al., 2012).

First, the methyltransferase complex that deposits m^{6}A scrupulously installs the mark in the DRACH consensus sequence (D = A,G,U; R= A,G; H = A,C,U) (Dominissini et al., 2012; Harper et al., 1990; Meyer et al., 2012). Yet thousands of DRACH motifs are not methylated, suggesting that the writers have additional means to control where methylation occurs (Zaccara et al., 2019).

Second, m^{6}A exhibits a specific pattern along the transcript body, with enrichment in the 5'UTR, CDS, and 3'UTR, and most highly around the stop codon (the last being linked to the terminal exon-exon junction likely for regulation of alternative polyadenylation and 3'UTRs (Ke et al., 2017)) (Bodi et al., 2012; Dominissini et al., 2012; Linder et al., 2015; Meyer et al., 2012;

Schwartz et al., 2014). This topography is conserved across cell types, where m^{6}A tags in the 3'UTR and near stop codons are largely constitutive, suggesting tight regulation of these sites, while those in the 5'UTR or CDS are less conserved, implying more dynamic control in these regions (An et al., 2020; Schwartz et al., 2014; Zhang et al., 2020a).

Third, substantial evidence indicates that methylation is introduced co-transcriptionally onto nascent transcripts (Barbieri et al., 2017; Bertero et al., 2018; Haussmann et al., 2016; Huang et al., 2019a; Ke et al., 2017; Knuckles et al., 2017; Lence et al., 2016; Slobodin et al., 2017). Incorporation likely occurs during RNA PolII elongation, as METTL3 and RNA PolII interact in plants (Bhat et al., 2020), and prior to splicing, as m^{6}A can be detected in introns and splice junctions (Louloupi et al., 2018). Deposition of m^{6}A to nascent transcripts suggests that the act of transcription likely influences writer specificity or guides the m^{6}A enrichment pattern (Slobodin et al., 2017; Zaccara et al., 2019).

Fourth, the selectivity of m^{6}A addition is determined by both the main components of the writer complex and its cofactors (Schwartz et al., 2014). The catalytic core, METTL3 and METTL14, are suggested to dictate broad m^{6}A deposition in canonical regions, while the cofactors modulate m^{6}A at more context specific sites (Wang et al., 2021). Subunit proteins may recognize their own binding motifs and thus recruit the writer to neighboring m^{6}A sequences, thereby controlling where the transcript is methylated (Patil et al., 2016; Zhang et al., 2020c). Modulation in the expression and activity of the methyltransferase complex may explain differential m^{6}A modifications across cell and developmental states.

Together, these features of m^{6}A deposition demonstrate that the methylation landscape is highly specific and can be attenuated to diverse physiological contexts. Understanding the pattern of m^{6}A can provide key insight into how this mark controls gene expression. Yet, current

knowledge of where m^6A is located is limited by its mapping techniques (McIntyre et al., 2020). These approaches traditionally rely on antibody capture coupled with high throughput sequencing, which preclude determination of site specific stoichiometries and are associated with immunoprecipitation biases (McIntyre et al., 2020). Additionally, many of these mapping techniques cannot distinguish m^6A from another modification, $N^6,2'$-O-dimethyladenosine (m^6A_m), which also influences transcript stability (Linder et al., 2015; Mauer et al., 2017). Numerous new approaches are being developed to overcome these limitations, which often rely instead on fusion proteins, restriction endonucleases, and single-molecule direct RNA sequencing (Anreiter et al., 2021; Linder and Jaffrey, 2019). As the identification of m^6A becomes more quantitative, capable of capturing fractional abundance, and site specific, our understanding of the function importance of this epitranscriptomic mark will greatly improve.

1.2.3. The m^6A writer complex

METTL3 and METTL14

Discovery of the "writer" proteins that catalyze m^6A addition to mRNA greatly advanced the field of epitranscriptomics. Methyltransferase identification enabled mutagenesis studies that revealed how loss of methylation impacts gene expression, and showed that these enzymes are essential for numerous cellular and developmental processes (Clancy et al., 2002; Zhong et al., 2008). The m^6A methyltransferase complex is comprised of METTL3 and METTL14, which form a heterodimer to serve as the catalytic core (Bokar et al., 1997; Liu et al., 2014; Schöller et al., 2018; Śledź and Jinek, 2016; Wang et al., 2016a, 2016b, 2014b) (**Fig. 1.3.**). Several auxiliary cofactors facilitate m^6A deposition by interacting with the core to guide methylase localization, specificity, binding, and activity (**Fig. 1.2.**). These cofactors are still being identified, but are

known to include WTAP, VIRMA, RBM15, ZC3H13, and CBLL1/HAKAI (Garcias Morales and Reyes, 2021; Lence et al., 2019). Although both METTL3 and METTL14 contain a methyltransferase domain, crystal structure analysis has shown that only METTL3 has catalytic activity, while METTL14 functions as an allosteric adapter to stabilize interaction with the RNA and improve methylation efficiency (Huang et al., 2019b; Schöller et al., 2018; Śledź and Jinek, 2016; Wang et al., 2016a, 2016b). Notably the functions of METTL3 extend beyond its role as a methyltransferase, as this enzyme has also been found to promote translation in the cytoplasm (Choe et al., 2018; Lin et al., 2016; Sorci et al., 2018).

Proper function of METTL3 and METTL14 is vital to development, as loss of these writers disrupts the methylome and subsequently impairs cellular reprogramming across organisms. For instance, METTL3 and METTL14 are required for early embryogenesis in mice, as genetic knockouts are lethal and depletion in mESCs inhibits differentiation (Aguilo et al., 2015; Batista et al., 2014; Chen et al., 2015; Geula et al., 2015; Meng et al., 2019; Wang et al., 2014b). Similarly, the homolog, MTA, is essential for embryogenesis and growth in *Arabidopsis thaliana* (Bodi et al., 2012; Shen et al., 2016; Zhong et al., 2008), and inactivation of core methyltransferase components Ime4 and Mum2 in yeast prevents meiosis and sporulation (Agarwala et al., 2012; Bodi et al., 2010; Clancy et al., 2002; Schwartz et al., 2013). The methylases are also crucial for spermatogenesis and oogenesis in zebrafish and mice, where they regulate gene expression at multiple stages of maturation, including in the germ cells (Lin et al., 2017; Sui et al., 2020; Xia et al., 2018; Xu et al., 2017). In *Drosophila*, they are necessary for sex determination (Haussmann et al., 2016; Lence et al., 2016). This extensive range of developmental functions across organisms demonstrate the importance of m^{6}A and its writers in modulating gene expression during key developmental milestones and transcriptome turnover.
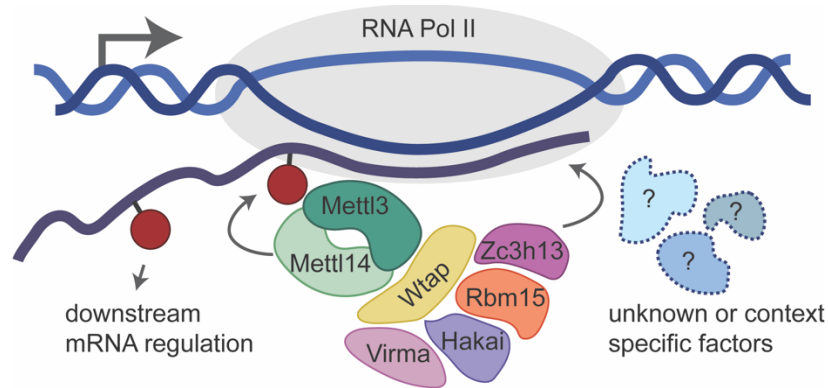
Figure 1.3. The methyltransferase complex adds m⁶A to mRNAs co-transcriptionally
The m⁶A modification is added to mRNA by the methyltransferase complex, which is comprised of two core components, METTL3 and METTL14, as well as several cofactors that help determine the activity, localization, and specificity of the complex, including WTAP, VIRMA, HAKAI, RBM15, and ZC3H13. The methyltransferase interacts with RNA polymerase II to install the modification co-transcriptionally, and methylation on transcripts leads to their downstream regulation. Other unknown or cellular context specific factors may also contribute to methyltransferase activity and specificity.

WTAP

WTAP, also called Fl(2)d in flies, is a central adapter of the methyltransferase complex, and its interaction with METTL3 is required for m⁶A formation in yeast and mammals (Agarwala et al., 2012; Horiuchi et al., 2013; Ping et al., 2014; Schwartz et al., 2014). WTAP helps recruit and anchor the methylases to target RNAs, and thereby guide the levels and specificity of methylation (Liu et al., 2014; Ping et al., 2014; Schöller et al., 2018). In *Drosophila*, WTAP is involved in sex determination and dosage compensation through regulation of *Sxl* alternative splicing (Granadino et al., 1990; Penn et al., 2008), although the extent to which this relies on its function in the methyltransferase complex is unclear. WTAP is also essential for proper m⁶A levels on transcripts encoding stem cell fate regulators during plant development (Shen et al., 2016). Similarly, conditional deletion of WTAP in mouse Sertoli cells impairs sperm stem cell self-renewal and differentiation, again reflecting the central function of m⁶A in stem cell fate decisions and spermatogenesis (Jia et al., 2020).

VIRMA

VIRMA, also called Virilizer or KIAA1429, is another methyltransferase subunit that helps establish the pattern of m^{6}A through recruitment of the methylases (Hu et al., 2020; Liu et al., 2018a; Schwartz et al., 2014). VIRMA's function as an alternative splicing regulator is critical during female development. In *Drosophila*, VIRMA works with WTAP to regulate *Sxl* splicing and control sex determination (Hilfikert et al., 1995; Ortega et al., 2003). In mice, KIAA1429 is essential for oocyte competence, likely by promoting localization of SRSF3 and YTHDC1 to nuclear speckles, where they assist with splicing (Hu et al., 2020).

RBM15

RBM15 and its paralog RBM15b are RBPs responsible for METTL3 and WTAP recruitment to mRNA and the lncRNA, *Xist*, where RBM15 binds to U-rich sequences near DRACH motifs, thus helping to specify m^{6}A target sites (Knuckles et al., 2018; Lee et al., 2020; Moindrot et al., 2015; Patil et al., 2016). Like other subunits in the methyltransferases complex, the RBM15 homolog in *Drosophila* (called Spenito) contributes to sex determination via regulation of alternative splicing of *Sxl* (Kan et al., 2017; Lence et al., 2016; Yan and Perrimon, 2015). Loss of RBM15 is lethal in *Drosophila* and mice (Lence et al., 2016; Patil et al., 2016), suggesting that its functions in m^{6}A regulation are essential for viability.

ZC3H13

Three concurrent studies revealed that ZC3H13 (also called Flacc in flies) is another component of the methyltransferase, functioning as an adapter protein between WTAP and

RBM15 in *Drosophila* and mice, and controlling complex nuclear localization (Guo et al., 2018; Knuckles et al., 2018; Wen et al., 2018). ZC3H13 regulates mESC self-renewal by promoting methylation of genes involved in pluripotency and differentiation, and deletion of its homolog, Xio in *Drosophila* results in female specific lethality, defects in wing development, and nervous system impairment (Knuckles et al., 2018; Wen et al., 2018). Unsurprisingly, absence of Xio phenocopies loss of other central writer complex components in *Drosophila*, obstructing *Sxl* alternative splicing and sex determination (Guo et al., 2018; Knuckles et al., 2018).

CBLL1/HAKAI

Known as both CBLL1 and HAKAI, this conserved E3 ubiquitin ligase is found in the WTAP interactome (Horiuchi et al., 2013) and its deletion reduces m^{6}A levels in *Arabidopsis*, suggesting it is another factor involved in m^{6}A deposition (Růžička et al., 2017). Yet, while HAKAI deletion causes embryonic defects, mutants are viable, unlike knockouts of METTL3, METTL14, VIRMA, and WTAP in *Arabidopsis*, indicating it may be an auxiliary factor controlling methyltransferase specificity (Růžička et al., 2017). Indeed, confirmation of HAKAI as a component of the writer complex awaits study of its impact on *Sxl* splicing in *Drosophila*.

These many methyltransferase cofactors are essential to both m^{6}A distribution and gene regulation. Yet, it remains unclear which subunits are necessary for all sites versus a select subset of modifications. Knockdowns of Fl(2)d, Nito, Flacc, and Vir in *Drosophila* lead to differential expression of both shared and unique mRNAs (Knuckles et al., 2018), suggesting that methylation patterns can be attuned by altering the composition of the writer complex. Even inactivation of METTL3 and METTL14 does not always abolition all modifications (Batista et al., 2014; Lin et

al., 2017), potentially due to other compensatory methyltransferases. Alternatively, incomplete loss of m⁶A upon methylase mutagenesis may reflect a hypomorphic phenotype, as partial loss of core writer components is frequently observed when complete knockouts are lethal (Sharpe and Cooper, 2017; Zaccara et al., 2019).

While these many proteins guide and specify m⁶A installation, it is likely that other, yet unidentified cofactors also help recognize candidate methylation sites. Additionally, METTL3 and METTL14 may interact with indirect regulators, like TRA2A and CAPRIN1 (An et al., 2020; Horiuchi et al., 2013; Zhang et al., 2020b). These recently identified factors control m⁶A catalysis on specific transcripts and in select cell types, suggesting they are not constitutive subunits but rather transient interactors of the methylases (An et al., 2020). Because trans-factors like these can modulate writer activity and selectivity without being integral for methylation, the topology of m⁶A can be temporally and spatially tailored to distinct biological contexts.

Finally, it is possible that these proteins have functions beyond their roles in the methyltransferase complex. For example, Fl(2)d and Nito localize outside of the complex in flies (Kan et al., 2017), and their depletion can result in stronger phenotypes than knockouts of METTL3 and METTL14 (Knuckles et al., 2018). It is often unclear if these transcriptomic and developmental phenotypes stem from global or transcript specific elimination of m⁶A, or from activities unrelated to RNA methylation. Further, many mutagenesis studies of the methylases rely on full gene knockouts and transcript dysregulation is observed for both methylated and non-methylated transcripts. Discerning the direct versus indirect consequences of m⁶A absence will require the use of catalytically dead METTL3 and METTL14 mutants, to preserve non-methylase dependent functions. Regardless, it is clear that the many factors responsible for writing the m⁶A modification are crucial for gene expression regulation and developmental progressions.

1.2.4. Erasers of RNA methylation

The demethylases ALKBH5 and FTO are m^6A erasers that catalytically remove the modification from specific transcripts (Rajecka et al., 2019). Discovery of the erasers initially led to the view that m^6A is dynamically regulated, where it is added and removed to rapidly control gene expression in a manner akin to epigenetic marks (Zhao et al., 2016). Yet, the scope of demethylase activity now appears to be limited to specific tissues, diseases, or stress responses (Darnell et al., 2018). Indeed, unlike m^6A writers and readers, the erasers are not highly conserved and function only in vertebrates (Robbens et al., 2008; Zheng et al., 2013), suggesting that demethylation is a specific rather than universal mechanism of gene expression control (Heck and Wilusz, 2019).

FTO

Initially believed to be a major remover of RNA methylation, the relevance of FTO as an m^6A demethylase is now highly debated (Jia et al., 2011; Mauer et al., 2019; Rajecka et al., 2019). FTO can demethylate a broad spectrum of substrates and targets m^6A_m with much higher affinity than m^6A (Mauer et al., 2019; Meyer et al., 2015; Wei et al., 2018). Yet, some transcripts do exhibit reduced m^6A levels upon FTO depletion, although FTO majorly prefers small nucleolar and nuclear RNAs (Koh et al., 2019; Su et al., 2018; Wei et al., 2018; Yu et al., 2018). As FTO activity and specificity can be modulated by protein partners, such as TRMT10A and SFPQ, RNA structure, subcellular distribution, and cell lineage (Ontiveros et al., 2020; Song et al., 2020a; Wei et al., 2018; Zhang et al., 2019b; Zou et al., 2016), it is likely that the function of FTO as an m^6A demethylase is context dependent.

FTO expression is largely nuclear (Gerken et al., 2007; Jia et al., 2011), indicating that any demethylation will occur prior to mRNA export (Mauer and Jaffrey, 2018), and even suggesting that FTO prohibits m^6A addition rather than actively erasing the mark (Koh et al., 2019). Yet some instances of FTO demethylation have been observed in the cytoplasm during heat shock, DNA damage responses, and cancerous states, (Cui et al., 2017; Li et al., 2017d; Xiang et al., 2017; Zhang et al., 2016), reflecting that this may be a highly specialized pathway.

Disruption of FTO is linked to increased mRNA levels, potentially due to loss of destabilizing m^6A modifications, or to defects in pre-mRNA processing and alternative splicing, which are likely the main FTO functions (Bartosovic et al., 2017; Louloupi et al., 2018; Mauer et al., 2019; Su et al., 2018; Wei et al., 2018; Zhao et al., 2014). FTO can also modulate translation upon cellular stress (Meyer et al., 2015; Zhou et al., 2015).

Loss of FTO in mice is linked to reduced postnatal growth and viability (Boissel et al., 2009; Fischer et al., 2009), disrupted neuronal development (Engel et al., 2018; Gao et al., 2010; Ho et al., 2010; Li et al., 2017c), impaired adipogenesis (Church et al., 2010; Gulati et al., 2013; Merkestein et al., 2015; Tung et al., 2015; Wang et al., 2015a; Zhang et al., 2015; Zhao et al., 2014), and repressed sperm proliferation (Huang et al., 2019c). Thus FTO is essential for adipogenesis, neurogenesis, and spermatogenesis (Rajecka et al., 2019). Intriguingly, mouse mutant phenotypes of the m^6A_m methylase PCIF1 often mirror those of FTO depletion, suggesting that FTO function in these developmental contexts may be dependent on m^6A_m rather than m^6A (Pandey et al., 2020). Yet, given that FTO targets multiple modifications as well as multiple RNA types (Gulati et al., 2013; Wei et al., 2018), future work is required to address whether FTO influences methylated RNA metabolism during development.

ALKBH5

The second known demethylase ALKBH5 is more likely to serve as a specific eraser of m^{6}A, as its expression consistently correlates with reduced methylation in mice and human tissues (Liu et al., 2020a; Zheng et al., 2013). Further, crystal structure analysis has revealed that ALKBH5 has an m^{6}A-specific binding pocket and uses a distinct demethylation mechanism from FTO that lend it greater selectivity (Aik et al., 2014; Chen et al., 2014b; Feng et al., 2014; Toh et al., 2020; Xu et al., 2014a; Zhang et al., 2019b). These structural and mechanistic differences between FTO and ALKBH5 likely reflect unique substrate preferences, which in turn increase the breadth of spatiotemporal dynamics through which m^{6}A is removed from RNAs. Similar to FTO, ALKBH5 exhibits nuclear localization, indicating that cytoplasmic demethylation is largely nonexistent (Thalhammer et al., 2011; Zheng et al., 2013).

Yet, while ALKBH5 is more specific for m^{6}A than FTO, methylation increases by only about 10% upon its knockdown in mice, indicating that it is not a global regulator of methylated mRNAs (Zheng et al., 2013). Depletion of murine ALKBH5 results in misregulated mRNA processing and export (Zheng et al., 2013), and in spermatocytes, aberrant splicing and 3'UTR usage, as well as accelerated transcript degradation due to higher m^{6}A levels (Tang et al., 2017). These molecular defects in ALKBH5 mouse mutants manifest as smaller testes, abnormal spermatozoa, and sterility, indicating that this eraser is essential for spermatogenesis, although the mice are viable (Tang et al., 2017; Zheng et al., 2013). ALKBH5 also functions during the development of many cancers, in which it frequently contributes to hypoxia response (Chen et al., 2019; Ma et al., 2018; Shen et al., 2020; Wang et al., 2020a; Zhang et al., 2016, 2017b). Given the lack of overt phenotypes for most tissues upon loss of ALKBH5, this demethylase may have a narrow regulatory focus for select cellular and physiologically processes. Ultimately, future

research is needed to determine the extent to which the m⁶A erasers contribute to gene expression changes during development.

1.2.5. Shared and unique features of the YTH m^{6}A readers

While m^{6}A does not disrupt the coding capacity of mRNA, its presence dramatically expands the functional diversity of RNA, allowing for dynamic regulation of gene expression (Lence et al., 2019). The operational significance of m^{6}A is dictated by the reader proteins, which recognize and bind to the mark, and subsequently employ effectors to specify transcript splicing, processing, stability, translation, and localization (Patil et al., 2018). While many proteins mediate methylated transcript regulation, only a few are bona fide readers, with the capacity for direct binding (Patil et al., 2018; Zaccara et al., 2019). These include the YTH-domain containing family, which rely on specific residues and conformations of their YTH domain to interact with the methyl moiety on the RNA molecule, as demonstrated through crystal structure studies (Li et al., 2014, 2021; Luo and Tong, 2014; Theler et al., 2014; Xu et al., 2014b, 2015; Zhu et al., 2014). Other m^{6}A regulators act indirectly, either through weak binding to m^{6}A (as well as non-methylated mRNAs) as is the case for FMRP (Edupuganti et al., 2017; Worpenberg et al., 2021; Zhang et al., 2018), or via m^{6}A-structural switches, where presence of the mark induces conformational changes favorable to protein binding, as observed for IGF2BPs (Edupuganti et al., 2017; Huang et al., 2018) and HNRNPs (Alarcón et al., 2015a; Liu et al., 2015, 2017; Roost et al., 2015; Wu et al., 2018). Regardless of the mechanism by which m^{6}A interpreters engage with the transcript, these factors are known to play pivotal roles in transcriptome remodeling.

The YTH family of readers contain five central factors, YTHDF1, YTHDF2, YTHDF3, YTHDC1, and YTHDC2. These factors are highly conserved, with YTHDF and YTHDC1-like

proteins found in organisms ranging from plants to humans (Patil et al., 2018), although YTHDC2 is largely limited to mammals (Jain et al., 2018). In vertebrates, amino acid sequence homology is high within the YTH domains for all five readers, but YTHDC1 and YTHDC2 also exhibit distinct sequences and domain organization, suggesting they may have additional unique roles (Patil et al., 2016). Lower organisms, like *Drosophila* express only one YTHDF protein (and one DC1), instead of three separate paralogs as in vertebrates (Kan et al., 2017), suggesting that the DFs share a single conserved function. Indeed, the sequence homology of the YTHDFs is extensive both within the YTH domains and within their low complexity regions (Patil et al., 2018), indicating that differences in m^{6}A-recognition may stem from distinctive expression patterns rather than individual binding profiles. Transcriptome-wide binding analyses by CLIP-sequencing demonstrate that all YTHs bind to the m^{6}A motif (Hsu et al., 2017; Li et al., 2017a; Patil et al., 2016; Wang et al., 2014a, 2015b; Xiao et al., 2016), but whether each reader has additional sequence preferences is yet to be determined. Across multiple cell types, the YTHDFs consistently recognize the same sites throughout the transcriptome (Li et al., 2017a; Patil et al., 2016; Shi et al., 2017), again suggestive of potentially redundant functions. YTHDC1 largely binds to nuclear methylated mRNAs, including lncRNAs, while YTHDC2 has a unique binding profile that includes some non-modified transcripts (Patil et al., 2016; Xiao et al., 2016). It is possible that the unique regions of the YTHDCs confer their specificity for certain RNAs, in addition to differences in subcellular localization or interacting partners (Kasowitz et al., 2018; Li et al., 2014; Wojtas et al., 2017; Xu et al., 2014b, 2015; Zhu et al., 2014). Indeed, YTHDC1 exhibits nuclear localization (Xiao et al., 2016), the YTHDFs are largely cytoplasmic (Shi et al., 2017; Wang et al., 2014a, 2015b), and YTHDC2 is found in both the nucleus and cytoplasm (Hsu et al., 2017). Finally, the DFs and YTHDC1 contain low complexity regions (Patil et al., 2018), which enable the proteins

to undergo phase separation, allowing them to target methylated transcripts to non-membrane organelles like P-bodies, stress granules, and other ribonucleoprotein (RNP) complex granules (Fu and Zhuang, 2020; Gao et al., 2019; Ries et al., 2019; Wang et al., 2020b, 2014a).

Yet, whether the YTHDF readers have shared or independent functions remains debated (**Fig. 1.4.**) (Patil et al., 2018; Shi et al., 2019). The extensive overlap in protein sequence and structure, shared sets of m^{6}A targets, overlapping interactomes, and similar cytoplasmic distributions, indicate that the YTHDFs have the capacity to regulate methylated mRNAs through common mechanisms (Zaccara and Jaffrey, 2020). Further, double or triple YTHDF depletion often results in more severe phenotypes than single mutants, potentially owing to compensation upon loss of a single reader (Lasman et al., 2020a; Li et al., 2017a; Zaccara and Jaffrey, 2020).

Additionally, the YTHDFs interact within the cell (Jin et al., 2020; Shi et al., 2017), but whether this reflects overlapping functions, competition, or ordered binding remains unclear. For instance, all three YTHDFs can induce phase separations (Ries et al., 2019), suggesting that any combination of readers is acceptable to partition modified mRNAs, as long as they meet the threshold for phase transition to occur. Alternatively, binding by one reader may recruit a second reader, allowing them to target a single transcript with multiple regulatory mechanisms (Liu et al., 2020b; Shi et al., 2017).

Some studies have uncovered specific roles for each reader (Liu et al., 2018b), as well as different degrees to which each factor is required for development (Lasman et al., 2020a). This may indicate that the cell type or physiological state determines the reader activity (Shi et al., 2019). Alternatively, these differences may reflect distinct expression patterns between the readers (Lasman et al., 2020a). Moreover, many studies limit their assessment to a single reader, and thus common functions may be overlooked. Ultimately, a thorough analysis of all three YTHDF

proteins and their interactions is essential to test if their roles converge or diverge to control m^{6}A-mediated cell fate decisions.
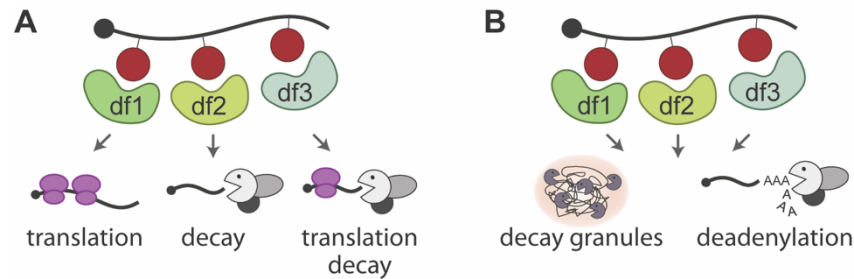
Figure 1.4. The two predominant models of YTHDF reader function
The degree to which the YTHDF m^{6}A readers share common functions can be explained by two main models: (A) the YTHDFs exert unique functions to regulate methylated mRNAs, with YTHDF1 promoting translation, YTHDF2 facilitating decay, and YTHDF3 contributing to both enhanced translation and degradation, or (B) the YTHDFs functional redundantly, as observed in their regulation of mRNA destabilization through localization to decay granules or interaction with deadenylases.

1.2.6. YTHDF reader function in mRNA decay

Upon its discovery, RNA methylation was quickly linked to transcript instability (Sommer et al., 1978). Now, m^{6}A is cemented as a central regulator of decay, with numerous studies showing that mRNA half-lives increase upon loss of methyltransferase function (Batista et al., 2014; Ke et al., 2017; Liu et al., 2014; Schwartz et al., 2014). YTHDF2 was the first identified mediator of methylated transcript degradation (Wang, et al., 2014a), but all three YTHDFs and YTHDC2 are now known regulators of mRNA decay (Patil et al., 2018). In some contexts, the YTHDFs exert redundant functions on methylated transcript elimination (Kennedy et al., 2016; Lasman et al., 2020a; Lu et al., 2018; Tirumuru et al., 2016; Zaccara and Jaffrey, 2020), although YTHDF2 is the dominant or sole regulator in others (Park et al., 2019; Wang et al., 2014a; Zhao et al., 2017). Mechanistically, the YTHDFs can promote transcript elimination through three main pathways: deadenylation, endoribonucleolytic cleavage, and localization to P-bodies (Du et al., 2016; Lee et al., 2020; Park et al., 2019; Wang et al., 2014a). This YTHDF triggered decay is especially

important during developmental transitions (Huang et al., 2020; Paris et al., 2019; Zhang et al., 2017a; Zhao et al., 2017), where recognition of m^{6}A enables rapid changes in mRNA fate and gene expression.

Localization to phase separated granules

The first mechanism used by the YTHDF readers to ensure short mRNA half-lives is sequestration of methylated transcripts into phase-separated compartments (Fu and Zhuang, 2020; Gao et al., 2019; Ries et al., 2019; Wang et al., 2020b, 2014a). In human cells, YTHDF2 induces modified mRNA degradation through targeting to P-bodies (Wang et al., 2014a), which are enriched in decapping and decay machinery (Luo et al., 2018). Similarly, YTHDF1, 2, and 3 drive methylated transcript localization to stress granules upon heat shock, where their translation is inhibited (Ries et al., 2019). Notably, transcripts with multiple, clustered m^{6}A residues exhibit the greatest decay, potentially because they attract more YTHDF readers and thus enhance their own entrapment to repressive, phase-separated compartments (Zaccara et al., 2019). Because all three YTHDF readers share the capacity to partition methylated transcripts into RNA-protein droplets (Ries et al., 2019), it is likely to be a universal mechanism for clearance.

Deadenylation

The second mechanism of the YTHDFs is recruitment of deadenylation machinery to promote poly(A) tail removal (Du et al., 2016). All three YTHDFs interact with the CCR4-NOT deadenylase complex (Zaccara and Jaffrey, 2020), and tethering of each reader accelerates reporter deadenylation in human cells (Du et al., 2016). Yet, in somatic reprogramming of mouse embryonic fibroblasts (MEFs), YTHDF2 and YTHDF3 function by independent deadenylation

mechanisms, with YTHDF2 again interacting with CCR4-NOT and YTHDF3 exclusively recruiting the PAN2-PAN3 deadenylase complex (Liu et al., 2020b). Given that these deadenylases exhibit distinct tail length substrates and rates of tail removal (Wahle and Winkler, 2013), these unique YTHDF interactions may help target multiple machineries to shared methylated targets and ensure their complete deadenylation. Future work should address how the YTHDFs achieve specificity in deadenylation machinery recruitment, especially given the high degree of protein homology and common m^{6}A targets (Zaccara et al., 2019).

Other decay pathways

Third, the YTH readers can facilitate cleavage of target transcripts. For instance, YTHDF2 promotes endoribonucleolytic cleavage of m^{6}A-containing mRNAs and circRNAs through recruitment of the adapter protein HRSP12 and subsequent binding of the endoribonuclease RNase P/MRP in human cells (Park et al., 2019). YTHDF1 and YTHDF3 can also interact with HRSP12, suggesting this may be a common mechanism (Park et al., 2019). The extent to which this program is employed is unclear, but HRSP12 binds preferentially to specific motifs (Park et al., 2019), suggesting that m^{6}A sequence context helps determine how degradation will proceed. YTHDC2 also expedites cleavage, by recruiting the cytoplasmic 5'-3' exoribonuclease XRN1 (Kretschmer et al., 2018; Wojtas et al., 2017), which was also recovered in the YTHDFs' interactomes (Zaccara and Jaffrey, 2020)

Finally, although initially believed to be inconsequential for mRNA abundance, (Wang et al., 2015b), YTHDF1 also promotes destabilization in some contexts. In human cancer cells, YTHDF1 facilitates m^{6}A-dependent Epstein-Barr viral RNA decay through recruitment of degradation machinery DCP2, DDX17, and ZAP, demonstrating that this factor has the capacity

to downregulate transcript expression (Xia et al., 2021). Whether other readers also encourage decapping is unknown, although some m^{6}A marked transcripts are dependent on Dcp2 activity for their destabilization (Luo et al., 2020b). Additionally, some factors, like HuR, TRA2A, ZFP217, and SMAD2/3 modulate methylated mRNA stability by manipulating methyltransferase activity, thereby increasing or decreasing m^{6}A levels on specific transcripts to flag them for downstream regulation (Aguilo et al., 2015; An et al., 2020; Bertero et al., 2018; Panneerdoss et al., 2018).

The extent to which these clearance pathways are used by the m^{6}A readers is unknown, as is how specific mRNAs are selected for each mode of regulation, and how the YTHDFs coordinate message removal. It is likely that the YTHDFs share redundant roles in transcript destabilization, especially considering that triple depletion is often necessary to inhibit methylated mRNA clearance to the same degree as METTL3 mutation (Lasman et al., 2020a; Zaccara and Jaffrey, 2020). Further, precisely how stability is influenced by methylation sequence and structural context, cooperation with other decay pathways, and physiological state remains undefined.

mRNA Stability

Rather than promoting transcript clearance, several readers have been identified as methylated mRNA stabilizers. The IGF2BP family helps maintain modified transcript abundance (Huang et al., 2018), and are known to shield mRNAs from decay in cytoplasmic granules, although it is unknown if this particular function is m^{6}A-dependent (Bell et al., 2013). IGF2BPs act during numerous developmental transitions, including embryogenesis in mice and flies (Boylan et al., 2008; Geng and Macdonald, 2006; Munro et al., 2006; Nielsen et al., 1999), as well as zebrafish, where IGF2BP3 is proposed to promote maternal mRNA stability during the MZT (Ren et al., 2020). Yet, whether the IGF2BPs are true "readers" of methylation is debated. IGF2BP3

26

was initially proposed to directly recognize m[6]A (Huang et al., 2018), but other work finds that IGF2BP3 binds nonspecifically to regions of high mRNA accessibility (Sun et al., 2019), such as those as induced by m[6]A (Liu et al., 2015; Roost et al., 2015). Because IGF2BPs can also bind in the absence of methylation (Huang et al., 2018; Müller et al., 2019), it is likely that these factors are indirect modulators of methylated mRNAs rather than specific readers.

FMRP is another indirect m[6]A regulator, as its sequence preference overlaps the DRACH motif, but the factor itself does not require m[6]A for binding (Worpenberg et al., 2021; Zhang et al., 2018). In *Drosophila*, YTHDF recruits the FMRP homolog FMR1 to methylated transcripts, where it represses translation to restrict axonal growth (Worpenberg et al., 2021). FMRP also co-binds with YTHDF2 in the mouse cerebral cortex, although here it competes promote stability while YTHDF2 engenders decay (Zhang et al., 2018). Additionally, PRRC2A stabilizes methylated mRNAs in mouse oligodendrocytes (Wu et al., 2019b), although it too binds unmethylated transcripts. Another indirect regulator is the mRNA-stabilizing stress granule protein G3BP1, which is repelled by m[6]A, and thus absence of its stabilizing effect results in enhanced degradation (Edupuganti et al., 2017). ELAVL1, or HuR, functions through a similar mechanism; when it binds to its AU-rich recognition elements near m[6]A sites, transcript stability increases likely because interaction with decay inducing readers is blocked (Wang et al., 2014b).

While these indirect effectors promote stability, it remains unclear how opposite consequences can be incurred on the same methylated transcripts, especially in conditions where readers with contrasting functions are simultaneously expressed, such as early embryogenesis (Ren et al., 2020; Zhao et al., 2017). It is possible that stabilizing factors occupy unique localities within the cell, antagonize the YTHDFs, or recognize distinct m[6]A sequences, as suggested for the IGF2BPs versus YTHDF2 (Huang et al., 2018). Careful comparison of each reader's methylome

preferences and cellular activities is required to better dissect the roles of m^{6}A effectors on transcript clearance.

1.2.7. m^{6}A and YTHDF regulation of translation

RNA methylation is capable of both stimulating and inhibiting global mRNA translation across organisms and cellular contexts (Meyer, 2019). The cellular conditions, location of the methylation within the transcript, local secondary structure, codon identity, ribosomal interactions, and association with different trans factors all shape how m^{6}A will modulate translation. These regulatory functions of m^{6}A on translation and protein synthesis have a developmental impact, including on embryogenesis, oogenesis, spermatogenesis, cancer cells, and neurons.

m^{6}A in the 5'UTR

The position of m^{6}A within the transcript dictates its role in translation. Methylation in the 5'UTR represents only about 10% of the total m^{6}A along the transcript body (Mao et al., 2019). Yet these 5'UTR residues enable ribosome loading and promote non-canonical translation in the absence of cap-binding proteins, especially in response to stressors like heat shock (Meyer et al., 2015; Zhou et al., 2015). This mechanism appears specific to 5'UTR methylation (Zhou et al., 2015), and may impact only a select handful of mRNAs (Luo et al., 2020a), but it represents a unique means by which m^{6}A ensures protein synthesis from transcripts when traditional translational pathways are impaired. m^{6}A in the 5'UTR can also downregulate translation. In human cancer cells, methylation in the 5'UTR of transcripts lengthens ribosomal dwell time around the start codon, delaying initiation and restricting translational output (Dong et al., 2021).

As YTH reader binding was not detected around these 5'UTR m^{6}A sites, it remains unclear which factor mediates these inhibitory effects on translation.

m^{6}A in the CDS

An estimated 36% to 52% of m^{6}A residues are located within the CDS in human cells, which impact translation in multiple ways (Louloupi et al., 2018; Mao et al., 2019). First, higher m^{6}A levels in the CDS correlate with decreased translation efficiency in MEF cells (Mao et al., 2019), and with lower protein production from reporters in human cells (Slobodin et al., 2017). Indeed, clustered or multiple marks have even greater inhibitory effects (Hoernes et al., 2019; Luo et al., 2020a; Slobodin et al., 2017). Inactive translation of these transcripts may be explained by the observation that coding region m^{6}A delays tRNA accommodation and thus slows translational elongation, as determined from single molecule measurements *in vitro* (Choi et al., 2016) and transcriptomic analysis in cell culture (Mao et al., 2019).

Conversely, m^{6}A in the CDS also correlates with enhanced translation. Loss of coding region m^{6}A through METTL3 knockdown reduces translation efficiency in mouse and human cells (Mao et al., 2019). This discrepancy may reflect the effect of the RNA structure underlying the modification (Mao et al., 2019). When methylation helps resolve highly structured CDSs, ribosome pausing is alleviated and translation efficiency increases. Alternatively, m^{6}A in unstructured transcripts slows tRNA accommodation and impedes translation. RNA unfolding is mediated by YTHDC2, indicating that the presence of specific readers also helps modulate translation (Mao et al., 2019). The codon identity and position of m^{6}A within codons also influences translation, with different codons exhibiting different degrees of ribosome pausing and occupancy, and evolutionary conservation patterns, indicating that m^{6}A-codon interactions may

affect ribosomal decoding (Barbieri et al., 2017; Choi et al., 2016; Hoernes et al., 2019; Liu et al., 2018c; Mao et al., 2019). Thus, the effects of CDS m⁶A on translation appear to be context dependent, where the codon identity, local structure, recruited factors, and ribosomal interactions dictate the translational output for each transcript.

m⁶A in the 3'UTR

Up to 55% of methylated residues are harbored in the 3'UTR, and these modifications are largely linked to enhanced translation (Meyer, 2019). Loss of 3'UTR methylation through METTL3 depletion decreases mRNA translation efficiency (Mao et al., 2019), and YTHDF1 and YTHDF3 are thought to promote cap-dependent translation via marks in this region (Shi et al., 2017; Wang et al., 2015b). How these factors facilitate translation through the 3'UTR is unclear, though a looping mechanism dependent on the eukaryotic translation initiation factor eIF3 has been proposed.

It is possible that the effects of m⁶A on translation are linked to its role in mRNA degradation. Indeed, m⁶A in the 3'UTR is associated with transcript decay (Wang et al., 2014a), meaning m⁶A can attenuate the levels of transcript availabile for translation (Meyer, 2019). Further, some readers like YTHDC2 enhance both mRNA clearance and translation (Mao et al., 2019; Wojtas et al., 2017), and can thus coordinate these processes to fine tune gene expression control. Together, these studies reveal that the consequences of methylation on mRNA translation are diverse and dependent on many trans factors and transcript features.

YTHDFs and translation

As the consequences of methylation on mRNA translation vary extensively, the interacting reader proteins help determine the regulatory outcome. The first identified effector of m⁶A-dependent translation is YTHDF1, whose depletion in human cells decreases translation efficiency (Wang et al., 2015b). Since then, YTHDF1 is found to upregulate translation of specific methylated mRNAs across cellular contexts, including in stem cells, cancer, immune response, and neural development, suggesting this regulatory function is conserved (Han et al., 2020, 2019a; Huang et al., 2018; Liu et al., 2020c; Weng et al., 2018; Wu et al., 2019c; Zhuang et al., 2019).

YTHDF1 may regulate translation by binding to 3'UTR m⁶A, and looping the mRNA through recruitment of eIF3, to facilitate ribosome loading near the 5'end (Han et al., 2019a; Wang et al., 2015b). Yet, other work suggests that interactions between the YTHDFs and eIF3 are non-specific (Zaccara and Jaffrey, 2020). YTHDF1 can also promote translation via CDS methylation, potentially by engaging with elongation factors, as seen in cancer cells (Lin et al., 2019).

YTHDF1 also downregulates translation. Up to a third of YTHDF1 m⁶A targets increase in translational efficiency upon DF1 depletion (Zhang et al., 2020c), and DF1 recruits the translational suppressor FMR1 to methylated transcripts in *Drosophila* cells (Worpenberg et al., 2021). Thus, multiple mechanisms and factors likely influence the impact of YTHDF1 on translation simultaneously.

YTHDF3 is another translation regulator (Chang et al., 2020; Li et al., 2017a; Shi et al., 2017; Wu et al., 2021; Zhang et al., 2019c), and is proposed to cooperate with YTHDF1 to enhance target translation (Li et al., 2017a; Shi et al., 2017). Yet, YTHDF3 may also function independently, as loss of DF3 alone is sufficient to drive down translation of specific transcripts (Chang et al., 2020; Wu et al., 2021). YTHDF3 also promotes cap-independent translation of methylated circRNAs (Yang et al., 2017a), and may even control protein synthesis in the absence

of m^{6}A, as observed during the innate immune response (Zhang et al., 2019c), although m^{6}A-independent DF functions are rare.

Yet, it is possible that the YTHDFs do not universally influence translation, as conclusions from major studies of DF1 and DF3 were recently challenged (Zaccara and Jaffrey, 2020). In this work, neither individual nor triple YTHDF knockdowns affected translation efficiency, and reanalysis of ribosome profiling data from Wang et al., 2015 and Shi et al., 2017 uncovered no consequences of DF1 or DF3 depletion on translation (Zaccara and Jaffrey, 2020). Yet, the YTHDFs mediate translational output in other systems, and thus may serve as transcript specific if not global regulators. Future work is required to conclusively establish the impact of the YTHDFs in translation across unique biological contexts.

YTHDC2 and translation

The reader YTHDC2 also promotes translation, and employs its helicase domains to directly unwind methylated mRNA structures in the CDS, thereby relieving ribosomal stalling (Mao et al., 2019). This remodeling activity of YTHDC2 is not limited to the CDS, as DC2 also unwinds highly structured 5'UTRs to promotes translation initiation in human cells under hypoxia (Tanabe et al., 2016). Further, YTHDC2 binds directly to the 40S small ribosomal subunit (Kretschmer et al., 2018), together suggesting a mechanism by which YTHDC2 recognizes m^{6}A, unwinds RNA structures, and favorably interact with the ribosome to enhance target translation. Yet, how many mRNAs are subject to translational upregulation by YTHDC2 remains unclear (Tanabe et al., 2016), and future study is warranted to establish the prevalence of this m^{6}A-mediated regulatory mechanism.

METTL3 as a "reader" of m⁶A in translational control

In addition to its function as an m^{6}A writer, cytoplasmic METTL3 can associate with ribosomes to promote translation of specific mRNAs in human cancer cells (Choe et al., 2018; Lin et al., 2016). In this context, catalytically dead METTL3 promotes reporter translation without impacting mRNA abundance, indicating that METTL3 exclusively regulates translation, and does so independently of its methylase activity (Choe et al., 2018; Lin et al., 2016). Mechanistically, METTL3 facilitates translation by interacting with the cap-binding complex and eIF3, although how this occurs with METTL3 binding in the 3'UTR is unclear (Choe et al., 2018). This translation promoting function of METTL3 contributes to human lung cancer cell growth (Choe et al., 2018; Lin et al., 2016), but it remains to be determined if METTL3 serves as an m^{6}A "reader" in other physiological states. Because METTL3 does not bind to most m^{6}A sites, but METTL3 depletion does globally repress translation, downstream loss of methylation likely accounts for the majority of misregulation (Meyer, 2019).

Indeed, METTL3 also promotes translation through m^{6}A deposition. In acute myeloid leukemia cells, METTL3 association with transcript promoters is linked to enhanced CDS methylation of the corresponding mRNAs (Barbieri et al., 2017). These higher m^{6}A levels correlate with greater translation, suggesting that promoter-bound METTL3 boosts protein synthesis by increasing methylation (Barbieri et al., 2017). The precise mechanisms underlying this connection between DNA binding, m^{6}A deposition, and translation efficiency remain unclear.

eif3 and non-canonical m⁶A translation

eIF3 is another regulator of translation via m^{6}A. eIF3 can directly bind methylation in the 5'UTR and recruit translational machinery independent of cap binding proteins (Meyer et al.,

2015). This pathway is employed in response to cell stressors, like heat shock, during which m^{6}A is highly redistributed to the 5'UTR (Meyer et al., 2015; Zhou et al., 2015). The ATP-binding cassette protein, ABCF1 functions similarly, and recruits translation initiation machinery to methylated transcripts in stress conditions (Coots et al., 2017). Although eIF3 and ABCF1 regulation is often limited to a select subset of mRNAs, m^{6}A-dependent cap-independent translation is likely a universal means to control protein output when canonical pathways are restricted. Indeed, numerous other examples of m^{6}A promoting non-canonical translation in response to cell stress are documented, although the reader responsible may vary by each case. (Fry et al., 2017; Miao et al., 2019; Shen et al., 2019; Xiang et al., 2017; Zhou et al., 2018).

1.2.8. m^{6}A and microRNA biogenesis and function

RNA methylation and microRNAs interact in multiple ways. These pathways can integrate their functions to decay the same transcripts or indirectly control gene expression by regulating one another's activities (Chen et al., 2020b; Fazi and Fatica, 2019). Thus, crosstalk between m^{6}A and miRNAs can be divided into three main types: m^{6}A controlling miRNA biogenesis and activity, miRNAs modulating m^{6}A deposition and function, and miRNAs and m^{6}A coordinately degrading shared targets.

First, RNA methylation is known to modify miRNAs to regulate their maturation and expression (Alarcón et al., 2015b; Berulava et al., 2015; Bhat et al., 2020). Loss of m^{6}A through depletion of METTL, or its homolog MTA, impairs miRNA biogenesis in human cells and *Arabidopsis*, respectively (Alarcón et al., 2015b; Bhat et al., 2020). This most likely arises from improper miRNA processing, as m^{6}A stabilizes the pri-miRNA stem loop structure, and thus is crucial for recognition by microprocessor components (Alarcón et al., 2015b; Bhat et al., 2020).

Additionally, METTL3, METTL14, and the reader HNRNPA2B1 can regulate miRNA biogenesis directly by recruiting and interacting with the processing enzymes (Alarcón et al., 2015a, 2015b; Knuckles et al., 2017; Ma et al., 2017). Methylation may also modulate miRNA activity by altering expression of transcripts encoding other miRNA regulatory factors, like AGO2 and DROSHA (Min et al., 2018). It remains unclear if m^6A-dependent miRNA processing is universal, as biogenesis of some miRNAs is unaffected by METTL3 or HNRNPA2B1 knockdown (Alarcón et al., 2015a, 2015b), although it appears to be a central mechanism mediating carcinogenesis (Chen et al., 2020a; Han et al., 2019b; Ma et al., 2017; Peng et al., 2019; Zhang et al., 2019a).

Second, miRNAs can influence m^6A deposition and function. Dicer or miRNAs may facilitate cellular m^6A installation by promoting METTL3 binding (Chen et al., 2015), although how this is achieved is unclear. miRNAs also target m^6A regulatory proteins to directly control their expression. For example, miR-33a downregulates METTL3 mRNA in non-small-cell lung carcinoma cells, (Du et al., 2017) and the same strategy is employed by miR-4429 in gastric cancer cells (He et al., 2019) and miRNA let-7g in breast cancer cells (Cai et al., 2018). Similarly, miR-145 targets the 3'UTR of YTHDF2 in cancer cells, thereby increasing overall m^6A-modified mRNA stability (Li et al., 2020; Yang et al., 2017b). miRNA control over m^6A interpreters also helps regulate key developmental events, as when miR-670 targets *Igf2bp1* to facilitate mouse embryogenesis (Hao et al., 2020). This mechanism may represent a means by which miRNAs can rapidly expand the pool of transcripts under their regulatory umbrella without necessitating a binding sequence.

Finally, m^6A and miRNAs can combinatorially regulate transcripts. Transcriptome wide analysis in humans and mice reveals that m^6A peaks are enriched at miRNA target sites (Chen et al., 2015; Liu et al., 2020a). Similarly, ~60-80% of m^6A-modified mRNAs are estimated to harbor

at least one miRNA binding site (Liu et al., 2020a; Meyer et al., 2012). miRNAs are also known to pair with mRNA at methylated residues, with the consensus motif inversely complementary to the seed of hundreds of miRNAs (Chen et al., 2015; Liu et al., 2020a). The outcome of this pairing is unclear, as m^{6}A within 3'UTRs can both destabilize miRNA duplex formation (Briand et al., 2020; Konno et al., 2019), and promote favorably interactions with miRNAs (Cheng et al., 2020). Thus, the nature of interaction between m^{6}A and miRNAs on the same transcript may depend on the cellular context and mRNA identity.

Together, these examples demonstrate extensive crosstalk between m^{6}A and miRNAs to control gene expression at the posttranscriptional level. These collaborative interactions and cross regulatory pathways may help exert precise control over mRNA levels and timing of decay. The precise nature of m^{6}A and miRNA regulation is likely determine by the expression and localization of each pathways components, and the specific cell state.

1.3. RNA methylation regulates developmental transitions

RNA methylation is a regulator of message metabolism in numerous physiological transitions, with functions in stem cell differentiation, neuronal development, hematopoiesis, gametogenesis, cancer development, and immunity. These reprogramming events often rely on methylation to promote transcriptome turnover, where m⁶A helps balance expression of mRNAs between the old and new programs of gene expression. While the specific targets of methylation, and the activities of its writers and readers vary by developmental context, the universal importance of m⁶A on cell fate specification is clear, as loss of m⁶A writers or readers frequently disrupts both pluripotency and differentiation (Heck and Wilusz, 2019). Here, I will discuss the diverse cell state changes mediated by RNA methylation, with an emphasis on how m⁶A reshapes the posttranscriptional landscape to establish new patterns of gene expression and facilitate development.

1.3.1. RNA methylation in stem cells

Embryonic stem cells have the capacity to self-renew and maintain their pluripotent capacities, or to differentiate into the unique cell lineages that give rise to all embryonic tissues. The establishment, maintenance, and transition of stem cells from a pluripotent to differentiated state requires coordinated changes in gene expression, which are executed by transcriptional, epigenetic, and posttranscriptional pathways. m⁶A appears to contribute to stem cell fate by modulating the balance between self-renewal and differentiation, where it regulates expression of genes encoding the existing cell state. For instance, in mouse and human embryonic stem cells (ESCs), m⁶A marks mRNAs encoding core pluripotency transcription factors like *Nanog*, *Klf4*, and *Myc* for decay (Batista et al., 2014). Loss of methylation on these transcripts through genetic

inactivation of METTL3 in mouse or human ESCs prolongs their expression and blocks the exit from self-renewal toward differentiation (Batista et al., 2014). Alternatively, a second study finds that reduction of m^{6}A upon METTL3 knockdown causes mESCs to lose their capacity for self-renewal, likely through repressed decay of developmental regulators and continued expression of pluripotency factors like *Nanog* and *Sox2* (Wang et al., 2014b). While these studies agree that m^{6}A marks and regulates determinants of both self-renewal and lineage-commitment, their findings regarding the role of methylation in the maintenance of pluripotency appear contradictory. This conflict is resolved by the discovery that the timing of m^{6}A depletion determines the consequences on development, where absence of METTL3 in naïve ESCs traps cells in pluripotency, while in primed cells, METTL3 depletion blocks self-renewal and accelerates differentiation (Geula et al., 2015). Because m^{6}A controls the half-life of transcripts governing both the naïve and primed state, loss of METTL3 prolongs expression of whichever genes dominant the current cell state, thus locking cells in an either hyper differentiated or pluripotent state (**Fig. 1.5.**) (Geula et al., 2015).
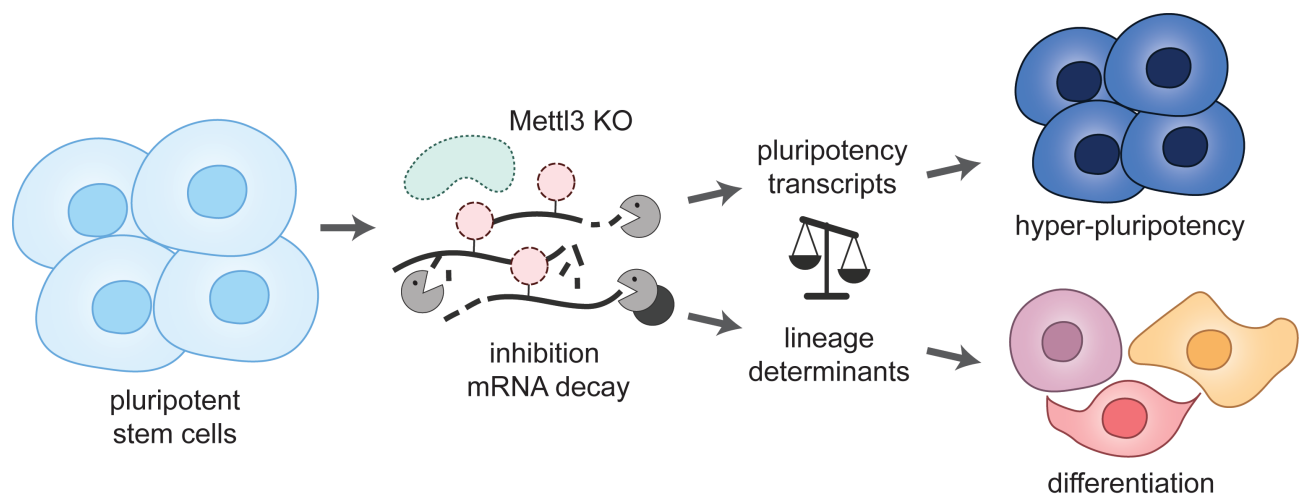
Figure 1.5. m^{6}A regulates the balance between stem cell self-renewal and differentiation.
RNA methylation and METTL3 control the balance between pluripotency and differentiation in stem cells by promoting degradation of transcripts maintaining the current cell state. When METTL3 is removed from pluripotent stem cells in the naïve state, mRNAs encoding pluripotency regulators fail to degrade, causing the cells to assume a hyper-pluripotent state. When METTL3 is lost in primed

pluripotent stem cells, transcripts for lineage determinants are stabilized, resulting in differentiation and cell death.

These effects are not limited to core writer components, as loss of ZC3H13 also impairs self-renewal and triggers mESC differentiation, and knockdown of WTAP, KIAA1429, or HAKAI likewise alters expression of transcripts controlling pluripotency and differentiation (Wen et al., 2018). This suggests that any misregulation of m^{6}A deposition disrupts developmental determination. Similarly, in porcine iPSCs, loss of METTL3 debilitates self-renewal and enhances differentiation, by reducing m^{6}A levels on *JAK2* and *SOCS3* mRNAs and inhibiting subsequent YTHDF1-dependent translation, and YTHDF2-dependent degradation, respectively (Wu et al., 2019c). Because proper levels of these factors in the JAK-STAT pathway are needed to transcriptionally activate *KLF4* and *SOX2* for prolonged self-renewal, maintenance of iPSCs pluripotency is deterred (Wu et al., 2019c). This same mechanism of m^{6}A and YTHDFs facilitating multipotency by regulating the JAK-STAT cascade is also observed in porcine bone marrow stem cells, prior to their differentiation into adipose tissue (Yao et al., 2019), in mouse neural stem/progenitor cells developing into neurites (Li et al., 2018), and in T cell homeostasis and differentiation (Li et al., 2017b), suggesting a conserved function across organisms and tissues. Further, loss of m^{6}A interpretation hinders lineage determination, as triple YTHDF knockouts in mice are unable to differentiate due to protracted expression of pluripotency markers, closely paralleling the METTL3 hyperpluripotency phenotype (Lasman et al., 2020a). Yet, single YTHDF knockouts in mESCs differentiate properly, and m^{6}A mRNA half-lives increase only upon triple reader ablation, indicating that all three readers share common roles in transcript decay during stem cell development (Lasman et al., 2020a).

Additionally, some factors manipulate methyltransferase activity to control methylation levels and thereby transcript stability. For example, in mESCs, ZFP217 interacts with METTL3 to

decrease modification of pluripotency factors, enabling their persisted expression and fostering self-renewal (Aguilo et al., 2015). In human ESCs, SMAD2/3 interacts with METTL3-METTL14-WTAP to upregulate methylation on pluripotency regulators, enhancing their degradation and facilitating differentiation in response to changes in activin/TGFβ signaling (Bertero et al., 2018).

RNA methylation also regulates efficient somatic cell reprogramming into pluripotent stem cells through transcriptome remodeling. In MEFs, early METTL3 knockout inhibits reprogramming (Geula et al., 2015), while higher m^{6}A levels promote reprogramming (Chen et al., 2015). The YTHDF readers appear to be responsible for modulating these effects of m^{6}A on somatic cells (Liu et al., 2020b). YTHDF2 and YTHDF3 are required to transform MEFs into iPSCs, by enhancing deadenylation of somatic-specific transcripts to accelerate the mesenchymal-to-epithelial transition, a process required to initiate reprogramming (Liu et al., 2020b). YTHDF2 has also been linked to m^{6}A-mediated destabilization of neural-specific factors to promote pluripotency during neural differentiation of iPSCs (Heck et al., 2020). This indicates that the YTHDFs may globally regulate clearance of lineage determinants, although how they target only a subset of methylated transcripts to prime cells for reprogramming remains unclear.

The impact of m^{6}A on cell fate transitions extends into numerous other systems, including hematopoiesis (Vu et al., 2019; Weng et al., 2019), neural development (Livneh et al., 2020; Vissers et al., 2020), adipogenesis (Song et al., 2020b; Wu and Wang, 2021), muscle development (Zhang et al., 2020b), and cancer progression (Delaunay and Frye, 2019; Liang et al., 2020), reflecting the universality of this modification in balancing pluripotency and differentiation. To facilitate these transitions, RNA methylation primarily promotes clearance of transcripts establishing the current state, thus priming cells for rapid shifts in gene expression. Given that the timing and stage of the transition dictate which mRNAs are regulated by m^{6}A (Geula et al., 2015),

understanding how the YTHDFs distinguish transcripts for degradation will be essential. Future research is needed to fully illuminate how RNA methylation and the YTHDFs posttranscriptionally regulate gene expression to potentiate stem cell fate decisions.

1.3.2. RNA methylation functions in gametogenesis

RNA methylation, its writers, and its readers play critical roles at multiple stages of gametogenesis, from the germ cells to fully functional oocytes and sperm (Lasman et al., 2020b). Similar to other cellular contexts, m^6A primarily promotes gametogenesis by regulating transcript stability and translation (Qi et al., 2016). RNA methylation is pivotal for gametogenesis across organisms, as evidenced by the frequent enrichment of m^6A-associated factors in reproductive organs, and the copious studies showing that loss of writer or reader function causes infertility (Hongay and Orr-Weaver, 2011; Hu et al., 2020; Jia et al., 2020; Kan et al., 2017; Lin et al., 2017; Pan et al., 2005; Xia et al., 2018; Xu et al., 2017; Zhong et al., 2008). For instance, almost all components of the methyltransferase complex are required for female development, fertility, and sex determination in *Drosophila* (Granadino et al., 1990; Guo et al., 2018; Haussmann et al., 2016; Hilfikert et al., 1995; Hongay and Orr-Weaver, 2011; Kan et al., 2017; Knuckles et al., 2018; Lence et al., 2016; Yan and Perrimon, 2015). Examples like these demonstrate that m^6A is a master mediator of the gene expression changes required for successful reproductive development.

Spermatogenesis

Spermatogenesis is the process of producing mature sperm from the primordial germ cells, and it occurs continuously in the seminiferous tubules of the testes. Spermatogenesis begins with the spermatogonial stem cells (SSCs), which balance self-renewal with lineage commitment into

sperm progenitors, and undergo mitosis to form primary spermatocytes (Griswold, 2016; Holstein et al., 2003). The primary spermatocytes next undergo meiosis I to generate secondary spermatocytes, which then undergo meiosis II to form haploid spermatids. Finally, the spermatids transition into mature haploid spermatozoa through the process of spermiogenesis (Griswold, 2016; Holstein et al., 2003). The methylation pathway regulates spermatogenesis in multiple organisms, through various effects of the m^6A writers METTL3 and METTL14, the erasers, ALKBH5 and FTO, and the readers YTHDC1, YTHDC2, and YTHDF2 (Lasman et al., 2020b).

In mice, the methyltransferase complex is required in both early and late spermatogenesis. Early primordial germ cell knockouts of METTL3 or METTL14 reduce methylation on genes required for SSC proliferation and differentiation, disrupting their translation and causing sterility (Lin et al., 2017). Similarly, testes specific METTL3 deletion leads to infertility, reduces the number of germ cells, impairs spermatogonial differentiation, and disrupts meiosis initiation in mice, potentially through dysregulation of alternative splicing and transcript expression (Lasman et al., 2020a; Xu et al., 2017). Loss of Mettl3 in zebrafish also impairs sperm maturation and reduces motility (Xia et al., 2018). In this case, neither the germ cells nor meiosis are affected, and fertility decreases but is not fully compromised (Xia et al., 2018), suggesting either that Mettl3 is nonessential for zebrafish spermatogenesis, or that this mutant is a hypomorph, as other instances of Mettl3 deletion are larval lethal (see Section 4.4). Other writer components are also required for spermatogenesis. Like METTL3 and METTL14, WTAP in mice is necessary for SSC maintenance, spermatogonial differentiation, and fertility, likely through the influence of m^6A on splicing, stability, and translation (Jia et al., 2020). Indeed, even in humans, higher m^6A, *METTL3*, and *METTL14* levels are associated with reduced sperm motility (Yang et al., 2016). Intriguingly, the writers are not required for spermiogenesis or mature sperm function, as spermatid specific

loss of METTL3 has no impact on fertility in mice (Lasman et al., 2020a). This is likely because spermatids are transcriptionally inactive and the methylases largely function co-transcriptionally. Together, these studies demonstrate that the m^{6}A writers are crucial for spermatogenesis across organisms.

The eraser ALKBH5 also functions in spermatogenesis, and is required for fertility and testes development in mice (Tang et al., 2017; Zheng et al., 2013). Loss of ALKBH5 disturbs mRNA export, processing, splicing, and transcript stability, and thus inhibits spermatocyte progression (Tang et al., 2017; Zheng et al., 2013). ALKBH5 may also influence circular RNA biogenesis and translation in male germ cells in mice, suggesting that demethylation controls spermatogenesis through multiple pathways (Tang et al., 2020). Finally, inhibition of the other demethylase, FTO, via meclofenamic acid treatment increases m^{6}A modification, and thus enhances degradation of cyclin dependent kinases required for sperm cell proliferation during meiosis (Huang et al., 2019d).

The most famous m^{6}A-mediator in spermatogenesis is YTHDC2, which facilitates meiosis in both male and female mice (Bailey et al., 2017; Hsu et al., 2017; Jain et al., 2018; Wojtas et al., 2017). Knockout of YTHDC2 causes infertility, reduces testes size, impairs differentiation of male germ cells, and halts the transition from mitosis to meiosis, likely through downregulation of meiotic genes and upregulation of mitotic genes (Bailey et al., 2017; Jain et al., 2018; Wojtas et al., 2017). YTHDC2 also controls transcript abundance and translation in sperm, (Hsu et al., 2017), interacts with the exoribonuclease Xrn1 (Wojtas et al., 2017), and localizes to RNA granules in the testes (Bailey et al., 2017). Whether these posttranscriptional roles of YTHDC2 in spermatogenesis are m^{6}A-dependent remains unclear.

Other readers also guide male reproductive development. YTHDC1 deletion reduces mature sperm levels, and causes loss of germ cells and male sterility, potentially through its function as a splicing regulator (Kasowitz et al., 2018). Mouse knockouts of YTHDF2 exhibit disrupted sperm cell morphology, migration, and proliferation, stemming from stabilization of transcripts involved in sperm cell adhesion (Huang et al., 2020). Further, YTHDF2 mouse mutants have seminiferous tubule degeneration, loss of sperm, and hypofertility, again due to dysregulated transcript decay (Lasman et al., 2020a). The main functions of YTHDF2 are likely late in spermatogenesis, as YTHDF2 is highly expressed in spermatocytes, while YTHDF1 and YTHDF3 expression is limited to spermatogonia (Lasman et al., 2020a). These differences in expression may account for differences in their activity during sperm maturation, although the role of YTHDF1 and YTHDF3 in male reproductive development is yet to be explored. Taken together, these studies demonstrate that the writers, eraser, and readers of RNA methylation are essential for spermatogenesis, where loss of any one factor dramatically disrupts male fertility.

Oogenesis

Generation of the mature egg, or ovum, is achieved through oogenesis. Oogenesis begins with mitosis of a diploid germ cell into a primary oocyte, which subsequently enters meiosis I (Marlow, 2018; Sánchez and Smitz, 2012). Here, the primary oocyte arrests in the germinal vesicle (GV) stage, until hormones trigger its re-entry into meiosis I. The oocyte then divides asymmetrically, forming the secondary oocyte and the first polar body. The secondary oocyte matures in the ovary until it begins meiosis II, where it arrests in metaphase II until fertilization (Marlow, 2018; Sánchez and Smitz, 2012). Because early embryogenic success depends on proper oocyte development and maternally supplied RNAs and proteins, the maternal transcriptome must

be faithfully assembled during this process (Marlow, 2018). Further, because there is no transcription past the GV stage, posttranscriptional regulation controls gene expression during late oogenesis and early zygotic development (Ivanova et al., 2017). RNA methylation greatly contributes to this posttranscriptional regulatory landscape, and both m^6A readers and writers are critical to ensure production of healthy oocytes (Lasman et al., 2020b).

The writers of m^6A, METTL3 and KIAA1429, are both essential for oocyte maturation and competence. In zebrafish, loss of METTL3 stalls oogenesis and greatly reduces the number of mature oocytes produced (Xia et al., 2018). In mice, loss of METTL3 early in murine oogenesis results in complete sterility and abnormal ovary morphology, while later absence of METTL3 causes failure of meiosis I and stalls oocyte maturation in the GV stage, again leading to sterility (Lasman et al., 2020a). Deletion of METTL3 specifically at the GV stage causes major transcriptomic defects, and interferes with both translational efficiency and maternal transcript degradation (Lasman et al., 2020a; Sui et al., 2020). In *Drosophila*, hypomorphs of the METTL3 homolog IME4 exhibit oogenesis defects, which cannot be rescued by a catalytic dead IME4, indicating that the methylase activity is required for oogenesis (Hongay and Orr-Weaver, 2011). KIAA1429 is also required for oocyte competence in mice, where oocyte specific deficiency disrupts maturation of the ovarian follicle, a shell of somatic cells surrounding the immature oocyte (Hu et al., 2020). These defects may stem from abnormal RNA processing and splicing, as co-localization between YTHDC1, SRSF3, and KIAA1429 to nuclear speckles is impaired in the mutants (Hu et al., 2020). YTHDC1 is also required for oogenesis, and absence of this reader blocks oocyte growth at the primary follicle stage (Kasowitz et al., 2018). This is likely due to disruptions of alternative polyadenylation and splicing, which cannot be rescued by an m^6A-

binding-deficient YTHDC1 (Kasowitz et al., 2018). These studies demonstrate that RNA methylation is essential to regulate maternal transcriptome assembly and secure oogenic success.

Other m[6]A readers are also key mediators of oogenesis. In mice, YTHDF2 is required for oocyte maturation and the wave of maternal RNA degradation that establishes the meiosis II transcriptome (Ivanova et al., 2017). Loss of YTHDF2-dependent changes in transcript abundance causes oocyte incompetence, female specific infertility, and failure of early zygotic development (Ivanova et al., 2017; Lasman et al., 2020a). Similarly, the MZT stalls in zebrafish YTHDF2 mutants, potentially due to delayed maternal mRNA clearance, although the extent to which this relies on methylation remains unclear (Kontur and Giraldez, 2017; Zhao et al., 2017). YTHDF1 and YTHDF3 knockouts have no impact on murine oogenesis, likely because they are not highly expressed in the developing oocytes (Lasman et al., 2020a), although YTHDF1 is required for female germline stem cell self-renewal in mice (Zhao et al., 2021). The IGF2BPs are also enriched in mouse and zebrafish ovaries, where they are important for germline development and embryogenesis, although dependence on m[6]A for these IGF2BP functions has not been demonstrated (Liu et al., 2019; Ren et al., 2020; Vong et al., 2020).

YTHDC2 is also pivotal for oogenesis in mice, and knockouts have smaller ovaries, loss of germinal vesicles, and infertility, likely due to transcriptome misregulation (Bailey et al., 2017; Hsu et al., 2017; Wojtas et al., 2017). Thus, the timing of reader mutant phenotypes in oogenesis correlates with the readers molecular activities. The YTHDFs impact late oocyte maturation when transcription has ceased and posttranscriptional regulation dominants. Alternatively, the YTHDCs phenocopy loss of the writers, reflecting an earlier role in oogenesis when transcription and m[6]A addition are still ongoing. Together, these studies uncover significant contributions of RNA

methylation, its writer, and its readers in ensuring proper maternal transcriptome establishment and successful oocyte generation across organisms.

1.3.3. RNA methylation and embryogenesis

Embryogenesis is the process through which multiple cell fate decisions guide an embryo to differentiate and create the complex tissues and organs required for life. Because embryogenesis parallels stem cell differentiation, development of the zygote relies on many of the same regulatory pathways to control transcript fate. Thus, it is unsurprising that RNA methylation is an essential mediator of embryogenesis.

Across organisms, loss of the methyltransferase is embryonic lethal, including in mice (Geula et al., 2015; Meng et al., 2019), flies (Granadino et al., 1990; Hilfikert et al., 1995; Kan et al., 2017; Knuckles et al., 2018), zebrafish (Zhang et al., 2017a), pig (Cao et al., 2021), and plants (Bodi et al., 2012; Shen et al., 2016; Zhong et al., 2008). These dramatic phenotypes demonstrate that m^6A is required to regulate the intricate genetic programs driving embryogenesis. For example, blastocysts from mice lacking METTL3 develop normally through preimplantation, after which they exhibit developmental defects (Batista et al., 2014; Geula et al., 2015; Wang et al., 2014b). Transcriptome analyses of these mutant embryos show that pluripotency factors, like *Nanog*, *Sox2*, and *Klf4* lose methylation and have sustained expression, preventing the blastocyst from exiting pluripotency and differentiating (Batista et al., 2014; Geula et al., 2015). Similarly, ablation of METTL14 traps mouse embryos in naïve pluripotency and leads to embryonic arrest, again due to transcriptome dysregulation (Meng et al., 2019; Wang et al., 2018). Also is mice, ZC3H13 is required for embryonic stem cell self-renewal (Wen et al., 2018), RBM15 knockouts

are lethal (Raffel et al., 2009), and WTAP is required for mesoderm and endoderm differentiation, although this last phenotype is not yet linked specifically to methylation (Fukusumi et al., 2008).

Readers of methylation are also important in embryogenesis, though the degree of their impact varies for each reader and across organisms. For instance, in mice, YTHDC2 is dispensable for viability (Bailey et al., 2017; Hsu et al., 2017; Wojtas et al., 2017), but YTHDC1 deletion is embryonic lethal, likely because DC1 influences transcript splicing and export (Kasowitz et al., 2018). hnRNPA2/B1 is also required for early embryonic development in mice, as its knockdown arrests post-implantation embryo growth, likely due to decreased expression of pluripotency markers (Kwon et al., 2019).

Other readers, like YTHDF2, have a more mild impact on embryogenesis, potentially reflecting overlapping functions of the YTHDFs during embryogenesis. For example, in mice, maternal YTHDF2 is required for development past the 2-cell stage, but zygotic-only mutants are viable (Ivanova et al., 2017), although recovered at lower rates (Lasman et al., 2020a; Li et al., 2018). These YTHDF2 mutant mice exhibit defects in cortical development, arising from impaired neural stem/progenitor cell differentiation, indicating that DF2 reader function is necessary to properly execute neurogenesis (Li et al., 2018). In zebrafish, maternal-zygotic YTHDF2 mutants fully progress through embryogenesis into adulthood, indicating that this reader is not absolutely required for their development (Zhang et al., 2017a; Zhao et al., 2017).

Yet, triple YTHDF loss of function recapitulates METTL3 deletion phenotypes, and fully arrests embryonic growth (Lasman et al., 2020a). The YTHDF readers seem to control embryogenesis via a dosage dependent mechanism, as lack of YTHDF1 or YTHDF3 can be compensated by the remaining two readers (Lasman et al., 2020a). YTHDF2 may play a central role in maintaining viability, as its absence cannot be fully compensated, likely owing to its higher

expression level (Lasman et al., 2020a) Together, this suggests that the YTHDF readers exert overlapping activities during early development, and a specific threshold of their function must be met for embryogenesis to proceed.

Finally, the IGF2BPs have been proposed as critical regulators of maternal transcript stability in early embryogenesis (Hansen et al., 2004; Huang et al., 2018; Ren et al., 2020). IGF2BP1 knockdown reduces global methylation levels and hinders embryogenesis in parthenogenically activated mouse embryos (Hao et al., 2020). Similarly, IGF2BP2 knockout mouse embryos arrest at the 2-cell stage, but whether these phenotypes are linked to regulation of m^6A is unclear (Liu et al., 2019). In zebrafish, IGF2BP3 mutants are non-viable and have ectopic and reduced primordial germ cell development, suggesting that IGF2BPs are mandatory for embryogenesis across vertebrates (Vong et al., 2020). Together, these studies of RNA methylation and its regulatory factors demonstrate the importance of m^6A in controlling transcriptome changes during embryonic differentiation.

1.3.4. RNA methylation and the YTHDF readers role in the maternal-to-zygotic transition

The maternal-to-zygotic transition (MZT) is an essential first step in embryogenesis, in which developmental control is passed from the mother to the zygote through activation of the zygotic genome and clearance of the established maternal transcriptome (Vastenhouw et al., 2019). RNA methylation, its writers, and its readers are key contributors to posttranscriptional gene expression changes during the MZT. For instance, METTL3 depletion in parthenogenically activated mouse embryos impedes transcriptional activation and maternal mRNA degradation, and deters embryogenesis in the 2-cell stage (Sui et al., 2020).

The IGF2BPs are also proposed regulators of the MZT, through transcript upregulation in both mice and zebrafish (Liu et al., 2019; Ren et al., 2020). In mice, loss of IGF2BP2 reduces transcription of factors involved in developmental competence, and arrests embryos around the onset of ZGA (Liu et al., 2019). In zebrafish, IGF2BP3 is suggested to promote maternal transcript stability (Ren et al., 2020). Loss of IGF2BP3 impairs development as early as the 8-cell stage, potentially due to premature maternal clearance (Ren et al., 2020). It remains unclear how the IGF2BPs distinguish select methylated mRNAs for stabilization while the decay-inducing YTHDF readers are simultaneously active.

Finally, the reader YTHDF2 facilitates the MZT. In mice, YTHDF2 ablation blocks MZT progression, likely because of improper maternal transcript dosage (Ivanova et al., 2017). In goat, YTHDF2 mutants cannot develop past the 2-cell stage, exhibit abnormal abundances of maternal and zygotic transcripts, and have reduced expression of deadenylase and decapping machinery needed for clearance (Deng et al., 2020). In the zebrafish MZT, maternal mutants of YTHDF2 exhibit a lag in development, which was posited to result from a corresponding delay in maternal mRNA clearance and inhibition of zygotic genome activation (Zhao et al., 2017). Together, these studies illustrate the importance of RNA methylation and its effectors in transcriptome switching during the MZT. Yet, this work also raises several major questions regarding the roles of each factor and the mechanisms underlying m^{6}A-dependent gene expression changes.

First, as many of these factors are also required in oocyte maturation (Ivanova et al., 2017; Liu et al., 2019; Sui et al., 2020), it is unknown if impaired MZT in these m^{6}A mutants arises from failure to establish the maternal transcriptome versus an inability to clear maternal mRNAs. Further, absence of these proteins often results in both increased and decreased mRNA expression, convoluting the direct impact of these methylation effectors on transcript fate during the MZT.

Carefully controlled analyses are required to better dissect the origins of transcriptome changes upon loss of m^{6}A function.

Second, the extent to which writer or reader phenotypes depends on methylation is unknown. Most studies present the broad impact of methylation mutants on the maternal or zygotic transcriptome without assessing consequences on the pool of endogenously modified mRNAs. Indeed, misregulated mRNAs in zebrafish and mouse YTHDF2 mutants are both methylated and unmethylated (Ivanova et al., 2017; Zhao et al., 2017), suggesting that either disrupted gene expression resulted indirectly from loss of YTHDF2, or that YTHDF2 exerts a regulatory function independent of m^{6}A. The consequences of m^{6}A-mediator absence on methylated transcripts must be specifically and separately addressed.

Third, it is unclear if m^{6}A-dependent defects in maternal mRNA clearance subsequently impede ZGA, if disrupted clearance is a consequence of delayed transcriptional activation, or if methylation independently impacts both processes. For instance, although m^{6}A predominantly drives decay, it is known to globally promote translation (Wang et al., 2015b). In the context of the MZT, m^{6}A could boost translation of key activators of zygotic transcription. In the case of zebrafish YTHDF2 mutants, it is noted that many transcripts dependent on DF2 are also targets of the zygotically supplied microRNA, miR-430 (Zhao et al., 2017). Delayed ZGA would reduce miR-430 abundance, thus causing a lag in maternal clearance that could be misattributed to loss of YTHDF2 (Kontur and Giraldez, 2017). The role of methylation in maternal mRNA clearance versus zygotic genome awakening must be carefully dissected.

Fourth, while many studies revolve around YTHDF2, the impact of the other YTHDF proteins is frequently ignored. Given that these factors can function redundantly (Lasman et al., 2020a; Zaccara and Jaffrey, 2020), a thorough assessment of reader function is necessary to

comprehensively understand how methylation guides transcriptome turnover during the MZT. For instance, in goat, YTHDF1 and YTHDF3 exhibit dramatically higher expression than YTHDF2, but are neglected for mutagenesis (Deng et al., 2020). In zebrafish, 2,653 methylated transcripts are unaffected by loss of DF2, suggesting that other factors compensate to clear these maternal messages (Kontur and Giraldez, 2017). Characterizing how all of the YTHDF factors contribute to maternal mRNA decay during the MZT is essential to fully comprehend m^6A-dependent control of gene expression during this foundational developmental event.

CHAPTER 2: RNA methylation regulates maternal mRNAs in early embryogenesis

In early embryogenesis, animal development is initially dictated by maternally inherited gene products (Laver et al., 2015; Wagner et al., 2004). During the maternal-to-zygotic transition (MZT), developmental control shifts to the zygote through massive remodeling of the mRNA landscape, characterized by the awakening of the zygotic genome and clearance of maternal mRNAs and proteins (Lee et al., 2014; Tadros and Lipshitz, 2009; Vastenhouw et al., 2019; Yartseva and Giraldez, 2015). Removal of these maternal mRNAs is essential for transcriptome reprogramming during the MZT and thus a host of posttranscriptional decay mechanisms contribute to maternal clearance (DeRenzo and Seydoux, 2004; Despic and Neugebauer, 2018; Stitzel and Seydoux, 2007; Tadros and Lipshitz, 2009; Yartseva and Giraldez, 2015). Yet, the impact of RNA m^6A methylation, a known regulator of decay, on the degradation of maternal transcripts remains undefined.

Herein, I explored the role of the RNA modification m^6A on maternal mRNA clearance during the MZT. Using zebrafish embryos as a model organism, I characterized m^6A as a facilitator of maternal transcript deadenylation, decay, and translation. I identified m^6A-mediated clearance as a component of the zygotic mode of decay, and uncovered combinatorial regulation between m^6A and the microRNA miR-430, revealing interplay between these distinct pathways of transcript turnover.

Chang et al., 2018 and Subtelny et al., 2014. mRNA-sequencing in the MZdicer and LNA conditions was performed by Minsun Jeong, and mRNA-sequencing in the dominant negative Caf1 and Dcp2 conditions (unpublished data) was done by Carter Takacs.

2.1. RNA methylation promotes maternal mRNA deadenylation during the zebrafish MZT

2.1.1. m⁶A-containing maternal mRNAs are differentially deadenylated

Maternally deposited transcripts in the early embryo are known to contain m^6A modifications, suggesting that this mark may tag specific mRNAs for tailored regulation during the MZT (Aanes et al., 2019; Ivanova et al., 2017; Zhao et al., 2017). Yet, whether methylation dictates changes in maternal mRNA abundance has not been thoroughly addressed. Thus, I sought to establish the effects of m^6A on transcript stability directly, by examining how endogenously methylated mRNAs behave *in vivo* during the zebrafish MZT. To determine if m^6A primarily impacts maternal mRNA decay or deadenylation, I compared the stability and polyadenylation status of maternal mRNAs that were found to contain m^6A to a control set of mRNAs found to be unmodified, as detected by previously reported m^6A-sequencing in zebrafish embryos (Zhao et al., 2017). I observed that methylated transcripts were significantly more deadenylated than unmethylated ones when I analyzed the poly(A) tail lengths, which were determined from two previously published datasets in zebrafish embryos, PAL-seq (Subtelny et al., 2014) and TAIL-seq (Chang et al., 2018) (**Fig. 2.1.a**) ($P = 4.2e-08$; $P = 3.5e-03$, respectively, Mann-Whitney U test 6 hours post fertilization (hpf)). Differential deadenylation was observed for methylated mRNAs even upon controlling for transcript co-regulation by miR-430 (**Fig. 2.1.b**), which is also known to promote deadenylation (Bazzini et al., 2012; Giraldez et al., 2006). This data suggests that modification by m^6A drives poly(A) tail shortening during the MZT.
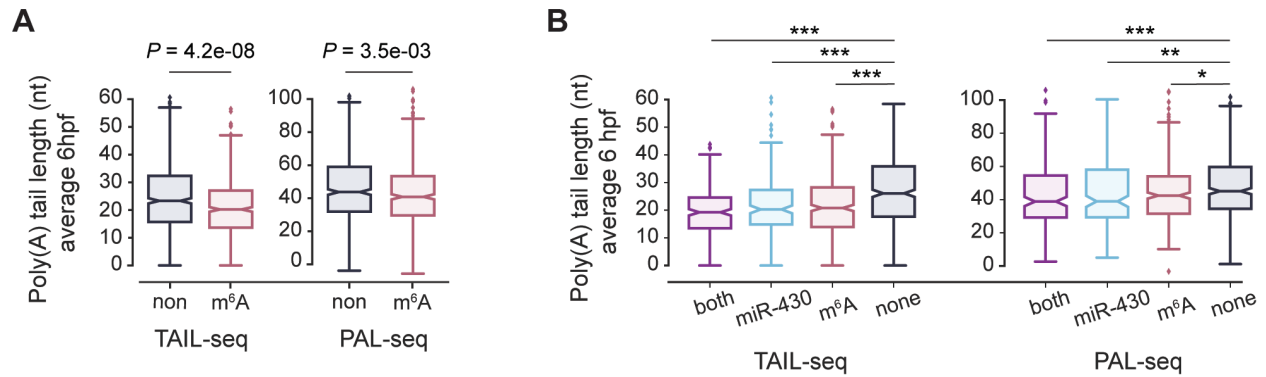
Figure 2.1. m⁶A methylation correlates with shorter poly(A) tails
(A) Correlation between m^{6}A RNA methylation and shorter average poly(A) tail length at 6 hpf for maternal m^{6}A-modified transcripts (m^{6}A, n = 675, pink) and non-modified transcripts (non, n = 841, grey) for both PAL-seq and TAIL-seq datasets. P-values were computed using a Mann-Whitney U test. Box, first to last quartiles; whiskers, 1.5x interquartile range; center line, median; diamonds, outliers.
(B) Average poly(A) tail lengths at 6 hpf for maternal mRNAs that were m^{6}A methylated (m^{6}A, n = 418, pink), contain a miR-430 seed (miR-430, n = 207, blue), have both methylation and a miR-430 seed (both, n = 229, purple), or contain neither (none, n = 519, grey) for both PAL-seq and TAIL-seq datasets. P-values were computed using a Mann-Whitney U test. * P < 0.05; ** P < 0.01; *** P < 0.001. Box, first to last quartiles; whiskers, 1.5x interquartile range; center line, median; diamonds, outliers.

2.1.2. m⁶A is associated with greater initial adenylation and greater deadenylation

Next, I analyzed changes in mRNA abundance from an mRNA-sequencing time course of zebrafish embryos (Vejnar et al., 2019), to determine if the shorter poly(A) tails observed for methylated mRNAs coincide with changes in transcript levels. I found that the abundance of endogenous methylated mRNAs was significantly decreased over time relative to controls in the poly(A)-selected (poly(A)) mRNA-sequencing (P = 7.7e-21, Mann-Whitney U test, 6 vs. 2 hpf) (**Fig. 2.2.a**). The differential effect of m^{6}A on transcript levels was less pronounced on mRNA decay than on deadenylation, as changes in total mRNA abundance were more similar for methylated and unmethylated transcripts in rRNA-depleted (ribo0) mRNA-sequencing (P = 9.6e-04, Mann-Whitney U test, 6 vs. 2 hpf) (**Fig. 2.2.b**).

To further assess the relative impact of methylation on maternal mRNA deadenylation and decay, I compared the ratio of poly(A) to ribo0 (p(A)/r0) mRNA abundances for methylated and non-methylated transcripts (**Fig 2.2.c**). The p(A)/r0 ratio was initially high for m^{6}A-modified mRNAs, but dramatically decreased over the course of the MZT, until the p(A)/r0 ratio of methylated transcripts fell below that of non-methylated transcripts at 6 hpf. This dynamic of m^{6}A-modified mRNAs suggests that methylated transcripts were initially more adenylated, but were also more actively deadenylated by 6 hpf than non-modified mRNAs. Conversely, the non-methylated transcripts exhibited a much lower p(A)/r0 ratio over time, reflecting a lower overall expression, less initial adenylation, and a less rapid rate of deadenylation relative to methylated transcripts.
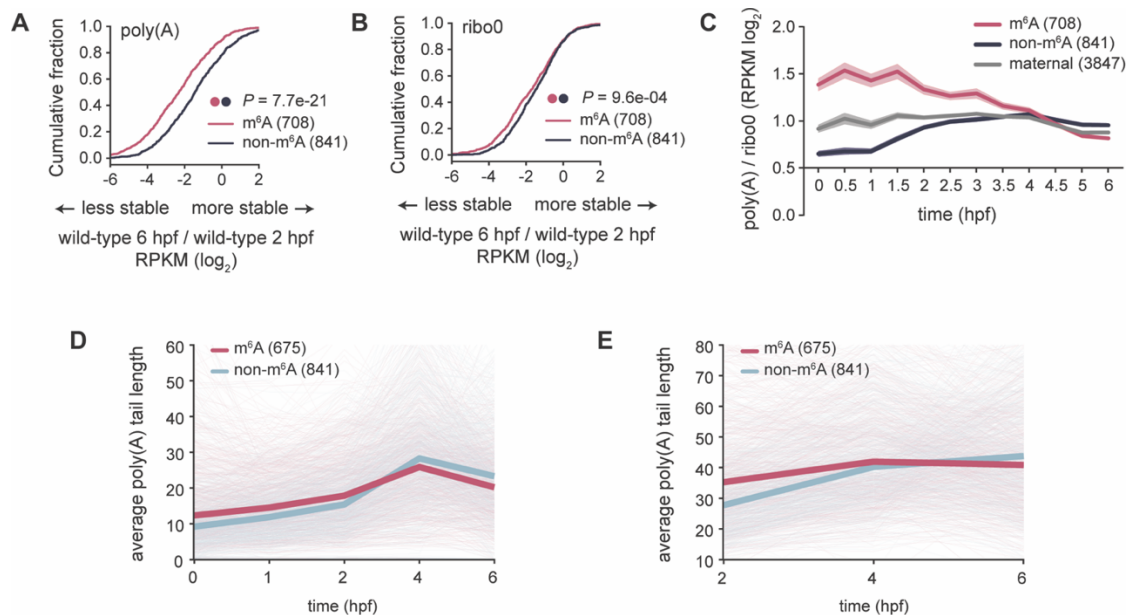
Figure 2.2. m^{6}A-containing maternal mRNAs start more adenylated but become less adenylated during the MZT

(A and B) Cumulative distributions of fold change in maternal mRNA abundance (log$_2$ RPKM) between 6 and 2 hpf in wild-type embryos, displaying decreased levels of m^{6}A-modified (red, $n = 708$) relative to non-modified transcripts (black, $n = 841$), from poly(A) (A) or ribo0 (B) mRNA-sequencing. *P*-values were computed using a Mann-Whitney U test.

(C) The ratio of poly(A) to ribo0 mRNA abundance (log$_2$ RPKM) at multiple time points (hpf) throughout the MZT for m^{6}A-modified (red, $n = 708$), non-modified (blue, $n = 841$), and all strictly maternal transcripts (grey, $n = 3847$).

(D and E) Average poly(A) tail length of individual maternal transcripts for m⁶A-modified transcripts (m⁶A, n = 675, maroon) and non-methylated mRNAs (non-m⁶A, n = 841, green) from either TAIL-seq (D) or PAL-seq (E) datasets. Solid lines represent mean value for all transcripts in each group. m⁶A-modified transcripts were significantly more adenylated at early time points, TAIL-seq (D): 0 hpf, P = 1.6e-15; 1 hpf, P = 1.1e-11; 2 hpf, P = 2.7e-06; PAL-seq (E): 2 hpf, P = 2.3e-17. At later time points, m⁶A-modified transcripts were significantly less adenylated than non-modified mRNAs; TAIL-seq (D): 4 hpf, P = 2.3e-03; 6 hpf, P = 4.2e-08. PAL-seq (E); 4 hpf, P = 0.11; 6 hpf, P = 3.5e-03. Differences between m⁶A-modified and non-modified transcripts were computed by Mann-Whitney U test.

I reasoned that this differential deadenylation of methylated mRNAs could arise from either stronger deadenylation by 6 hpf or from longer initial poly(A) tails, following the major wave of cytoplasmic polyadenylation that occurs in early embryogenesis (Chang et al., 2018; Subtelny et al., 2014; Ulitsky et al., 2012). To address this, I compared polyadenylation (Chang et al., 2018; Subtelny et al., 2014) at multiple time points throughout the MZT, which revealed that methylated mRNAs were more adenylated early at 0 and 2 hpf (P = 1.6e-15; P = 2.7e-06, respectively, from TAIL-seq, Mann-Whitney U test), and had significantly shorter tails at 6 hpf (average tail length of 21 vs. 25 nucleotides, m⁶A-modified and unmodified, respectively, P = 4.2e-08, from TAIL-seq, Mann-Whitney U test) (**Fig. 2.2.d-e**). This indicates that methylation is associated with greater initial adenylation, in accordance with previous findings (Aanes et al., 2019), and that it enhances later mRNA deadenylation, relative to unmodified mRNAs. Collectively, these analyses suggest that m⁶A promotes maternal mRNA deadenylation of its endogenous target transcripts during the MZT.

2.1.3. m⁶A-methylation promotes deadenylation and decay of reporter mRNA

To definitively determine if RNA methylation induces transcript deadenylation, I generated an mRNA reporter, made with or without m⁶A-modified nucleotides, but otherwise identical in sequence (**Fig. 2.3.a**). The reporter was designed without adenosines in the CDS, to

specifically test the effects of m^{6}A in the 3'UTR, because this region is highly linked to regulation of transcript stability (Charlesworth et al., 2013; Rabani et al., 2017; Semotok et al., 2005; Vejnar et al., 2019; Voeltz and Steitz, 1998) and is known to harbor m^{6}A modifications (Dominissini et al., 2012; Meyer et al., 2012). To test whether m^{6}A specifically drives tail shortening, I polyadenylated the reporters *in vitro*. Prior to injection, the incorporation of m^{6}A modification and poly(A) tail addition were validated using dot blot analysis and an RNase H assay with gel electrophoresis, respectively (**Fig. 2.3.b-c**). Reverse transcription followed by Sanger sequencing of the methylated reporter mRNA confirmed proper incorporation of m^{6}A only as specified by the plasmid sequence.

Upon injection of reporter mRNA into wild-type zebrafish embryos, I first observed enhanced deadenylation of the m^{6}A-modified reporter between 0 and 4 hpf relative to the unmodified mRNA. Second, I noted that the m^{6}A reporter exhibited greater degradation by 6 hpf than the unmethylated one (**Fig. 2.3.d**). Thus, m^{6}A both accelerated deadenylation and enhanced subsequent reporter mRNA degradation. This supports the finding that methylation contributes to maternal mRNA clearance by promoting maternal transcript deadenylation, and reveals that m^{6}A may also regulate mRNA decay.
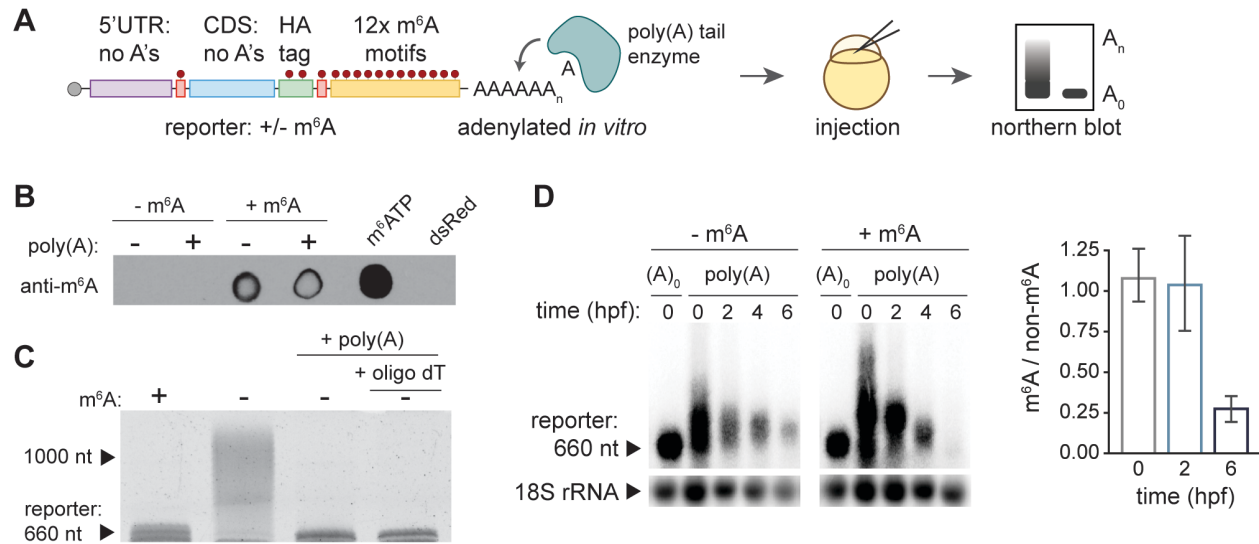
Figure 2.3. Validation and Northern blot analysis of methylated reporter mRNA

(A) Schematic of the methylated mRNA reporter assay. The capped mRNA reporter has a 5'UTR without adenines, AUG start codon, CDS without adenines, UAG stop codon, and 3'UTR with 12x repeats of the m^6A motif (GGACT). The reporter was *in vitro* transcribed either with or without m^6A-modified adenines, and then polyadenylated *in vitro* by the poly(A) tailing enzyme. Reporter mRNA was injected into embryos and mRNA abundance and polyadenylation were visualized by Northern blotting.

(B) Dot blot for m^6A demonstrates that methylated adenines were incorporated into the m^6A reporter but not the non-methylated reporter, for both polyadenylated and non-adenylated mRNAs. Unincorporated m^6-ATP nucleotides were included as a positive control and unmethylated dsRed mRNA was included as a negative control.

(**C**) RNase H assay and polyacrylamide gel electrophoresis validation of reporter (~660 nt) generation. The reporter, with (+) or without (-) methylation, and the adenylated reporter (+ poly(A)) were subjected to digestion with RNase H and run on a polyacrylamide gel to confirm that they were the expected size. To test for successful polyadenylation, one sample included oligo dT, to specifically digest away the poly(A) tail.

(D) Northern blot (left) showing rapid deadenylation and subsequent decay of m^6A-modified (+ m^6A) versus unmodified (- m^6A) reporter at respective timepoints (hpf) in untreated wild-type embryos. Internal 18S rRNA loading control (~1900 nt) shown along bottom. Ratio of methylated versus non-methylated reporter mRNA abundance (normalized to 18S rRNA) quantified from five replicates is shown on right. A_0, reporter injected without poly(A) tail.

To determine if the impact of m^6A extends to both deadenylation and decay, as indicated by the reporter assay, I assessed the abundance of methylated transcripts in two dominant negative (DM) conditions, where the catalytically inactive form a decay or deadenylation enzyme was overexpressed. These two enzymes are central components of key degradation pathways: Dcp2 is

part of the decapping machinery and Caf1 (also called Cnot7) is an exonuclease subunit of the Ccr4-Not deadenylase complex (Makino et al., 2015; Mishima and Tomari, 2016, 2017). To focus specifically on the consequences of m^{6}A modification, only transcripts that are not targets of miR-430 were included, as microRNAs often rely on the function of these enzymes to clear maternal transcripts (Bazzini et al., 2012; Giraldez et al., 2006). While abundance of almost all maternal transcripts increased in the a-amanitin, Dcp2-DM, and Caf1-DM conditions, methylated mRNAs were significantly, differentially more stabilized than non-methylated transcripts (**Fig. 2.4.**). This suggests that the m^{6}A modification may indeed rely on both decay and deadenylation pathways for its degradation. Together, these analyses indicate that m^{6}A methylation enhances maternal mRNA deadenylation and may also regulate mRNA decay, providing critical mechanistic insight into how m^{6}A specifies transcript life-times during the MZT.
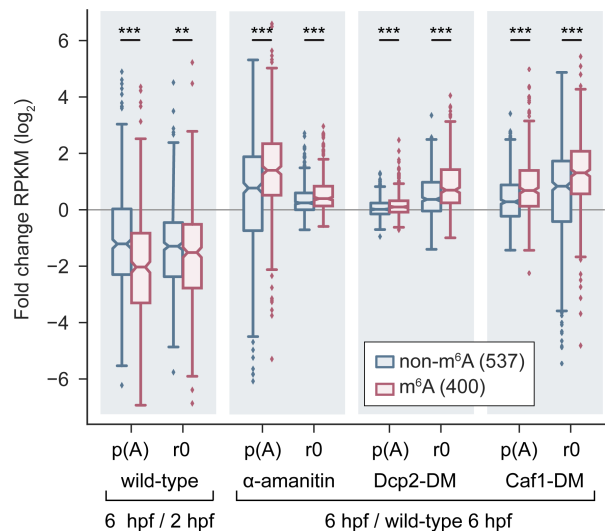
Figure 2.4. Methylated mRNA abundances in Caf1 and Dcp2 dominant-negative conditions Fold change (log$_2$ RPKM) of transcript abundance for maternal mRNAs that were either m^{6}A-modified (pink, n = 400) or not modified (blue, n = 537) from poly(A) (p(A)) or ribo0 (r0) mRNA-sequencing. Fold change in the wild-type condition (far left) represents 6 versus 2 hpf. Fold changes for treated embryos represent condition versus wild-type at 6 hpf. Wild-type p(A), P = 4.1e-14; wild-type r0, P = 1.1e-01; α-amanitin p(A), P = 3.8e-11; α-amanitin r0, P = 1.0e-07; Dcp2-DM p(A), P = 4.8e-06; Dcp2-DM r0, P = 1.0e-09; Caf1-DM p(A), P = 5.6e-11; Caf1-DM r0, P = 1.6e-09. P-values were computed using Mann-Whitney U test.

2.2. m⁶A-mediated maternal mRNA clearance depends on the zygotic program

It is unknown if elements of the RNA methylation pathway are part of the maternal or zygotic modes of gene expression. Considering the dramatic effect of methylation on maternal mRNA deadenylation, I sought to uncover whether this effect is mediated by maternally or zygotically encoded programs (Vejnar et al., 2019; Yartseva and Giraldez, 2015). I distinguished between these programs by blocking zygotic transcription with the RNA polymerase II inhibitor, α-amanitin (Kane et al., 1996; Lindell et al., 1970; Vejnar et al., 2019), which revealed that m⁶A-modified maternal mRNAs were differentially stabilized relative to unmethylated ($P = 3.2e\text{-}17$; $P = 1.7e\text{-}05$; Mann-Whitney U test, untreated vs. α-amanitin at 6 hpf, poly(A) and ribo0 mRNA, respectively) (**Fig. 2.5.a-b**).

miR-430 is a zygotically encoded factor that promotes maternal clearance and significantly overlaps target transcripts with m⁶A (see Section 2.3, below). It is conceivable that the observed differential stabilization of methylated transcripts could have arisen from loss of miR-430 expression upon inhibition of ZGA. To control for possible convolution from miR-430 repression, I divided methylated transcripts into those with a miR-430 seed in their 3'UTR and those without (**Fig. 2.5.c**). As anticipated, miR-430 only targets were differentially stabilized in α-amanitin conditions ($P = 1.0e\text{-}16$; Mann-Whitney U test, untreated vs. α-amanitin at 6 hpf, poly(A) mRNA). Yet, methylated mRNAs that are not recognized by miR-430 also increased in abundance compared to controls ($P = 9.5e\text{-}13$; Mann-Whitney U test), indicating that the m⁶A pathway was indeed differentially reliant on zygotic transcription for mRNA clearance. Transcripts controlled by both miR-430 and m⁶A were the most up-regulated relative to non-targets ($P = 1.6e\text{-}36$; Mann-Whitney U test), perhaps reflecting the combined dependence of these pathways on the zygotic

mode. Collectively, this analysis of endogenous maternal mRNAs in α-amanitin conditions shows that the zygotic mode contributes to m^{6}A-mediated transcript clearance.

Next, I tested if m^{6}A-based degradation depends on zygotic transcription, by injecting my methylated reporter into α-amanitin treated embryos. When zygotic transcription was blocked, I observed that the m^{6}A-modified reporter was no longer decayed at 6 hpf, but unmethylated reporter decay was unaffected (**Fig. 2.5.d**). This inhibition of m^{6}A mRNA decay suggests that methylated transcripts were more dependent on the zygotic program than unmethylated transcripts. Notably, α-amanitin treatment slowed but did not inhibit methylated reporter deadenylation between 0 and 6 hpf, suggesting that both maternal and zygotic pathways control m^{6}A-mediated tail shortening. Ultimately, these results indicate that a program dependent on zygotic transcription contributes to the degradation of methylation containing mRNAs, but that their deadenylation is regulated by both maternal and zygotic programs.
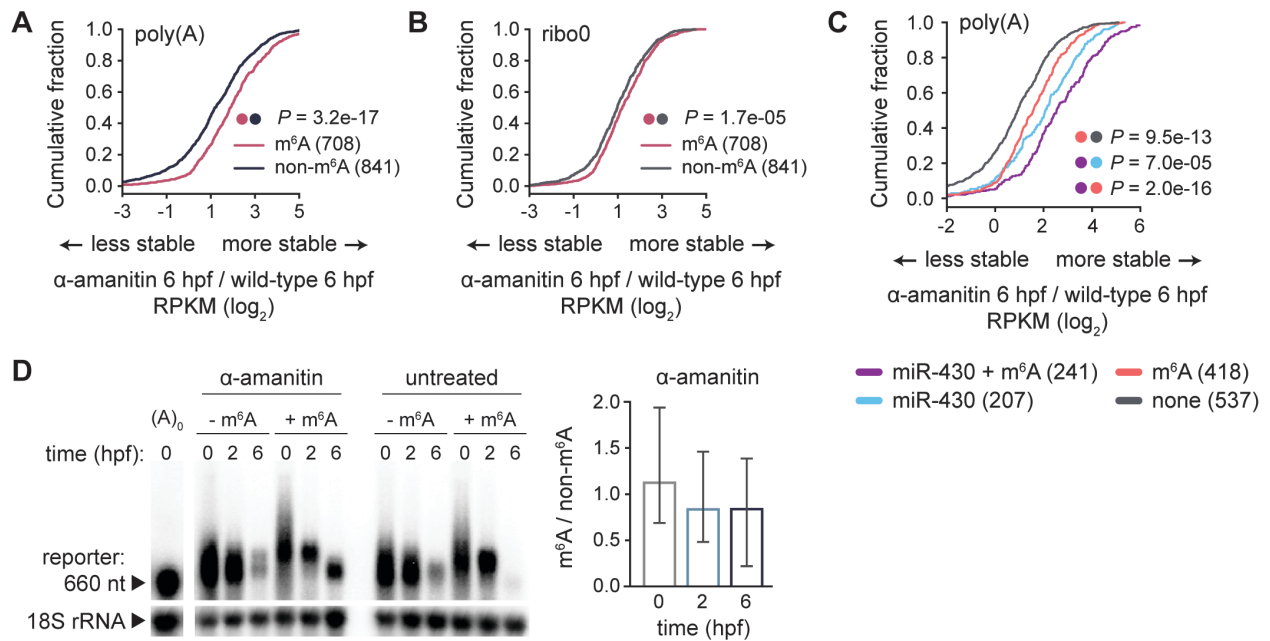
Figure 2.5. m^{6}A maternal mRNA clearance is differentially dependent on zygotic transcription
(**A and B**) Cumulative distributions of fold change in maternal mRNA abundance (log$_2$ RPKM) between α-amanitin treated and wild-type embryos at 6 hpf, displaying increased stabilization for m^{6}A-

modified (red, $n = 708$) relative to non-modified transcripts (black, $n = 841$), from poly(A) (A) or ribo0 (B) mRNA-sequencing. *P*-values were computed using a Mann-Whitney U test.

(**C**) Cumulative distribution of fold changes in maternal mRNA abundance ($\log_2$ RPKM) between α-amanitin treated and wild-type embryos at 6 hpf for poly(A) mRNA-sequencing. The combination of both m^6A-modification and a miR-430 seed in the 3'UTR (m^6A + miR-430, purple, $n = 241$) caused the greatest transcript stabilization. Transcripts that are miR-430 targets only (miR-430, blue, $n = 207$), or m^6A-modified only (m^6A, pink, $n = 418$), were less upregulated than co-target transcripts but were more stabilized than non-target mRNAs (none, grey, $n = 537$). Dots indicate which groups were compared to determine corresponding statistical significance. *P*-values were computed using a Mann-Whitney U test.

(**D**) Northern blot (left) comparing deadenylation and decay of m^6A-modified (+ m^6A) versus unmodified (- m^6A) reporter at respective timepoints (hpf) in α-amanitin and untreated embryos. Internal 18S rRNA loading control (~1900 nt) shown along bottom. Ratio of methylated versus non-methylated reporter mRNA abundance (normalized to 18S rRNA) for α-amanitin treated embryos quantified from three replicates is shown on right. A_0, reporter injected without poly(A) tail.

2.3. Methylation and miR-430 co-regulate maternal mRNAs

2.3.1. miR-430 and m^6A act independently and additively to regulate maternal transcript destabilization

Given that I have demonstrated that the RNA methylation pathway exhibits a dependence on the zygotic mode for transcript destabilization, I sought to establish whether a prominent zygotically encoded factor and known regulator of maternal clearance, miR-430 (Bazzini et al., 2012; Giraldez et al., 2006), is required to destabilize methylated maternal transcripts. Notably, I observed that more than a third of methylated maternal mRNAs also contain a miR-430 seed in their 3'UTR (**Fig. 2.6.a**), consistent with previous reports (Aanes et al., 2019; Zhao et al., 2017), and indicating that these pathways may attenuate stability of shared targets. Further, I observed a positive correlation between the strength of mir-430 seeds and the predicted number of m^6A modifications in maternal transcripts (**Fig. 2.6.c**), again reflecting potential co-regulation. I hypothesized that miR-430 and m^6A could act through several mechanisms to clear transcripts, functioning either cooperatively, resulting in a synergistic clearance of transcripts, independently,

wherein each mechanism separately contributes a certain degree of destabilization, or dependently, in which the activity of one pathway is dependent on the presence of the other (**Fig. 2.6.b**).
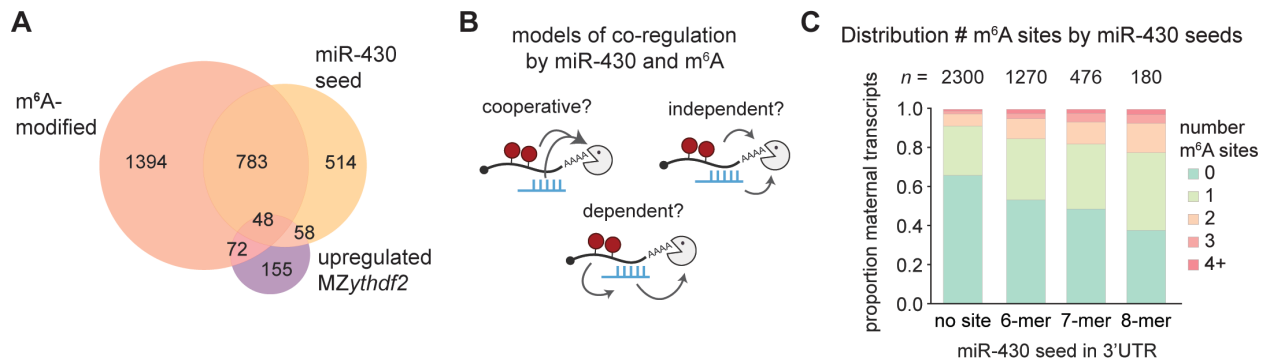
Figure 2.6. miR-430 and m⁶A pathways share common targets

(**A**) Venn diagram depicting numbers of maternal transcripts that contain a miR-430 seed in their 3'UTR, were m⁶A-modified, were stabilized in MZ*ythdf2* mutants (fold change (log₂ RPKM) > 0.5) or have an overlapping set of these features. More transcripts were both methylated and targets of miR-430, than were both methylated and stabilized in MZ*ythdf2*.

(**B**) Schematic of potential mechanistic models by which miR-430 and m⁶A could co-regulate maternal transcripts, tested in Figure 2.7. These pathways could function cooperatively, causing enhanced decay of common targets, behave independently, meaning their effects would act additively on common targets, or m⁶A could be dependent on miR-430, meaning loss of miR-430 would disrupt m⁶A-based mRNA degradation.

(**C**) Stacked bar plot displaying the proportion of maternal transcripts with a given number of predicted m⁶A sites, based on the strength of the miR-430 seed also present in the transcript. 8-mer corresponds to the strongest miR-430 site, followed by 7-mer, then 6-mer, and no-site denotes transcripts that are not targets of miR-430. The total number of transcripts with each miR-430 seed (*n*) is presented at the top of each bar.

To disentangle these possible roles of m⁶A and miR-430, I first compared the abundance of transcripts that contained m⁶A marks, miR-430 seeds, both, or neither during the MZT. mRNAs containing both m⁶A sites and miR-430 seeds were the most degraded, followed sequentially by miR-430 only targets, methylation-only mRNAs, and non-targets (6 vs. 2 hpf in wild-type embryos, poly(A) and ribo0 mRNA) (**Fig. 2.7.a-b**). I noted that the effects of m⁶A and miR-430 were greater in the poly(A) mRNA-sequencing, as changes in poly(A) mRNA abundance may reflect enhanced deadenylation driven by m⁶A and miR-430 (Bazzini et al., 2012; Giraldez et al., 2006), combined with their effects on transcript destabilization. Further, I found that loss of miR-

430 affected the abundance only of its cognate mRNAs and did obstruct turnover of methylation-only mRNAs, when I compared wild-type and MZ*dicer* or anti-sense LNA treated embryos (**Fig. 2.7.c-d**). Together, this suggests that m^{6}A drives mRNA deadenylation independently of miR-430, as observed in my poly(A) tail analysis (**Fig. 2.1.b**), and that these mechanisms function additively to co-regulate a subset of maternal mRNAs for stronger degradation. Thus, while miR-430 is not required for m^{6}A-mediated mRNA decay, it functions as an independent pathway to regulate their fate, acting combinatorially alongside methylation to co-regulate a subset of highly degraded targets.
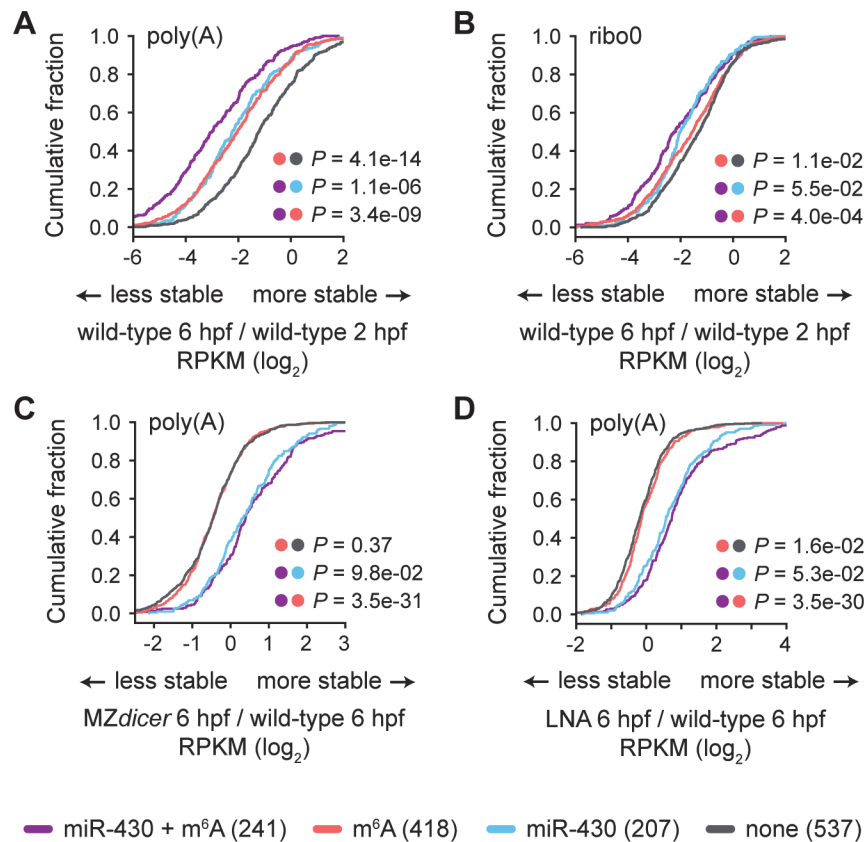
Figure 2.7. miR-430 and m^{6}A pathways are independent and additively regulate maternal transcripts for destabilization
(**A and B**) Cumulative distributions of fold changes in maternal mRNA abundance (log$_2$ RPKM) between 6 and 2 hpf in wild-type embryos, for poly(A) (A) or ribo0 (B) mRNA-sequencing, the combination of both m^{6}A-modification and a miR-430 seed in the 3'UTR (m^{6}A + miR-430, purple, *n* = 241) caused the greatest transcript destabilization. Transcripts that are miR-430 targets only (miR-

430 only, blue, $n = 207$), or m[6]A-modified only (m[6]A only, pink, $n = 418$), were less degraded than co-target transcripts but were more destabilized than non-target mRNAs (none, grey, $n = 537$).

(**C and D**) Cumulative distributions of fold changes in maternal mRNA abundance (log$_2$ RPKM) at 6 hpf between MZ*dicer* (C) or LNA-treated (D) embryos, which both lack functional miR-430, relative to wild-type, from poly(A) mRNA-sequencing. Only transcripts that are miR-430 targets (purple and blue) were stabilized in MZ*dicer* or LNA-treated embryos, regardless of m[6]A-modification, while m[6]A-modified targets (pink) were unaffected by loss of miR-430, relative to non-targets (grey).

For (A-D): transcripts in each group and corresponding labels are the same, and are presented in the legend along the bottom. Colored dots indicate which groups were compared to determine corresponding statistical significance. *P*-values were computed using a Mann-Whitney U test.

2.3.2. Ythdf3 is regulated by miR-430

miRNAs are known to target the Ythdf m[6]A readers to modulate their expression, and consequently, the extent of m[6]A function (Li et al., 2020; Yang et al., 2017b). I noticed that the mRNA expression of the reader *ythdf3* dramatically decreased around 4 hpf (**Fig. 2.8.a**, poly(A) and ribo0 mRNA), by which ZGA is majorly underway, and miR-430 is highly expressed. Examination of the *ythdf3* transcript revealed two miR-430 seed sequences within the 3'UTR (**Fig. 2.8.c**), suggesting that *ythdf3* transcript levels are controlled by miR-430. Indeed, western blot analysis revealed that Ythdf3 protein expression increased in MZ*miR-430* mutant embryos (Liu et al., 2013) relative to wild-type controls (**Fig. 2.8.b**). Although the effects of miR-430 inhibition on *ythdf3* mRNA levels remain unclear, this protein analysis suggests that loss of miR-430 function impaired *ythdf3* clearance. miR-430 regulation of Ythdf3 implies a possible feedback mechanism to control the balance or timing of methylated mRNA decay. Notably, *ythdf2* transcription increases at the same time that *ythdf3* levels decrease, revealing potential means through which the embryo modulates Ythdf reader dosage via miR-430 to ensure the proper degree of m[6]A-driven regulation. Future work should address the mechanism through which this miR-430 down-regulation of *ythdf3* is achieved.
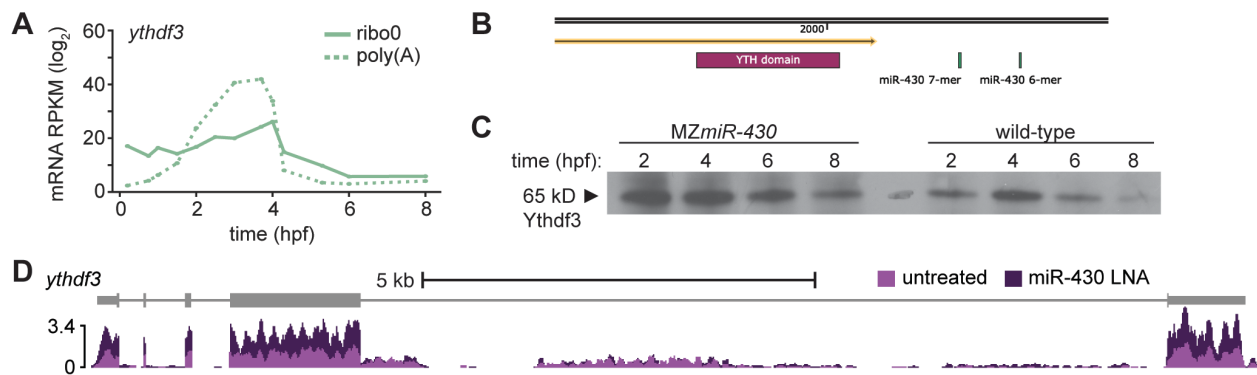
Figure 2.8. Ythdf3 is a miR-430 target
(**A**) *ythdf3* mRNA expression (log$_2$ RPKM) during the MZT, from poly(A) (dashed line) and ribo0 (solid line) mRNA-sequencing, displaying a dramatic drop in expression around 4 hpf.
(**B**) *ythdf3* mRNA transcript contains two miR-430 seed sequences in the 3'UTR (green bars). The yellow arrow indicates the end of the CDS, which contains the YTH domain (maroon).
(**C**) Western blot of Ythdf3 protein expression during the MZT (time, hpf) in MZ*miR-430* mutant embryos and wild-type controls.
(**D**) Genome tracks at 6 hpf of increased *ythdf3* poly(A) mRNA abundance in LNA-treated embryos (dark purple) relative to untreated embryos (light purple).

2.4. m⁶A influences maternal mRNA translation

During the MZT, there is a direct correlation between maternal transcript poly(A) tail length and translation (Vastenhouw et al., 2019). Given that m^{6}A modification correlates with higher initial polyadenylation and greater deadenylation (section 2.1.), I sought to determine if methylation also influences maternal mRNA translation. To achieve this, I compared global differences in translation efficiency between methylated and non-methylated mRNAs. Because the expression levels of modified and unmodified transcripts varies dramatically (**Fig. 2.9.a**), and expression is a major determinant of translation levels, I stratified transcripts by their abundance (ribo0 mRNA) at 2 hpf. Comparison of global translation revealed that m^{6}A marked maternal mRNAs were significantly more efficiently translated at 2 hpf than unmarked ones, for all expression levels (**Fig. 2.9.b**). Yet, this differential translation largely disappeared by 6 hpf,

perhaps because the majority of methylated transcripts were being cleared by this time point and were no longer available for translation (**Fig. 2.9.c**). Overall, this analysis suggests that m^6A modification promotes maternal transcript translation early in the MZT, although the extent to which this is linked to poly(A) tail regulation should be further tested.
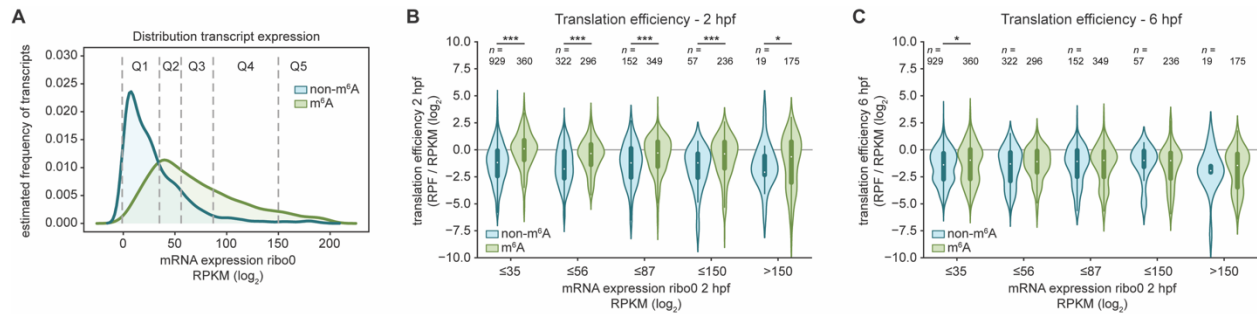
Figure 2.9. m^6A correlates with increased translation efficiency in the early MZT
(**A**) Kernel density estimate plot of methylated (m^6A, green, $n = 4832$) and non-methylated (non-m^6A, blue, $n = 3667$) maternal transcripts, displaying relative frequency of transcripts with a given mRNA expression level from ribo0 mRNA-sequencing. To control for differences in expression in (B-C), transcripts were binned into quintiles (Q1-Q5), with roughly equal numbers of methylated transcripts in each bin.
(**B-C**) Violin plots comparing translation efficiency (RPF / RPKM ribo0 mRNA (log_2)) of methylated (m^6A, green) and non-methylated (non-m^6A, blue) maternal transcripts at 2 hpf. Transcripts were binned into quintiles according to mRNA abundance (log_2 RPKM) from ribo0 mRNA-sequencing shown in (A). Expression cutoffs for each bin are shown on the x-axis and the number of transcripts in each bin (n) is presented along the top. P-values correspond to comparison of m^6A-modified (m^6A, green) and non-modified transcripts (non-m^6A, blue) for each bin, computed by a Mann-Whitney U test; *** $P < 0.001$; * $P < 0.05$.

CHAPTER 3: Ythdf reader regulation of the maternal transcriptome during the MZT

The functional consequences of m^{6}A modification on gene expression are determined by the "reader" proteins, which interpret the mark and recruit regulatory effectors to the transcript. The YTH-domain containing family of readers is well characterized, as these proteins have the capacity to bind the modification directly and induce changes in mRNA splicing, export, localization, translation, and decay (Boo and Kim, 2020; Heck and Wilusz, 2019; Shi et al., 2019; Zaccara et al., 2019). All three Ythdfs in zebrafish have been identified as maternal mRNA binders through interactome capture experiments (Despic et al., 2017), suggesting that all three paralogs contribute to methylated maternal mRNA decay during the MZT. Yet, precisely how these Ythdfs impact m^{6}A-modified mRNA fate to promote transcriptome reprogramming remains unclear.

Recently, the Ythdf2 reader was linked to mRNA turnover during the MZT in zebrafish. In a study by Zhao et al. (2017), Ythdf2 mutants exhibited a developmental delay, which was posited to result from delayed maternal mRNA clearance and hindered zygotic genome activation. However, as only the global effect of Ythdf2 on all maternal mRNAs was addressed, how loss of Ythdf2 specifically impacts endogenously methylated mRNAs is yet to be determined. Further, both methylated and unmethylated mRNAs were misregulated in the Ythdf2 mutants, suggesting that either disrupted gene expression resulted indirectly from loss of Ythdf2 or that Ythdf2 exerts a regulatory function independent of m^{6}A. While work by Zhao et al. (2017) suggests an important role for Ythdf2 in the MZT, it remains unclear if the Ythdfs specifically guide methylated transcript decay and whether their activity is required for global transcriptome switching.

In this chapter, I disentangle the contributions of the Ythdf2 reader to methylated transcript stability, global maternal mRNA clearance, and zygotic transcription. Through generation and transcriptome analysis of individual Ythdf mutants I demonstrate that no single reader is required for m^{6}A-mediated mRNA degradation, although loss of Ythdf2 does minimally stabilize some modified transcripts. Together, this work demonstrates that the effects of m^{6}A on maternal mRNA deadenylation do not exclusively depend on Ythdf2, nor any other sole reader, overturning the model that Ythdf2 has a unique and essential function in maternal transcript clearance during the zebrafish MZT.

ATTRIBUTIONS
This chapter is modified from my first author paper published in December, 2020 in Cell Reports (Kontur et al., 2020), which I wrote with input from Antonio Giraldez. Data for the zebrafish developmental time course mRNA-sequencing was from Vejnar et al., 2019, Beaudoin et al., 2018, and Bazzini et al., 2016. m^{6}A-sequencing data was from Zhao et al., 2017 and Aanes et al., 2019 and ythdf2$^{\Delta8/\Delta8}$ mutants were obtained from Zhao et al., 2017.

3.1. m^{6}A writer, eraser, and reader expression during the MZT

To identify which factors play a role in m^{6}A-mediated regulation of the maternal transcriptome, I first sought to determine which components of the methylation life cycle (Shi et al., 2019; Zaccara et al., 2019) were expressed during zebrafish embryogenesis. I examined mRNA abundances of transcripts encoding m^{6}A regulators during the MZT using the mRNA-sequencing time course (Vejnar et al., 2019, Beaudoin et al., 2018, and Bazzini et al., 2016), which yielded several intriguing observations regarding expression of m^{6}A writers, readers, and erasers.
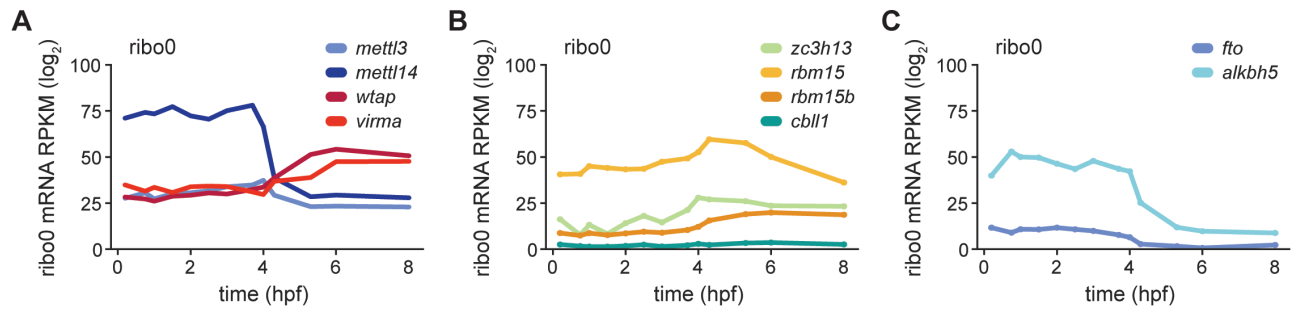
Figure 3.1. mRNA abundances of the m⁶A writers and erasers during the zebrafish MZT (**A-C**) mRNA levels (log$_2$ RPKM) of corresponding transcripts for components of the methyltransferase complex (A-B) and putative m⁶A erasers (C) from ribo0 mRNA-sequencing.

First, almost all components of the methyltransferase complex were maternally expressed (**Fig. 3.1.a-b**), including both core enzymes and cofactors, which guide writer specificity and activity (Garcias Morales and Reyes, 2021; Gu et al., 2021). *mettl14*, one half of the heterodimer catalyzing m⁶A addition (Liu et al., 2014; Wang et al., 2014b), exhibited especially high expression. Given that m⁶A is deposited co-transcriptionally (Ke et al., 2017), and the embryo is transcriptionally silent prior to ZGA, it will be exciting to determine the function of the writer complex prior to the onset of zygotic gene expression. Notably, most methyltransferase components increased in abundance after ZGA, around 4 hpf, suggesting that they will be required to methylate newly synthesized transcripts as development proceeds. Based on the observed high expression of *mettl14*, and the essential role of METTL3 and METTL14 in methylation and embryogenesis (Geula et al., 2015; Wang et al., 2014b), these enzymes were selected for mutagenesis.

Second, expression of both putative m⁶A erasers, *alkbh5* and *fto* decreased over the course of the MZT. While the activity of these proteins as demethylases is highly debated (Rajecka et al., 2019), their early expression pattern poses the intriguing possibility that some maternal transcripts could be regulated by demethylation prior to ZGA.

Third, all three *ythdf* readers and both *ythdc* readers were maternally expressed (**Fig. 3.2.a**). *ythdf2* displayed the greatest abundance, and *ythdf2*, *ythdc1*, and *ythdf1* all increased in abundance following the onset of ZGA, indicating that they may have continued function in later development. Indeed, Ythdc1 is a largely nuclear protein, with functions in mRNA splicing and export (Patil et al., 2016; Roundtree et al., 2017b; Xiao et al., 2016), which may explain why it is required once zygotic transcription is underway. Conversely, expression of *ythdf3* and *ythdc2* largely decreased following ZGA, which for *ythdf3* can be explained through potential down-regulation by miR-430 (see section 2.3.2.). Ythdc2 has been linked to mRNA degradation through its interaction with the 5'-3' exoribonuclease Xrn1 (Wojtas et al., 2017) and is also known to regulate translation (Mao et al., 2019), but is believed to largely function in germ cells and reproductive organs (Bailey et al., 2017; Hsu et al., 2017; Jain et al., 2018; Wojtas et al., 2017). Whether Ythdc2 exerts these regulatory functions in this developmental context is unexplored. Although the expression patterns of all Yth readers implied functionality during early embryogenesis, I opted to limit my mutagenesis approach to the Ythdf readers, as they are most strongly linked to cytoplasmic regulation (Patil et al., 2018; Zaccara et al., 2019). To confirm that the Ythdf proteins were maternally supplied alongside the mRNA, I performed western blot analysis for the Ythdfs, which revealed that all three proteins were indeed maternally deposited and expressed throughout the MZT (**Fig. 3.2.b**). Finally, while many other potential m^{6}A readers have been identified (An et al., 2020; Arguello et al., 2017; Edupuganti et al., 2017; Huang et al., 2018; Meyer et al., 2015), their assessment is beyond the scope of the work presented here. Exploration of these additional m^{6}A effectors will likely yield fruitful insights into the role of methylation in maternal transcriptome regulation.
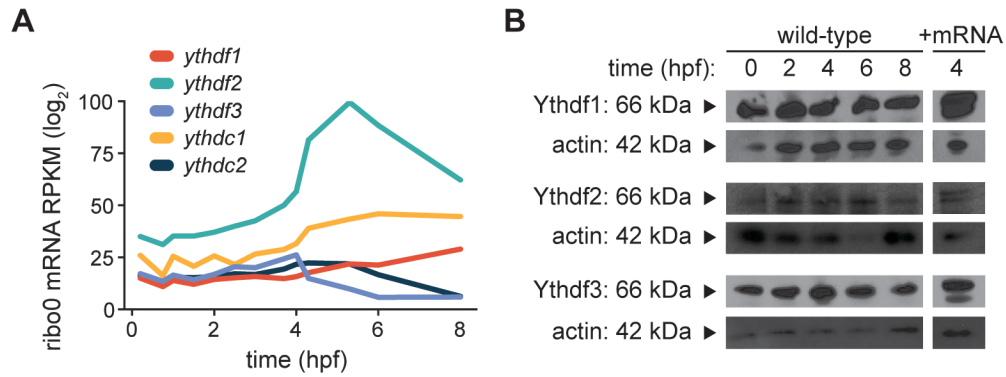
Figure 3.2. mRNA and protein levels of the YTH m⁶A readers during the zebrafish MZT
(**A**) *ythdf1*, *ythdf2*, *ythdf3*, *ythdc1*, and *ythdc2* transcripts were all maternally expressed ($\log_2$ RPKM) during the MZT, from ribo0 mRNA-sequencing.
(**B**) Western blotting shows that Ythdf1, Ythdf2, and Ythdf3 proteins were all maternally deposited (0 hpf) and expressed throughout the MZT in wild-type embryos. Injection of respective flag-tagged *ythdf* mRNAs served as positive controls (+mRNA). Actin levels were measured from immunoprecipitation inputs as loading controls.

3.2. Role of Ythdf readers in methylated mRNA clearance

3.2.1. Ythdf2 is not mandatory for global maternal mRNA clearance

To determine whether the Ythdf readers control m⁶A-mediated mRNA clearance during the zebrafish MZT, I first looked at the role of Ythdf2, as it had the highest maternal expression (**Fig. 3.2.a**) and has been extensively linked to the regulation of transcript decay (Du et al., 2016; Wang et al., 2014a; Yoon et al., 2017; Zhao et al., 2017). To determine if Ythdf2 is sufficient to drive m⁶A-mediated maternal mRNA turnover, I performed poly(A) mRNA-sequencing on maternal-zygotic (MZ) mutant embryos with the same Ythdf2 deletion allele as in Zhao et al. and on related, genetic background-matched wild-type controls (**Fig. 3.3.a**). Though Ythdf2 was reportedly required for maternal mRNA clearance, I found no significant differences in abundance for the majority of maternal mRNAs upon loss of Ythdf2 relative to controls, regardless of their methylation status (4 and 6 hpf, **Fig. 3.3.b-c**). Indeed, of 13642 maternally expressed genes, only

17 were found to be differentially expressed at either 4 or 6 hpf (determined by DESeq2 (Love et al., 2014); **Table 3.1.**), of which only 11 were stabilized and only 2 were predicted to be methylated. Thus, although Ythdf2 was proposed as a key regulator of maternal clearance, the fact that maternal transcripts were not majorly stabilized in MZ*ythdf2* mutants demonstrates that Ythdf2 is not obligatory for global maternal mRNA decay.
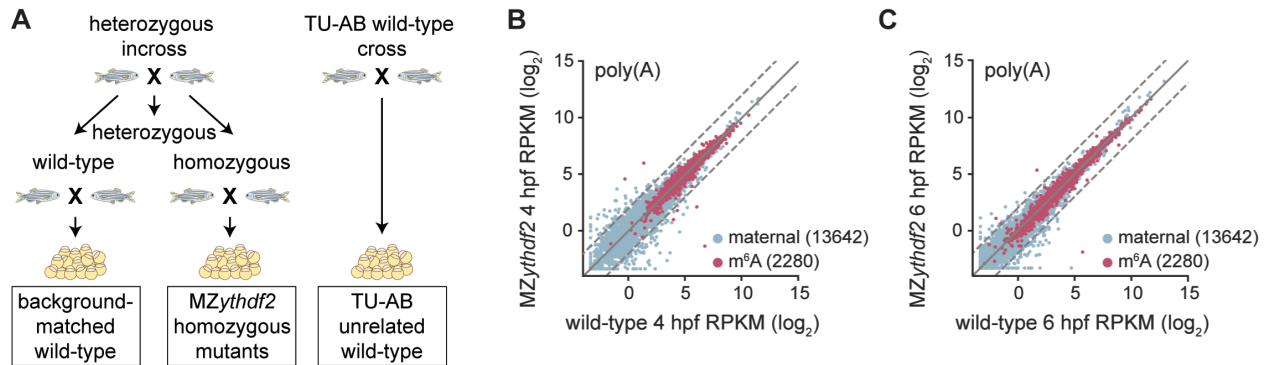
Figure 3.3. Loss of Ythdf2 does not disrupt global maternal mRNA levels
(A) Schematic of zebrafish crosses to generate MZ*ythdf2* and background-matched wild-type embryos. Sibling parents of wild-type or *ythdf2*^{-/-} homozygous genotype were incrossed to generate control and mutant embryos with matched backgrounds. Embryos from a cross of TU-AB strain zebrafish were included as an additional and unrelated wild-type control.
(B-C) Biplots of similar expression levels (log$_2$ RPKM) of maternal ($n = 13642$) and m^{6}A-modified maternal mRNAs ($n = 2280$) between background-matched wild-type and MZ*ythdf2* embryos at 4 hpf (B) or 6 hpf (C), from poly(A) mRNA. Dashed lines indicate two-fold change.

Table 3.1. Fold-changes and *P*-values for 17 differentially expressed maternal transcripts

gene ID	fold-change 4 hpf	*P*-value 4 hpf	fold-change 6 hpf	*P*-value 6 hpf	methylation status
ENSDARG00000002165	-2.8	1.0E-02	-1.96	9.0E-02	
ENSDARG00000005479	-1.86	2.0E-02	-0.86	n.s.	
ENSDARG00000014498	3.26	5.4E-13	1.23	n.s.	m^6A
ENSDARG00000017338	2.87	1.0E-02	1.63	n.s.	
ENSDARG00000024746	-1.09	n.s.	-2.01	4.0E-03	non-m^6A
ENSDARG00000037917	2.03	8.0E-03	1.45	n.s.	
ENSDARG00000052894	2.63	4.0E-02	0.47	n.s.	
ENSDARG00000054454	5.64	2.0E-03	0.46	n.s.	
ENSDARG00000061398	2.49	6.0E-02	0.1	n.s.	
ENSDARG00000071087	1.69	4.0E-03	-0.04	n.s.	non-m^6A
ENSDARG00000077712	-0.52	n.s.	-1.69	1.0E-03	
ENSDARG00000077740	5.59	6.1E-06	6.5	1.0E-03	
ENSDARG00000078016	2.99	8.0E-03	0.35	n.s.	
ENSDARG00000087937	-2.8	8.0E-03	-0.72	n.s.	non-m^6A
ENSDARG00000091111	0.21	n.s.	-1.38	8.0E-03	
ENSDARG00000091280	2.15	n.s.	3.79	1.2E-07	
ENSDARG00000094210	-2.05	4.0E-03	-0.65	n.s.	m^6A

Differential expression determined between time-matched MZ*ythdf2* and background-matched wild-type embryos at either 4 or 6 hpf in poly(A) mRNA-sequencing by DESeq2 (*P*-value < 0.05, corrected for multiple testing). n.s., not significant. No value for methylation status indicates unknown status.

3.2.2. Ythdf2 marginally contributes to m^6A-mediated clearance

As maternal transcript decay was largely unaffected in MZ*ythdf2* mutants, I next addressed how Ythdf2 specifically affects methylated mRNAs. When I compared the abundance of m^6A-modified and unmodified transcripts, methylated mRNAs were not differentially expressed at 4 hpf, but were marginally more stabilized in the MZ*ythdf2* mutants at 6 hpf, relative to controls (*P* = 0.16, 4 hpf; *P* = 4.4e-04, 6 hpf; Mann-Whitney U test) (**Fig. 3.4.a-b**). While this is consistent with a role for Ythdf2 in methylated mRNA decay, the stabilization of m^6A-mRNAs in MZ*ythdf2* mutants was negligible relative to the dramatic stabilization observed in the absence of other key decay regulators (6 hpf, **Fig. 3.4.c**). For instance, loss of miR-430 through antisense locked nucleic

acid (LNA) treatment, lead to an average 0.89-fold increase of target transcript abundance, while

the fold-change in MZ*ythdf2* mutants was only 0.05 for methylated mRNAs at 6 hpf. To further

assess the effects of Ythdf2 on m⁶A-mRNAs, I quantified abundance of several methylated

transcripts using qRT-PCR and visualized their expression by *in situ* hybridization. Loss of Ythdf2

did not significantly alter decay of either *zgc:162879* or *mtus1a*, both maternal, m⁶A-marked

transcripts, as levels were comparable to background-matched controls (**Fig. 3.4.d**). Conversely,

mtus1a, also a miR-430 target, was clearly stabilized in MZ*miR-430* mutants. Together, this data

shows that loss of Ythdf2 only nominally impedes methylated mRNA degradation, and that the

contributions of Ythdf2 to m⁶A-modified maternal transcript clearance are minimal relative to

established decay pathways.
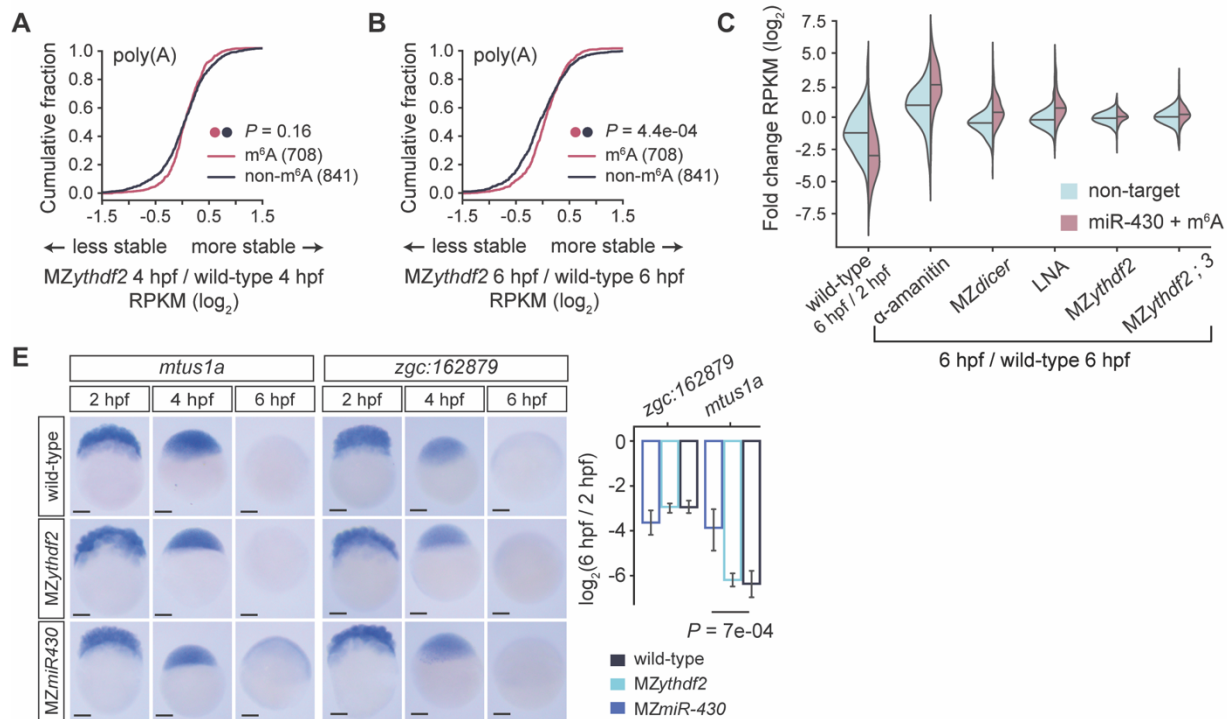
Figure 3.4. Loss of Ythdf2 marginally stabilizes methylated maternal mRNAs
(A-B) Cumulative distributions of fold change in maternal mRNA abundance (log₂ RPKM) between
MZ*ythdf2* and background-matched wild-type embryos at either 4 hpf (A) or 6 hpf (B), depicting slight
stabilization of m⁶A-modified (red, *n* = 708) relative to non-modified transcripts (black, *n* = 841), from
poly(A) mRNA. *P*-values were computed using a Mann-Whitney U test.

(G) Fold change ($\log_2$ RPKM) of transcript abundance for maternal mRNAs that were either m^{6}A-modified and contain a miR-430 seed (miR-430 + m^{6}A, $n = 241$) or were not modified nor miR-430 targets (non-target, $n = 537$). Fold change in wild-type condition represents 6 versus 2 hpf. Fold change for mutant or treated embryos represents condition versus wild-type (background-matched for MZ*ythdf2* mutants) at 6 hpf. Wild-type, $P = 1.1e\text{-}30$; a-amanitin, $P = 1.6e\text{-}36$; MZ*dicer*, $P = 4.4e\text{-}34$; LNA, $P = 4.8e\text{-}39$; MZ*ythdf2*, $P = 7.3\text{-}04$; MZ*ythdf2,3* $P = 1.1e\text{-}05$. *P*-values were computed using Mann-Whitney U test.

(E) *In situ* hybridization of methylated maternal transcripts *mtus1a* (left) and *zgc:162879* (right) in wild-type, MZ*ythdf2*, and MZ*mir-430* embryos at 2, 4, or 6 hpf. *mtus1a*, both a target of miR-430 and m^{6}A-modification, was stabilized in MZ*miR-430* but not MZ*ythdf2* embryos. Fold change ($\log_2$) in transcript abundance between 6 and 2 hpf for each genotype, as determined by qRT-PCR, is shown on the far right (mean $\pm$ s.d., $n = 3$ independent replicates). *P*-values were computed using a two-sided student's t-test. Scale bars, 100 μM.

Given the extensive effects of m^{6}A on mRNA deadenylation (see section 2.1.), the minor stabilization of maternal transcripts upon loss of Ythdf2 suggests that it is not the sole regulator of methylated mRNA stability. Indeed, I observed significant stabilization for only 2 of 11 methylated transcripts that were previously defined as Ythdf2 targets (Zhao et al., 2017), as measured by qRT-PCR in MZ*ythdf2* mutants and control embryos (**Fig. 3.5.a**). To further test if methylated transcripts can be degraded in the absence of Ythdf2, I injected my methylated reporter into MZ*ythdf2* mutants. I found no difference in the adenylation or decay dynamics of the m^{6}A-modified reporter between MZ*ythdf2* and background-matched wild-type embryos (**Fig. 3.5.b**), illustrating that Ythdf2 is dispensable for methylated reporter degradation. Collectively, these experiments reveal that Ythdf2 is not mandatory for clearance of all methylated maternal transcripts, indicating that redundant mechanisms may exist to regulate m^{6}A-mediated decay during the MZT in zebrafish.
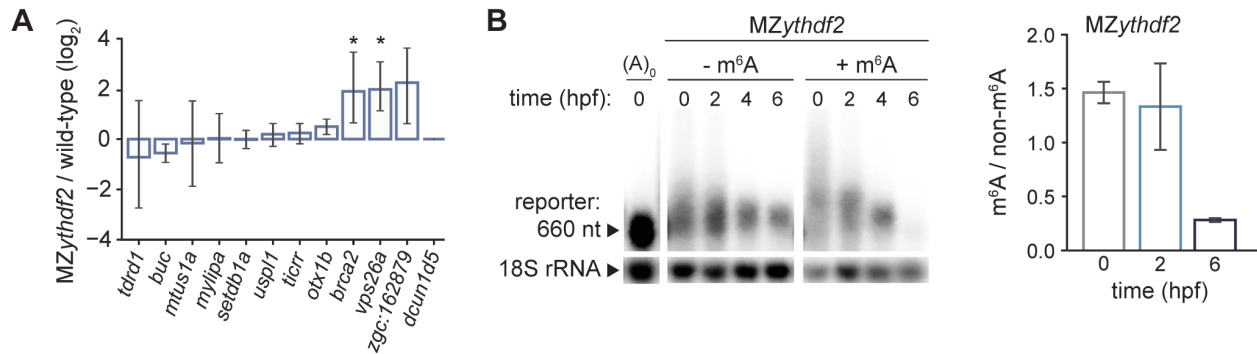
Figure 3.5. Loss of Ythdf2 stabilizes few methylated mRNAs
(A) Fold change from qRT-PCR measure of relative abundance of methylated maternal mRNAs between MZ*ythdf2* and background-matched wild-type embryos was insignificant for most transcripts at 4 hpf (mean ± s.d., $n = 3$ independent replicates). Only two transcripts were significantly stabilized, *brca2*, $P = 5.4\text{e-}03$; *vps26a*, $P = 6.3\text{e-}03$.
(B) Northern blot (left) of m^6A-modified ($+ m^6A$) versus unmodified ($- m^6A$) reporter at respective timepoints (hpf) in MZ*ythdf2* embryos. Internal 18S rRNA loading control (~1900 nt) shown on bottom. Ratio of methylated versus non-methylated reporter mRNA abundance (normalized to 18S rRNA) quantified from two replicates is shown on right. A_0, reporter injected without poly(A) tail.

3.2.3. Ythdf1 and Ythdf3 are not individually required for m^6A-mediated clearance

Given that Ythdf2 alone did not control methylated mRNA abundance during the MZT, I sought to establish whether Ythdf1 or Ythdf3 were dominant regulators of m^6A-modified transcripts. I used CRISPR/Cas9 gene editing to individually disrupt *ythdf1*, *ythdf2*, and *ythdf3* but deletion of any one was not sufficient to stabilize the previously defined m^6A-containing mRNAs (**Fig. 3.6.**). Thus loss of neither *ythdf1*, *ythdf2*, nor *ythdf3* individually prevented methylated transcript removal, suggesting that no single reader is required for m^6A-mediated maternal mRNA decay.
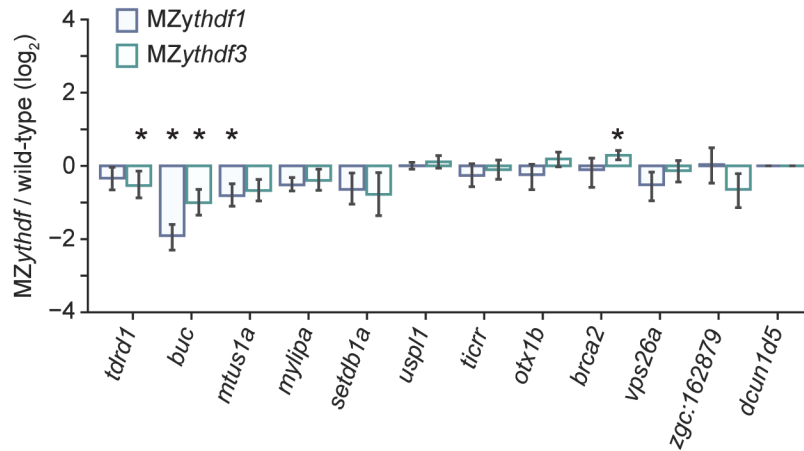
Figure 3.6. Loss of Ythdf1 or Ythdf3 does not stabilize most methylated mRNAs
Fold change from qRT-PCR measure of relative abundance of methylated maternal mRNAs between MZ*ythdf1* (blue) or MZ*ythdf3* (green) and wild-type embryos was insignificant for most transcripts at 4 hpf (mean ± s.d., *n* = 3 independent replicates, * *P* < 0.05). Only one transcript was significantly stabilized, *brca2* in MZ*ythdf3* mutants, *P* = 4.0e-02.

3.2.4. Ythdf2 and Ythdf3 together are not obligatory for m⁶A-mediated maternal mRNA clearance

As absence of individual Ythdf readers was not sufficient to block degradation for the majority methylated maternal mRNAs, I aimed to determine if double loss of *ythdf2* and *ythdf3* hindered maternal transcript clearance. When I performed poly(A) mRNA-sequencing on MZ*ythdf2;*MZ*ythdf3* mutants (see section 4.2.2.) and analyzed maternal mRNA expression, I found that very few transcripts were stabilized in MZ*ythdf2*;MZy*thdf3* mutants relative to wild-type controls (256 of 13642 maternal mRNAs with fold-change > 2.0 at 6 hpf), of which only 20 were found to be methylated (**Fig. 3.7.a**). Thus, double *ythdf2* and *ythdf3* deletion did not stabilize most maternal mRNAs, supporting the possibility that they are not compulsory to regulate global maternal transcript levels during the MZT.

To test if loss of *ythdf2* and *ythdf3* specifically affected decay of methylated mRNAs, I compared changes in maternal transcript abundance between m⁶A-modified and unmodified messages. As in MZ*ythdf2* embryos, I found that m⁶A-modified transcripts were slightly stabilized

in MZ*ythdf2;*MZ*ythdf3* mutants at 6 hpf relative to controls (P = 2.8e-14, Mann-Whitney U test,

Fig. 3.7.b). Further, I did not observe significant stabilization for any of the previously defined

m^{6}A-containing targets in MZ*ythdf2;*MZ*ythdf3* mutants relative to background-matched controls,

as measured by qRT-PCR (**Fig. 3.7.c**). This suggests that m^{6}A-based recognition and

deadenylation of cognate mRNAs was not fully impaired in MZ*ythdf2;*MZ*ythdf3* mutants.
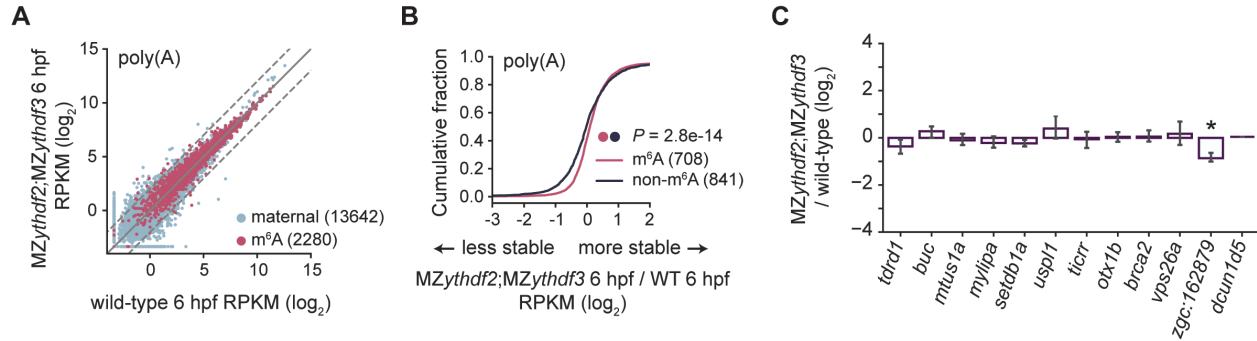
Figure 3.7. Methylated maternal mRNA clearance is unaffected by the absence of Ythdf2 and Ythdf3

(**A**) Biplot comparing similar expression levels (log$_2$ RPKM) of maternal transcripts (blue, n = 13642) and m^{6}A-modified transcripts (magenta, n = 2280) between background-matched wild-type and MZ*ythdf2*;MZ*ythdf3* mutant embryos at 6 hpf, from poly(A) mRNA.

(**B**) Cumulative distribution of fold changes in maternal mRNA abundance (log$_2$ RPKM) between MZ*ythdf2*;MZ*ythdf3* mutant and background-matched wild-type embryos, showing m^{6}A-modified mRNAs (magenta, n = 708) were slightly stabilized relative to non-modified transcripts (black, n = 841) at 6 hpf, from poly(A) mRNA. P-values computed by Mann-Whitney U test.

(**C**) Fold change from qRT-PCR measure of relative abundance of methylated maternal mRNAs between MZ*ythdf2*;MZ*ythdf3* and background matched wild-type embryos was insignificant for most transcripts at 4 hpf (mean ± s.d., n = 3 independent replicates, * P < 0.05).

3.3. Role of Ythdf2 in zygotic genome activation

Previous work indicated that loss of Ythdf2 delayed both zygotic genome activation (ZGA)

and gastrulation (Zhao et al., 2017), possibly due to slowed maternal clearance. Though my

analysis shows that loss of Ythdf2 did not prevent methylated or maternal mRNA clearance, I

sought to inspect if zygotic transcription was disrupted in MZ*ythdf2* mutants. To this end, I

compared zygotic gene expression between MZ*ythdf2* mutants and background-matched wild-type

control embryos. Several lines of evidence suggest that Ythdf2 deletion does not hinder the onset of ZGA. First, only 5 of 6477 zygotic genes were differentially expressed in MZ*ythdf2* mutants relative to controls, and only one of these was downregulated (4 and 6 hpf, **Fig. 3.8.a**) (DESeq2 analysis, $P < 0.05$, **Table 3.2.**). Second, when I analyzed the global proportion of intronic reads, used to detect zygotic transcription, I found that intron expression was unchanged in the MZ*ythdf2* mutants relative to wild-type controls, contrasting the sharp intronic read depletion in embryos treated with triptolide, an RNA Pol II inhibitor (**Fig. 3.8.b**). Third, I observed similar RNA levels for several of the earliest expressed zygotic genes including *aplnrb*, *klf17*, and *miR-430*, between MZ*ythdf2* mutants and controls (**Fig. 3.8.c**) (fold-changes of 0.04, -0.21, and -0.32, respectively, all $P < 0.05$, 6 hpf). These same genes were dramatically downregulated when zygotic transcription was blocked with triptolide (fold-changes of -2.67, -3.08, and -3.83, for *aplnrb*, *klf17*, and *miR-430*, respectively). Together, these results illustrate that loss of Ythdf2 does not disrupt zygotic gene expression and thus that Ythdf2 is not essential for the onset nor extent of ZGA.
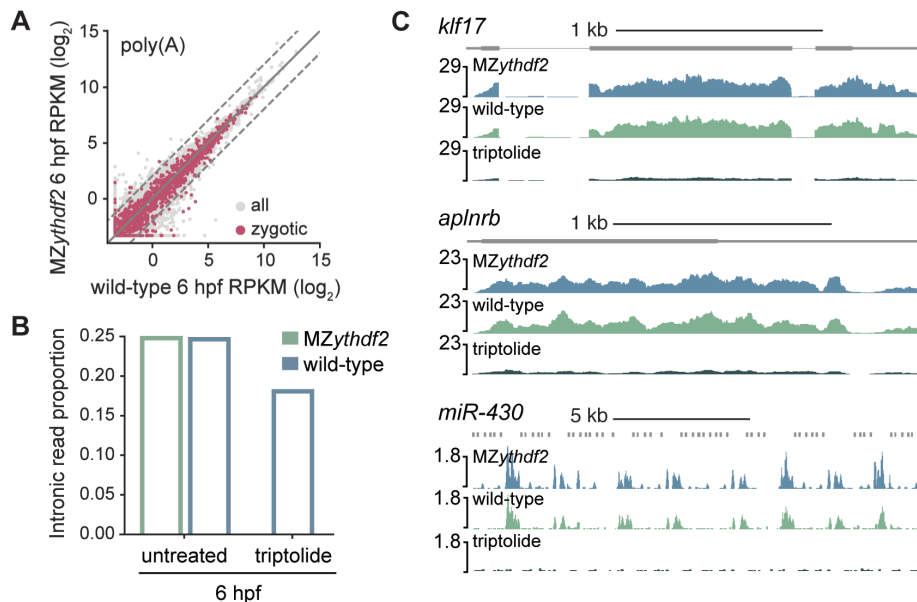
Figure 3.8. Loss of Ythdf2 does not hinder zygotic genome activation
(**A and B**) Biplot of similar expression levels (log₂ RPKM) of zygotic (magenta, $n = 1760$) and all mRNAs (grey, $n = 20119$) between background-matched wild-type and MZ*ythdf2* embryos at 6 hpf from poly(A) mRNA. Dashed lines indicate two-fold change.

(**C**) Proportion of intronic reads relative to total number of reads for background-matched wild-type (green), MZ*ythdf2* (blue), and triptolide-treated embryos at 6 hpf from ribo0 mRNA. Triptolide inhibits zygotic transcription, resulting in decreased count of intronic reads.

(**D**) Genome tracks at 6 hpf of similar levels of zygotic transcripts between MZ*ythdf2* mutants and background-matched wild-type compared to reduced mRNA levels in triptolide-treated embryos.

Table 3.2. Fold-changes and *P*-values for 5 differentially expressed zygotic transcripts

gene ID	fold-change 4 hpf	*P*-value 4 hpf	fold-change 6 hpf	*P*-value 6 hpf	methylation status
ENSDARG00000026236	0.71	n.s.	1.62	2.5E-02	non-m^{6}A
ENSDARG00000036107	2.05	7.8E-03	0.50	n.s.	non-m^{6}A
ENSDARG00000073695	1.53	n.s.	3.75	2.6E-02	
ENSDARG00000077618	-1.38	1.1E-03	-1.42	n.s.	
ENSDARG00000093131	2.88	n.s.	8.16	1.2E-03	

Differential expression determined between time-matched MZ*ythdf2* and background-matched wild-type embryos at either 4 or 6 hpf in poly(A) mRNA-sequencing by DESeq2 (*P*-value < 0.05, corrected for multiple testing). n.s., not significant. No value for methylation status indicates unknown status.

CHAPTER 4: Redundant functions of Ythdf readers in zebrafish development

m^{6}A methylation and its Ythdf readers are known to modulate mRNA fate to promote key developmental transitions, including stem cell differentiation, embryogenesis, and gametogenesis (Heck and Wilusz, 2019; Lasman et al., 2020b). For instance, m^{6}A facilitates decay of pluripotency promoting mRNAs in mouse embryonic stem cells to enable the shift from self-renewal to differentiation (Geula et al., 2015). Similarly, YTHDF2, YTHDC1, and YTHDC2 are all found to be essential for oogenesis and spermatogenesis in mice, (Bailey et al., 2017; Hsu et al., 2017; Ivanova et al., 2017; Jain et al., 2018; Kasowitz et al., 2018; Wojtas et al., 2017), suggesting several factors concurrently contribute to these developmental milestones. This multi-layered regulation by m^{6}A may reflect the fact that redundant mechanisms are needed to ensure robustness in gene expression changes during cellular reprogramming events.

Indeed, while the three YTHDF readers were initially attributed distinct functional roles (Wang et al., 2014a, 2015b), new evidence indicates that their cellular activities may instead overlap. Recent studies have found that the YTHDFs share m^{6}A binding sites and are simultaneously required for mRNA decay and cellular differentiation, demonstrating that these proteins function redundantly (Lasman et al., 2020a; Zaccara and Jaffrey, 2020). All three zebrafish Ythdfs are found to be maternally provided mRNA binders during the MZT (Despic et al., 2017), suggesting that the three paralogs contribute to transcriptome turnover in concert. Defining the exact roles of the Ythdfs during development is essential to understand precisely how methylation and its readers promote key cellular transitions.

Herein, I determined that the Ythdf readers function redundantly at multiple steps in zebrafish development. I employed single, double, and triple Ythdf mutants to show that individual

Ythdf readers are not required for embryogenesis, but concurrent loss of two Ythdfs impairs ovary development, and triple Ythdf deletion results in larval lethality. Through their overlapping functions, Ythdf1, Ythdf2, and Ythdf3 are likely key mediators of developmental transitions.

ATTRIBUTIONS
This chapter is modified from my first author paper published in December, 2020 in Cell Reports (Kontur et al., 2020), which I wrote with input from Antonio Giraldez. Daniel Cifuentes, a contributing author on the paper, generated the ythdf2 *and* ythdf3 *mutant alleles.*

4.1. Individual Ythdf readers are not required for embryogenesis

Previous work reported that loss of Ythdf2 delayed gastrulation of zebrafish embryos, potentially stemming from the corresponding lag in ZGA and maternal clearance (Zhao et al., 2017). Given that I showed that Ythdf2 deletion did not affect the timing of zygotic transcription or mRNA transcript removal, I sought to test if loss of Ythdf2 disrupts developmental progression during the zebrafish MZT. Consistent with a lack of transcriptomic differences between MZ*ythdf2* mutant and control embryos, I observed no difference in the onset of gastrulation in a live imaging developmental time course (**Fig. 4.1.a.**).
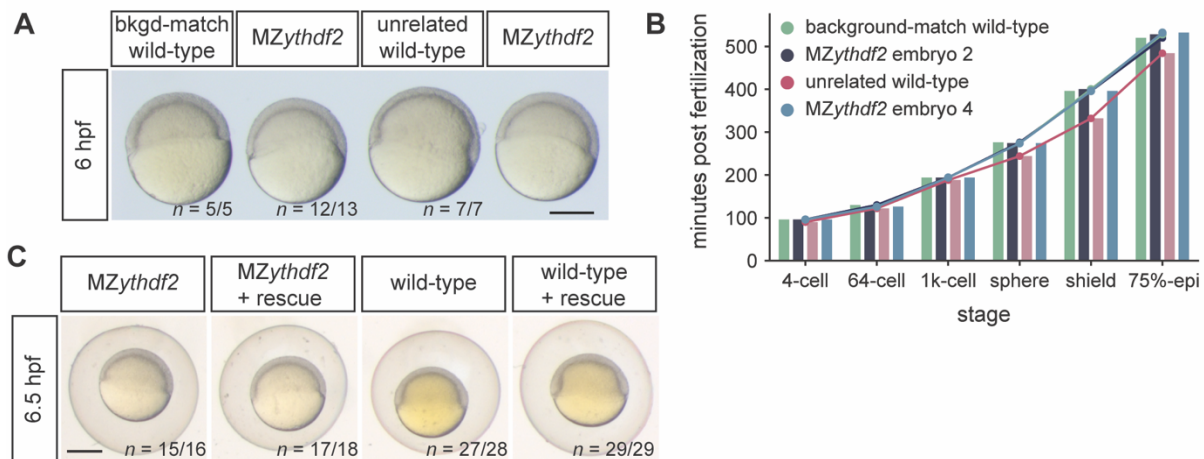
Figure 4.1. Loss of Ythdf2 does not delay gastrulation of zebrafish embryos
(A) Image of zebrafish embryos where MZ*ythdf2* and background-matched (bkgd-match) wild-type exhibit similar developmental delay relative to unrelated wild-type at 6 hpf. MZythdf2 embryos were

from the same clutch and share genetic background with the background-matched wild-type embryo. *n*, replicate number of embryos at the same developmental stage. Scale bar, 500 μM.
(B) Quantification of developmental rates of embryos in developmental time course shown in(A). Bars and dots indicate minutes post fertilization at which embryos reach corresponding developmental stage. MZ*ythdf2* embryo 2 and 4 correspond to the MZ*ythdf2* embryos second from the left and on the far right in (E), respectively.
(**C**) Representative images of MZ*ythdf2* and unrelated TU-AB wild-type embryos that were either uninjected or injected with *ythdf2* rescue mRNA. *n*, replicate number of embryos from the same clutch and condition at the same developmental stage. Scale bar, 400 μm.

In this time course, I compared MZ*ythdf2* mutants to both related, genetic background-matched wild-type and to unrelated, TU-AB background wild-type embryos (see **Fig. 3.3.a**). All embryos were at the 64-cell stage at approximately 2 hpf. However, both MZ*ythdf2* mutants and background-matched controls reached 50% epiboly at approximately ~5.9 hpf, while the TU-AB wild-type reached 50% epiboly about 40 minutes earlier, at ~5.2 hpf (**Fig. 4.1.b**). This ~40-minute delay is consistent with that observed by Zhao et al., but because this delay was exhibited by both MZ*ythdf2* mutants and background-matched wild-type, it is unlikely to be linked to the *ythdf2* deletion mutation. Indeed, when I injected *ythdf2* mRNA into MZ*ythdf2* mutants, I could not rescue the delay in gastrulation relative to the TU-AB wild-type embryos (**Fig. 4.1.c**).

To ensure that Ythdf2 deficiency does not disrupt embryonic development, I employed a second, independent mutant allele of *ythdf2* from CRISPR-Cas9 gene editing (MZ*ythdf2*[-223/-223]). I found no difference in the onset of gastrulation or developmental timing of MZ*ythdf2*[-223/-223] mutants relative to background-matched controls (**Fig. 4.2.**). Thus, loss of Ythdf2 does not disrupt the timing of gastrulation, supporting the idea of mechanistic redundancy in regulation of m^6A-mediated changes in gene expression during the MZT.
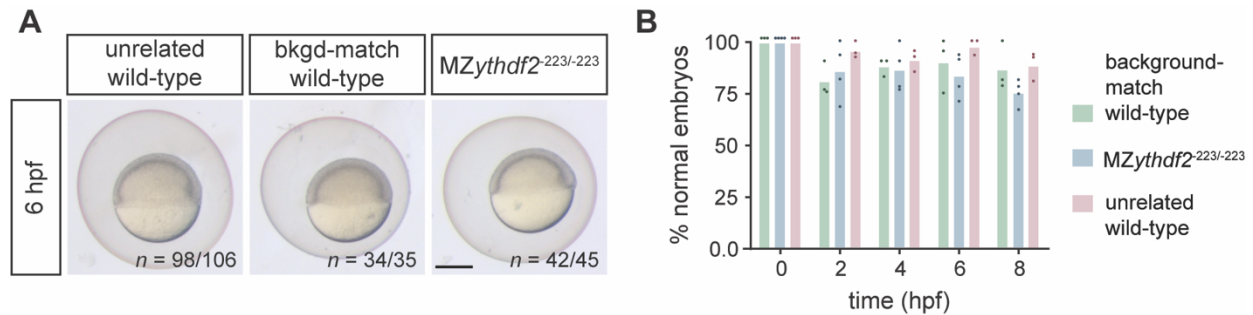
Figure 4.2. Ythdf2 deletion does not disrupt zebrafish embryogenesis
(**A**) Representative images of similar developmental stages of MZ*ythdf2*$^{-223/-223}$, background-matched (bkgd-match) wild-type, and unrelated wild-type embryos at 6 hpf. *n*, replicate number of embryos from the same clutch at the same developmental stage. Scale bar, 500 µM.
(**B**) Quantification of normally developing embryos was similar for each genotype. Dots indicate quantifications from three independent clutches and bars represent mean percentage of normally developed embryos at each time point (hpf) from all three clutches.

Given that Ythdf2 alone did not control zebrafish embryogenesis, I sought to establish potentially redundant roles for the Ythdf readers during development. As in humans, zebrafish have three Ythdfs, which exhibit high protein sequence similarity between themselves and with their human orthologs (**Fig. 4.3.**), suggesting conserved and common functions. To determine if Ythdf1 or Ythdf3 drive zebrafish development, I used CRISPR/Cas9 gene editing to individually disrupt *ythdf1* and *ythdf3*, but deletion of either reader did not result in developmental phenotypes (**Fig. 4.4.**). Together, this analysis demonstrates that individual Ythdf readers are not required for embryogenesis.
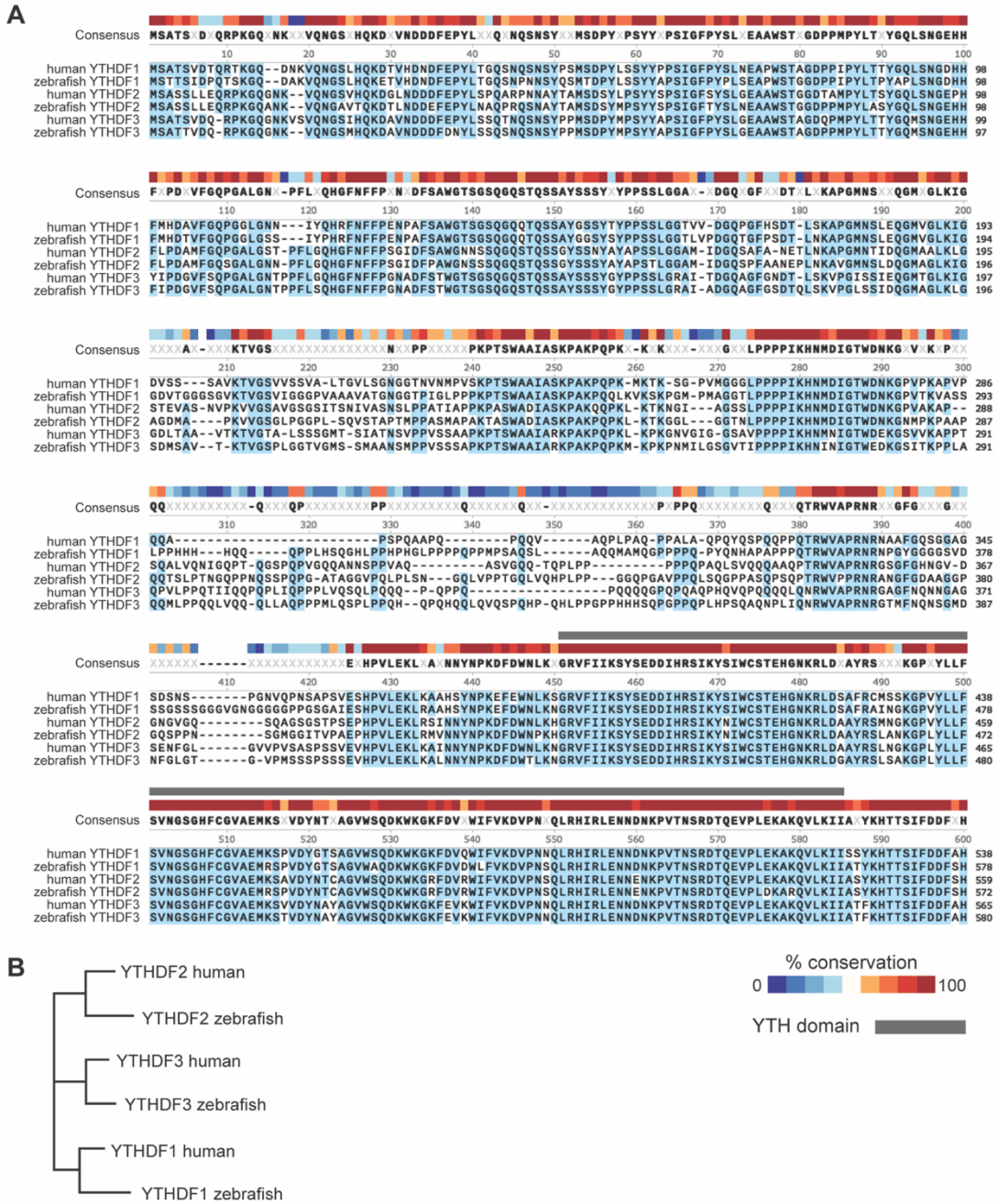
Figure 4.3. Zebrafish and human Ythdf homology

(**A**) Alignment of protein sequences for zebrafish and human Ythdf proteins shows high sequence similarity between paralogs and homologs of both species, especially in the YTH domain (grey bar). Sequence alignment was generated by Clustal Omega, where blue shading indicates alignment to the consensus sequence (top row, bolded) and the consensus threshold was set to > 50%. Colored blocks along the top indicate percentage of sequence conservation at each residue.

(**B**) Phylogenetic relationship of zebrafish and human Ythdf proteins generated from the protein sequence alignment. Branch lengths represent evolutionary distance in number of amino acid substitutions.
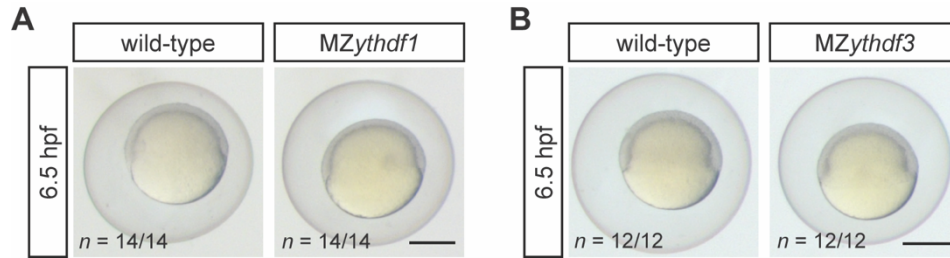
Figure 4.4. Ythdf1 and Ythdf3 mutant embryos develop normally
Representative images of MZ*ythdf1* (left) and MZ*ythdf3* (right) mutants exhibiting no developmental differences relative to respective background-matched wild-type controls at ~6.5 hpf. *n*, replicate number of embryos from the same clutch at the same developmental stage. Scale bars, 500 μm.

4.2. Ythdf2 and Ythdf3 are together required for ovary development

4.2.1. Double loss of Ythdf2 and Ythdf3 disrupts female gonad development

Because analysis of single *ythdf* mutants suggested that these proteins could function redundantly, I generated a double *ythdf2* and *ythdf3* mutant, as Ythdf3 is also linked to mRNA decay (Shi et al., 2017). Deletion of both *ythdf2* and *ythdf3* specifically disrupted female development, as no double homozygotes (*ythdf2$^{-/-}$;ythdf3$^{-/-}$*) were female, while control siblings (*ythdf2$^{-/+}$;ythdf3$^{-/-}$*) were an almost equal ratio of males and females (**Fig. 4.5.a**). This male-only phenotype was also observed in *ythdf1$^{-/-}$;ythdf2$^{-/-}$* mutants (**Fig. 4.5.b**), but appears specific to double *ythdf* deletion, as single *ythdf* homozygotes could still become female (**Fig. 4.5.c**). As sex determination and gonad development are interdependent in zebrafish (Santos et al., 2017), I hypothesized that loss of *ythdf2* and *ythdf3* prevented proper establishment of the ovaries. Histological staining of gonads from double *ythdf2$^{-/-}$;ythdf3$^{-/-}$* mutants revealed underdeveloped juvenile ovaries at 27 days post fertilization (dpf) relative to sibling controls (**Fig. 4.5.d**). By 34 dpf, all homozygous *ythdf2$^{-/-}$;ythdf3$^{-/-}$* mutants had developed testes, the default gonad upon disruption of ovary development (Nagabhushana and Mishra, 2016), whereas controls exhibited

both ovaries and testes (**Fig. 4.5.d**). Loss of *ythdf2* and *ythdf3* specifically affected ovaries, as male

fish developed healthy testes and were fertile at rates similar to wild-type (**Fig. 4.6.**). Together,

this phenotype of inhibited female gonad development provides evidence for redundant functions

of *ythdf2* and *ythdf3* in the establishment of the ovary prior to the MZT.
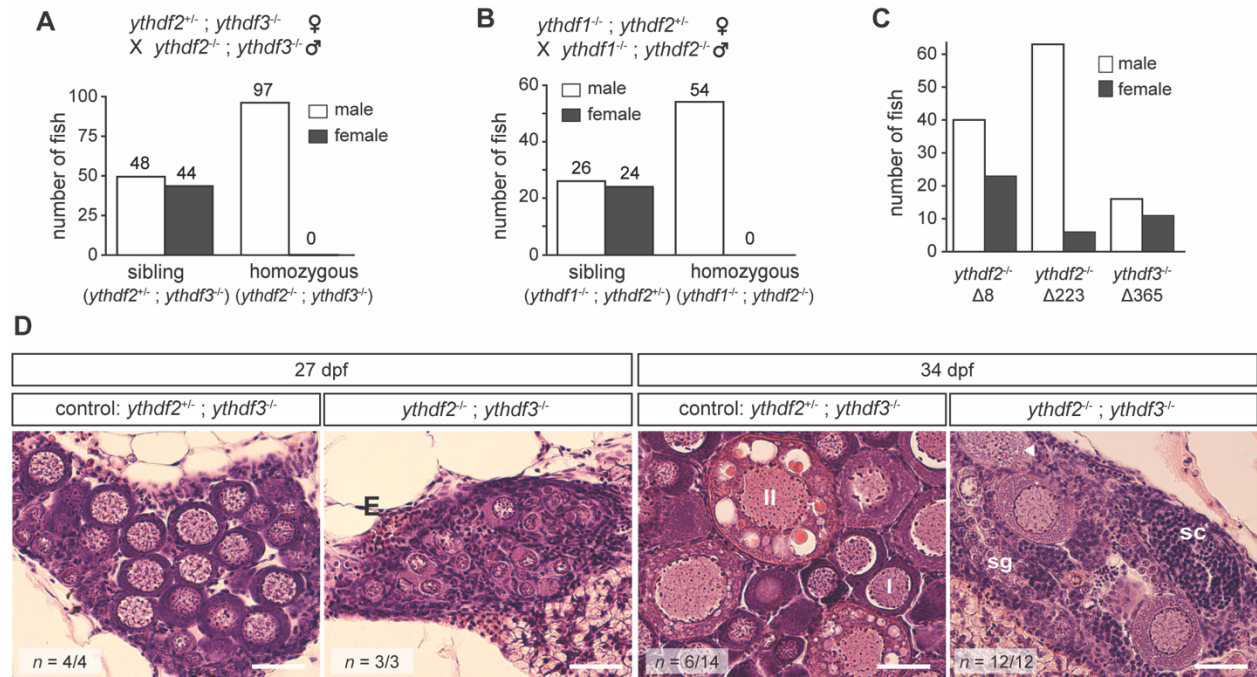
Figure 4.5. Double loss of Ythdf2 and Ythdf3 disrupts female gonad development
(**A-B**) Numbers of male and female fish of each genotype, quantifying male-only phenotype of double *ythdf2;ythdf3* (A) and *ythdf1,ythdf2* (B) homozygous mutants. Sibling controls and double homozygotes were offspring from the same crosses, depicted on top.
(**C**) Numbers of male and female fish of each genotype. Homozygous mutants of *ythdf2* (both Δ8 and Δ223 alleles) and *ythdf3* (Δ365) can develop into females.
(**D**) Gonad histology of *ythdf2$^{-/-}$;ythdf3$^{-/-}$* mutant fish and sibling controls (*ythdf2$^{+/-}$;ythdf3$^{-/-}$*) from same cross in (A). At 27 dpf, mutants exhibit less developed juvenile ovaries than siblings. At 34 dpf, 6 sibling fish had adult ovaries and 8 had testes, while all 12 *ythdf2$^{-/-}$;ythdf3$^{-/-}$* fish had developed testes. I, stage I oocytes; II, stage II oocytes; triangle, apoptotic oocyte; sg, spermatogonia; sc, spermatocytes. *n,* replicate number of each genotype with similar gonads. Scale bars, 40 μm.
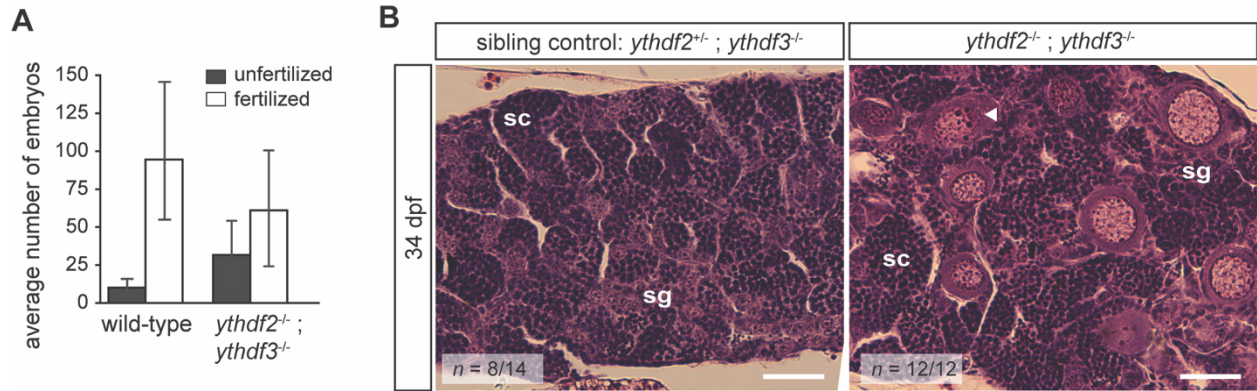
Figure 4.6. Testes develop normally in *ythdf2;ythdf3* double mutants
(**A**) Embryos from *ythdf2;ythdf3* homozygous males and unrelated TU-AB wild-type males were fertilized at similar rates (mean ± s.d., *n* = 3 independent biological clutches of each genotype).
(**B**) Testes histology from *ythdf2⁻ᐟ⁻;ythdf3⁻ᐟ⁻* mutant fish and sibling controls (*ythdf2⁺ᐟ⁻;ythdf3⁻ᐟ⁻*). At 34 dpf, both sibling and mutant fish exhibited healthy developing testes. triangle, apoptotic oocyte; sg, spermatogonia; sc, spermatocytes. *n,* replicate number of each genotype with similar gonads; for sibling the remaining six were ovaries. Scale bars, 40 μm.

4.2.2. Ythdf2 and Ythdf3 together are not mandatory for embryonic development

Though *ythdf2* and *ythdf3* function redundantly to establish the ovary, the extent of overlap in Ythdf reader function during embryogenesis remains unclear. To test the maternal function of *ythdf2* and *ythdf3*, I first had to overcome the defect in ovarian development. To this end, I treated growing double *ythdf2⁻ᐟ⁻;ythdf3⁻ᐟ⁻* mutants with 17α-ethinylestradiol (EE2), a synthetic estrogen agonist that promotes ovarian development and subsequently increases the number of female offspring (Örn et al., 2003). Double homozygous females were recovered following EE2 treatment (**Fig. 4.7.a**), enabling study of *ythdf2* and *ythdf3* during methylated RNA decay and embryonic development. MZ*ythdf2;*MZ*ythdf3* mutants appeared to be phenotypically normal relative to EE2-treated background-matched controls, as mutant embryos exhibited normal gastrulation, morphology, and developmental timing (**Fig. 4.7.b**).

90
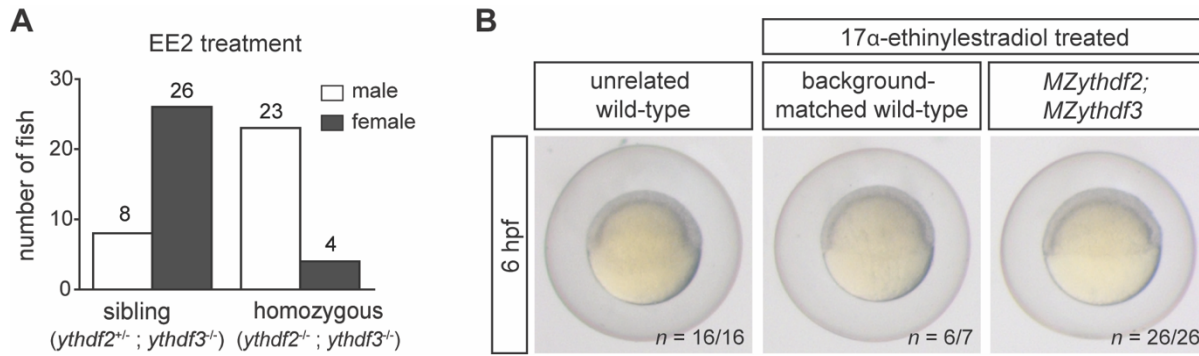
Figure 4.7. Embryonic morphology was normal in double *ythdf2;ythdf3* mutants
(**A**) Numbers of male and female fish of each genotype, following rescue of male-only phenotype in double *ythdf2;ythdf3* homozygous mutants by treatment with 17 α-ethinylestradiol (EE2). Sibling control and homozygous fish were offspring from the same cross as in (Fig. 4.5.a).
(**B**) MZ*ythdf2*;MZ*ythdf3* mutants, background-matched wild-type, and unrelated wild-type zebrafish embryos develop at similar rates. Parents of mutant or background-matched control embryos were 17 α-ethynylestradiol treated. *n*, replicate number of embryos of each genotype at the same developmental stage. Scale bars, 500 μm.

4.3. Triple Ythdf loss of function is lethal to zebrafish

Given that *ythdf2* and *ythdf3* double deletion did not stabilize methylated mRNAs or disturb embryogenesis, I generated a triple Ythdf loss of function mutant (**Fig. 4.8.a**). Triple *ythdf* disruption was lethal, as triple homozygous larvae could only survive until 9 dpf, likely due to maternally contributed Ythdf proteins (**Fig. 4.8.b**). Triple *ythdf* mutants were never observed in adulthood, and I recovered fewer zebrafish double homozygous for two *ythdf*s and heterozygous for the remaining *ythdf* than expected (**Fig. 4.8.c**). This suggests that the Ythdf proteins act redundantly to ensure zebrafish viability, likely in a dosage dependent manner, as fewer fish with only one functional *ythdf* copy survived. Unfortunately, the lethality phenotype prohibits analysis of triple Ythdf depletion on methylated mRNA stability and assessment of redundancy during the MZT. Yet, my double and triple Ythdf mutants demonstrate that dual loss of both Ythdf2 and Ythdf2 was not enough to disrupt preferential deadenylation of methylated mRNAs, and reveals that the redundant functions of all three Ythdf readers are required during early development.
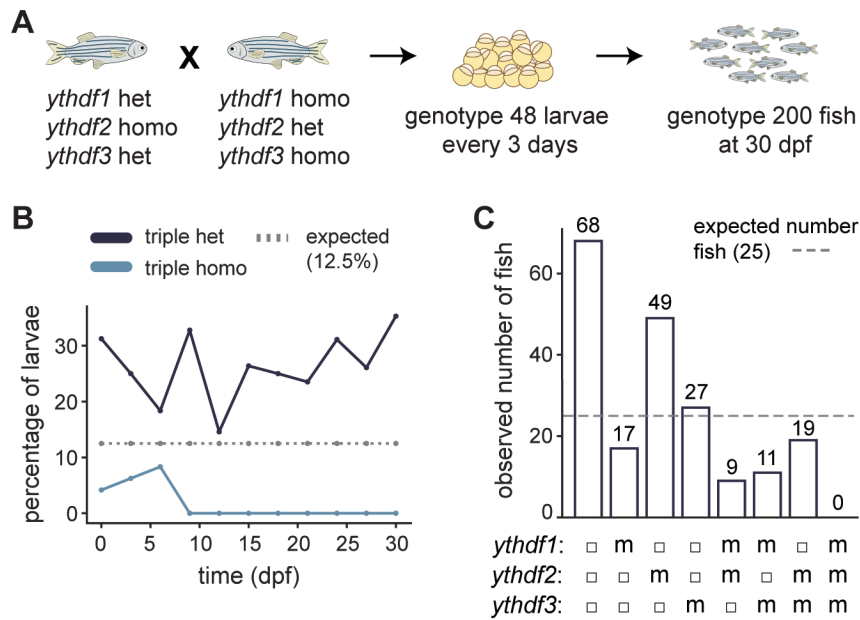
Figure 4.8. Triple loss of Ythdfs disrupts zebrafish development
(**A**) Schematic of cross and genotyping strategy to characterize triple Ythdf mutants. Female fish (genotype $ythdf1^{+/-};ythdf2^{-/-};ythdf3^{+/-}$) were crossed to males (genotype $ythdf1^{-/-};ythdf^{+/-};ythdf3^{-/-}$) to generate triple homozygous embryos (1 out of 8 possible genotypes). Every 3 days, 48 larvae were genotyped, and 200 additional fish were genotyped at 30 dpf to identify triple homozygotes.
(**B**) Percentage of triple heterozygous (dark blue, $ythdf1^{+/-};ythdf2^{+/-};ythdf3^{+/-}$) or triple homozygous (light blue, $ythdf1^{-/-};ythdf2^{-/-};ythdf3^{-/-}$) fish during development. Grey dotted line, expected percentage (12.5%) of fish with each possible genotype produced from cross in (D).
(**C**) Number of fish observed with each genotype produced from the cross in (D) at 30 dpf. For each $ythdf$ allele: open squares, heterozygous allele (+/-); m, homozygous allele (-/-). Grey dotted line indicates expected number of fish (25), equal for all genotypes.

4.4. Mettl3 or Mettl14 loss of function is lethal to zebrafish

To assess the role of m^6A globally in embryogenesis, I generated mutants of the core enzymes of the methyltransferase complex, *mettl3* and *mettl14*, aiming to determine if development can proceed in the complete absence of maternal m^6A modifications. Loss of function of Mettl3 or Mettl14 resulted in late stage larval lethality, in which no fish homozygous for the mutant alleles could be recovered past 35 days post fertilization (**Fig. 4.9.**). This suggests that some function of the methyltransferases is essential during zebrafish development, but prevents analysis of the maternal functions of m^6A during early embryogenesis
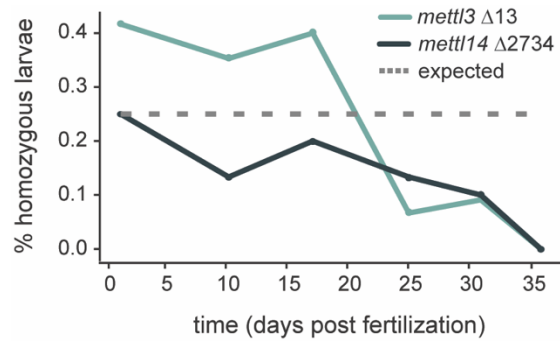
Figure 4.9. Mettl3 or Mettl14 loss of function is larval lethal

Percentage of fish homozygous for the corresponding mutant allele surviving over time during development. Grey dotted line, expected percentage (25%) of fish with homozygous genotype produced from in cross of two heterozygous fish.

CHAPTER 5: Discussion and Future Outlook

This work aimed to understand how RNA methylation and its reader proteins guide maternal transcriptome remodeling during early embryonic development. Here, I showed that m^{6}A modification promotes mRNA deadenylation during the MZT, establishing it as an additional facet of control over maternal transcript fate. Although the importance of m^{6}A is clear, future investigations are necessary to understand how this pathway integrates into the larger landscape of posttranscriptional regulation during embryogenesis.

To characterize the role of the Ythdf s, oogenesis, and zebrafish viability. Given that m^{6}A and its readers influence global changes in gene expression across developmental transitions, this study strengthens the model of RNA methylation as a universal mechanism to promote reprogramming.

5.1. RNA methylation contributes to maternal mRNA clearance

5.1.1. Discussion on the unknowns of m^{6}A-mediated maternal mRNA deadenylation

My analysis of maternal mRNA stability in zebrafish embryos revealed that RNA methylation contributes to transcript degradation during the vertebrate MZT and promotes poly(A) tail shortening of maternal mRNAs. This is consistent with early studies proposing m^{6}A as a key determinant of transcript lifetimes (Batista et al., 2014; Liu et al., 2014; Schwartz et al., 2014), and more recent findings that show m^{6}A promotes deadenylation in cell culture (Du et al., 2016). Thus, methylation may serve as a universal regulator of transcript stability, especially in the context of cell fate determination (Heck and Wilusz, 2019). Yet, the potential mechanisms underlying this activity are not fully clear, as the impact of m^{6}A on deadenylation and decay are

often intertwined. Indeed, I observed that the effects of m⁶A were greater on deadenylation than decay for endogenously methylated mRNAs (**Fig. 2.2.**), which may be due to the combined effects of poly(A) tail-shortening and mRNA decay driven by m⁶A when assaying poly(A)-selected mRNA. Further, the rapid deadenylation and enhanced degradation of the methylated reporter (**Fig. 2.3.**) may reflect its hypermethylated state, or indicate that m⁶A-mediated deadenylation enables subsequent and rapid decay. Thus, it remains difficult to determine the extent to which methylation driven deadenylation and decay are connected. Given that poly(A) tail shortening often proceeds decapping and decay (Chen and Shyu, 2011; Zheng et al., 2008), a stepwise pathway beginning with m⁶A-mediated deadenylation is likely, but this must be more thoroughly investigated.

The enzymes on which m⁶A relies to control mRNA deadenylation and decay during the zebrafish MZT also remain unclear. Methylation readers of the YTH family are associated with both the Pan2-Pan3 and Ccr4-Not deadenylase complexes, the 5'-to-3'exoribonuclease XRN1, and stress granule components (Du et al., 2016; Kretschmer et al., 2018; Liu et al., 2020b; Zaccara and Jaffrey, 2020), suggesting m⁶A may degrade transcripts through parallel pathways. Destabilization of m⁶A marked transcripts was demonstrated here to differentially depend on Dcp2 and Caf1, although whether this is a direct or indirect dependence is yet to be tested. The modification has also been linked to additional decay mechanisms, including endoribonucleolytic cleavage (Park et al., 2019) and localization to P-bodies and stress granules (Fu and Zhuang, 2020; Gao et al., 2019; Ries et al., 2019; Wang et al., 2014a). Future work should address which deadenylases control methylation-dependent deadenylation during the MZT and whether it is uncoupled or interconnected with the contributions of m⁶A to these other pathways. Further, the extent to which m⁶A-based deadenylation is essential for maternal mRNA clearance is unknown, as my attempts

to remove methylation from the maternal transcriptome were frustrated by the lethal phenotype exhibited by mutants of the methyltransferase complex, Mettl3 and Mettl14 (see section 4.4.). Despite this limitation, my work provides mechanistic insight that m⁶A fosters mRNA destabilization via deadenylation, establishing it as an important regulator of maternal mRNA clearance.

5.1.2. Zygotic mode dependence of m⁶A methylation

Analysis of m⁶A-modified messages upon failure of ZGA has revealed that methylated mRNA clearance is reliant on zygotic transcription. This reliance is unlikely to be a total dependency, as methylated reporter abundance did decrease somewhat by 2 hpf before ZGA, reflecting some maternal contributions. Further, methylated reporter deadenylation was unaffected by RNA PolII inhibition, suggesting that poly(A) tail modulation pre-MZT is executed by maternal elements. This is consistent with prior reports of polyadenylated mRNA abundance fluctuating prior to ZGA (Aanes et al., 2011; Eichhorn et al., 2016; Mathavan et al., 2005; Rabani et al., 2014; Subtelny et al., 2014; Winata et al., 2018). Indeed, this mechanism of deadenylating transcripts early, but delaying decay, was previously observed in embryogenesis, and may serve to carefully control maternal protein output from key developmental genes without necessitating transcript turnover (Despic and Neugebauer, 2018; Graindorge et al., 2008; Voeltz and Steitz, 1998).

A clearer understanding of the relative dependence of m⁶A-mediated decay on the maternal and zygotic programs may be achieved through a deep investigation of m⁶A-interactors. For instance, the Ythdf readers are all maternally supplied (see Section 3.1.) and thus have the capacity to influence early adenylation. Yet, their activity may be regulated by ZGA-dependent alterations in posttranslational modifications (Hou et al., 2021), localization, or protein partners (Vejnar et al.,

2019), enabling them to control downstream decay. Further study is required to illuminate the precise nature of the maternal and zygotic mode contributions to methylated mRNA clearance.

5.1.3. Interaction between m⁶A and other decay pathways

My dissection of the relation between m⁶A and miR-430 demonstrated that RNA methylation functions independently but additively with the miR-430 pathway to target maternal mRNAs for clearance. This is coherent with the observation that most unstable maternal mRNAs depend on multiple decay programs (Rabani et al., 2017; Thomsen et al., 2010; Vejnar et al., 2019). This sort of combinatorial regulation is thought to serve as a mechanism to ensure that selected transcripts are rapidly and robustly eliminated (Vejnar et al., 2019; Yartseva and Giraldez, 2015). Indeed, I found that those mRNAs targeted by both m⁶A and miR-430 were the most degraded (**Fig. 2.7.a**), reflecting faster elimination due to co-regulation. Thus, by combining multiple pathways, different transcripts are conferred different degrees of destabilization, allowing for dynamic regulation in the timing and extent of mRNA decay.

Given the extensive catalog of posttranscriptional pathways that contribute to maternal clearance, it will be exciting to establish possible interactions with m⁶A for each of them. For instance, co-occurrence of the m⁶A consensus site with other RBP binding motifs (Zhang et al., 2020c) could reflect coordinated regulation or indicate that these trans factors help specify the functional output of m⁶A on its targets. Methylated maternal transcripts in zebrafish were found to be enriched in sequence motifs similar to those bound by Dazl and Unr, two RBPs involved in translational regulation via the poly(A) tail (Aanes et al., 2019), suggesting potential co-regulation. Another intriguing possibility is that m⁶A modulates RBP binding through its function as a structural switch, either by masking or unmasking motifs, or creating favorable conformations for

RBP recognition, as it does for HNRNP proteins (Liu et al., 2015, 2017; Wu et al., 2018). Similarly, codon optimality is known to modulate poly(A) length through the translation of optimal and suboptimal codons (Bazzini et al., 2016; Buschauer et al., 2020; Mishima and Tomari, 2016; Presnyak et al., 2015), and m^{6}A can disrupt tRNA selection and translation elongation (Choi et al., 2016). Whether RNA methylation enhances the effects of codon optimality by contributing to ribosome pausing remains to be determined.

Finally, m^{6}A-dependent regulation may also cooperate with other RNA modifications. Ybx1, a reader of 5-methylcytosine (m^{5}C), is linked to the regulation of mRNA stability and translation during early embryogenesis (Sun et al., 2018; Yang et al., 2019), and the Ythdf proteins were recently implicated as readers and destabilizers of N^1-methyladenosine (m^{1}A) marked mRNAs (Dai et al., 2018; Seo and Kleiner, 2020; Zheng et al., 2020). Dual modification by m^{1}A and m^{6}A may enhance transcript recognition by the Ythdfs, guaranteeing down-regulation. Additionally, terminal uridylation is known to help degrade maternal transcripts with short poly(A) tails (Chang et al., 2018) during the MZT. m^{6}A may induce deadenylation of maternal mRNAs, after which uridylation facilitates their degradation. Simultaneous analysis of all RNA modifications decorating maternal transcripts will provide key insights into how m^{6}A function is integrated into the larger posttranscriptional regulatory landscape.

5.1.4. m^{6}A and the regulation of mRNA translation

Ribosome profiling analysis indicated that m^{6}A modification correlated with early maternal mRNA translation. This raises the intriguing possibility that translational regulation by methylation is linked to its modulation of polyadenylation, especially given that poly(A) tail length is a major determinant of translation during embryogenesis (Eichhorn et al., 2016; Subtelny et al.,

2014; Vastenhouw et al., 2019; Winata et al., 2018). Indeed, at 2 hpf, methylation was associated with both greater adenylation and enhanced translation efficiency, but these relations dissolved by 6 hpf, when modified mRNAs were instead differentially deadenylated. This pattern of dynamic regulation exhibited by methylated transcripts is consistent with the finding that the correlation between poly(A) tail length and translation efficiency diminishes following ZGA (Subtelny et al., 2014; Vastenhouw et al., 2019). Thus it is possible that m^{6}A contributes to the coupling of translation and adenylation during the MZT, although this mechanism requires further investigation of the connection between tail length, translation, and m^{6}A levels. Additionally, the factors mediating the effects of methylation on translation have yet to be identified. Studies in human cells link Ythdf1 and Ythdf3 to translational upregulation (Shi et al., 2017; Wang et al., 2015b), although other work suggests that the Ythdf readers have no impact on translation (Zaccara and Jaffrey, 2020), meaning the Ythdfs' role must be further explored. Ythdc2 is also found to promote translation, although it employs its helicase domains (not present in the DFs) to unwind mRNA structures and facilitate ribosome translocation (Mao et al., 2019). Finally, it will be worthwhile to assess how the fate of maternal mRNAs varies based on the location of m^{6}A within the transcript, as where the mark is deposited may help to determine the downstream translational consequences (Mao et al., 2019).

5.2. Ythdf2 is not the sole driver of methylated transcript turnover

Although my study showed that m^{6}A promotes maternal mRNA clearance, I could not establish Ythdf2, the proposed driver of methylated transcript turnover (Lee et al., 2020; Wang et al., 2014a; Zhao et al., 2017), as the sole mediator of these effects. Further, I found that Ythdf2 is not obligatory for the timing or success of maternal mRNA decay or zygotic genome activation,

in contrast to work that presents Ythdf2 as a critical regulator of mRNA fate during the zebrafish MZT (Zhao et al., 2017). Differences in the observed MZ*ythdf2* phenotype may arise from differences in the genetic background of control embryos (**Fig. 3.3.a**). Indeed, I found that the delay phenotype did not segregate with the *ythdf2* mutation, as it was no longer observed when the genetic background between MZ*ythdf2* mutants and wild-type controls was matched. Comparison of MZ*ythdf2* mutants to unrelated wild-type embryos also accounts for the transcriptomic phenotype; if the mutant embryos are a stage behind developmentally, their gene expression profiles will be consistent with that earlier developmental stage, rather than arising from mRNA dysregulation due to loss of *ythdf2*. Thus, my data challenges the view that Ythdf2 is required for proper transcript clearance and ZGA, and instead indicates that Ythdf2 is not obligatory to direct the MZT.

Additionally, I found only a minor role for Ythdf2 in the clearance of methylated transcripts. RNA-sequencing data from both this study and Zhao et al. (2017) demonstrates that loss of Ythdf2 stabilized only a small number of methylated transcripts, suggesting that other factors are required for turnover of most m^{6}A targets. Individual deletion of Ythdf1 and Ythdf3 was also unable to significantly stabilize select m^{6}A-modified transcripts, suggesting that no single Ythdf reader is sufficient to control methylated mRNA clearance. Notably, limitations from the technique used to map m^{6}A in the zebrafish embryos preclude knowledge of what fraction of a given transcript is methylated. This means that m^{6}A reader removal could have an appreciable impact on a small fraction of methylated transcripts, but that these effects would be masked by the unchanged stability for the larger, unmodified fraction of the same transcript. As m^{6}A-mapping techniques become more quantitative and precise (Linder and Jaffrey, 2019; McIntyre et al., 2020),

reader specificity for methylated maternal mRNAs should be carefully assessed, to fully resolve if the Ythdfs redundantly control m^6A-modified maternal transcript turnover.

5.3. Ythdf functional redundancy during development

My analysis of double and triple Ythdf mutants demonstrated that these factors work in concert to control mRNA fate during multiple developmental transitions (**Figure 5.1.**). This finding aligns with the newly emerged model of functional redundancy between the Ythdfs, and challenges the traditional view that each reader has a distinct regulatory role (Lasman et al., 2020a; Patil et al., 2018; Shi et al., 2019; Zaccara and Jaffrey, 2020; Zaccara et al., 2019). Indeed, recent evidence supports interchangeable activities for the Ythdfs. First, the Ythdfs contain the same protein domains across vertebrates, and some invertebrates, like *Drosophila*, have only one YTH homolog, reflecting a shared capacity for overlapping functions (Kan et al., 2017; Patil et al., 2018). Second, all three proteins are known to bind the same m^6A sites in multiple physiological contexts, suggesting that co-targeting between the readers is universal (Lasman et al., 2020a; Lu et al., 2018; Shi et al., 2017; Tirumuru et al., 2016; Zaccara and Jaffrey, 2020). Third, the interactomes of the Ythdfs markedly coincide, with key decay and deadenylation machinery associating with Ythdf1, Ythdf2, and Ythdf3 (Zaccara and Jaffrey, 2020). Fourth, significant stabilization of methylated transcripts is observed only upon triple Ythdf knockdown in cell culture, while individual knockdowns have minimal impact on m^6A-modified mRNAs, mirroring my observations in zebrafish embryos (Zaccara and Jaffrey, 2020). Together, these studies and my work affirm a model of functional redundancy between the Ythdfs in regulation of the methylated transcriptome.
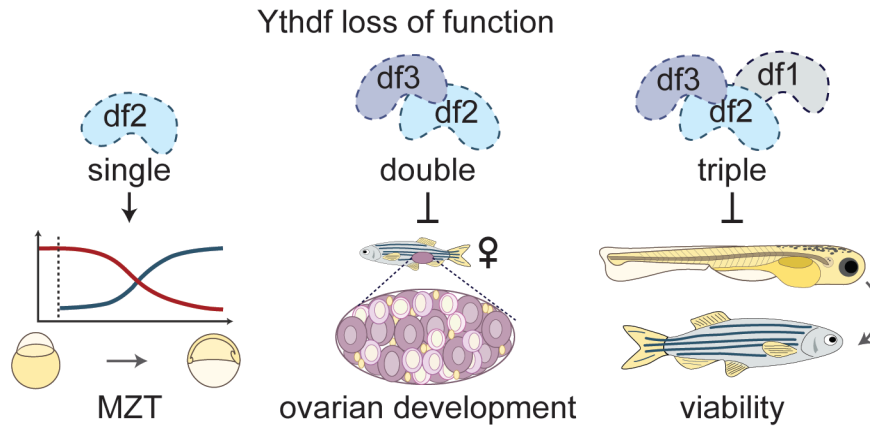
Figure 5.1. Single, double, and triple Ythdf zebrafish mutants reveal redundant functions in multiple stages of development.
My study shows that in zebrafish, single Ythdf knockouts of Ythdf1, Ythdf2, or Ythdf3 do not impact the maternal-to-zygotic transition (MZT) or embryogenesis. However, double loss of Ythdf2 and Ythdf3 impairs oogenesis and inhibits ovary development. Triple Ythdf deletion disrupts larval viability.

Notably, the Ythdf readers are found to target unique transcripts or exert distinctive functions in some biological contexts (Liu et al., 2018b; Wang et al., 2014a, 2015b). While this could arise from exclusive expression of a single paralog in a given cell or tissue type (Shi et al., 2019), compartmentalization of readers is unlikely during the zebrafish MZT, as all three Ythdf proteins are simultaneously expressed in the early embryo.

Indeed, redundant Ythdf activity is consistently observed in instances of cellular reprogramming (Lasman et al., 2020a; Zaccara and Jaffrey, 2020), suggesting that this multi-layered regulation is important to ensure robust changes in gene expression. For instance, a dosage-dependent mechanism controls embryonic viability in mice, as determined through single, double, and triple Ythdf knockouts (Lasman et al., 2020a). This is consistent with my results that individual knockouts did not impede maternal mRNA decay or embryonic development, but that dual loss of Ythdf2 and Ythdf3 impaired oogenesis, and triple Ythdf loss led to lethality. Indeed, I found that only triple reader deletion phenocopied Mettl3 or Mettl14 knockouts, suggesting that the

developmental impact of full reader absence is proportional to complete loss of methylation. This has also been similarly observed in mESCs, where triple YTHDF mutagenesis impairs differentiation to the same extent as METTL3 depletion (Lasman et al., 2020a). Together, this evidence supports a dosage-dependent functional redundancy of the Ythdf readers during development. Given that combinatorial decay is frequently employed to clear messages in the early embryo (Yartseva and Giraldez, 2015), redundant regulation by the Ythdfs may guarantee specific, timely, and orchestrated transcript turnover during key cellular transitions.

Finally, although it is clear that the Ythdfs coordinate their activity during early development, the impact of maternal Ythdf loss of function could not be assessed due to the non-viable phenotype. Ultimately, loss of all three Ythdf readers during the MZT is required to determine if these factors act redundantly to modulate methylated maternal mRNA fate. Additionally, recent work has greatly expanded the list of m^{6}A-associated factors (Arguello et al., 2017; Edupuganti et al., 2017), whose role in cellular transitions must be explored. For instance, the RBP IGF2BP3 was found to maintain maternal mRNA stability prior to transcript clearance during the zebrafish MZT (Huang et al., 2018), although the extent to which this relies on m^{6}A is debated (Sun et al., 2019). Given that multiple readers may contribute to equilibrium between methylated mRNA decay and stability, the specific role of each factor, especially the remaining YTH proteins, must be fully defined to completely understand how methylation governs maternal mRNA clearance.

5.4. The m^{6}A pathway regulates reproductive development

The m^{6}A modification pathway is increasingly recognized as a central regulator of stem cell differentiation and gametogenesis (Lasman et al., 2020b). I found that simultaneous mutation

of Ythdf2 and Ythdf3 impaired female gonad development, demonstrating an essential function of these proteins in zebrafish oogenesis. Intriguingly, this phenotype was restricted to female development, as spermatogenesis and male fertility were unaffected by loss of two Ythdfs, suggesting requirement for these readers arises after the germ cells are established. Consistent with my study in zebrafish, this role of m^6A and its effectors as regulators of gametogenesis is observed across organisms. YTHDF2 is required for murine oocyte maturation (Ivanova et al., 2017) and depletion of the m^6A writer, Mettl3, inhibits gamete maturation in zebrafish (Xia et al., 2018). Additionally, both YTHDC1 and YTHDC2, are found to be essential for proper spermatogenesis and oogenesis in mice (Bailey et al., 2017; Hsu et al., 2017; Jain et al., 2018; Kasowitz et al., 2018; Wojtas et al., 2017). It remains unclear exactly how YTHDF readers regulate mRNA stability during oogenesis, as loss of YTHDF2 in mouse oocytes results in both up- and downregulation of different transcripts (Ivanova et al., 2017). Alternatively, the YTHDFs may impact mRNA translation, as modulation of m^6A levels through methyltransferase mutants dysregulates translation in mouse and *Xenopus* oocytes (Qi et al., 2016; Sui et al., 2020), and other male-only phenotypes in zebrafish stem from defects in translation (Miao et al., 2017). Future work is needed to define exactly how m^6A readers govern transcriptome changes during gametogenesis.

Finally, it is notable that the dosage dependency of the Ythdfs extends to their function in reproductive development. I observed that single Ythdf mutants did not exhibit the male-only phenotype, and only upon double disruption was oogenesis repressed. Similarly, the severity of defects in mouse gametes depends on the extent of m^6A dysregulation. Knockout of Ythdf1 or Ythdf3 causes no reproductive defects, loss of Ythdf2 destroys oocyte competence and decreases sperm count, and early METTL3 mutation completely halts sperm and oocyte development (Huang et al., 2020; Ivanova et al., 2017; Lasman et al., 2020a; Lin et al., 2017; Xu et al., 2017).

Intriguingly, Ythdf2 appears to be the principal Ythdf controlling gametogenesis, as other readers cannot compensate for its loss in mice (Ivanova et al., 2017; Lasman et al., 2020a). Similarly, both of my double mutants included Ythdf2, although the combination of Ythdf1 and Ythdf3 was not tested. Why is Ythdf2 more essential than the other readers? This is likely attributable to expression or localization differences between Ythdfs in the developing gonads; in mice, only Ythdf2 expression persists between spermatogonia and spermatocytes, and it is the only reader with both nuclear and cytoplasmic distribution in developing oocytes (Lasman et al., 2020a). Thus, variation in the required dosage of the Ythdfs across various organisms and cellular contexts may reflect expression changes, although this is yet to be confirmed in zebrafish reproductive development.

5.5. Conclusions and perspective: RNA methylation as a master regulator of transcriptome switching

RNA modifications have become regarded as pivotal posttranscriptional regulators during cellular transitions (Frye et al., 2018). Because chemical marks offer a unique means to tie transcripts together for similar fates, m^{6}A has been proposed as a universal regulator of transcriptome switching during developmental reprogramming (Darnell et al., 2018; Frye et al., 2018; Heck et al., 2020; Roundtree et al., 2017a; Simen Zhao et al., 2018). Indeed, as one of the most abundant mRNA modifications, m^{6}A is known to control gene expression changes during stem cell differentiation, neurogenesis, cancer development, hematopoiesis, gametogenesis, and embryogenesis (Heck and Wilusz, 2019; Lasman et al., 2020b; Zhang et al., 2020b). Across these physiological contexts, m^{6}A tags specific sets of transcripts for coordinated regulation, and its effectors mediate the downstream consequences on mRNA metabolism. Thus m^{6}A ensures the proper genetic program is realized efficiently and correctly without requiring new transcription.

It is possible that RNA methylation and the Ythdf readers play a similar role in transcriptome remodeling and embryonic development in zebrafish (Zhao et al., 2017). My study demonstrated that the m^{6}A modification promotes maternal transcript removal, and that the Ythdf proteins are redundantly required at multiple stages of development, including oogenesis and larval viability. Thus methylation is another pathway woven into the landscape of posttranscriptional regulation orchestrating the MZT, functioning alongside RBPs, microRNAs, codon optimality, secondary structures, and other mechanisms to control maternal mRNA clearance and facilitate early embryogenesis.

Yet, interpretation of RNA methylation as a universal mediator of development must be considered cautiously, as it hinges on the capacity of m^{6}A to both promote and repress mRNA stability and translation, and to quickly switch its regulatory capacity while relying on the same effector proteins. Indeed the dynamic nature of m^{6}A deposition has been challenged (Darnell et al., 2018; Mauer and Jaffrey, 2018; Simen Zhao et al., 2018), and the directionality of m^{6}A's consequences on mRNA decay and translation vastly differ across physiological conditions (Patil et al., 2018; Shi et al., 2019; Zaccara et al., 2019). Future research regarding the full profile of mechanisms used by RNA methylation to control transcript fate across biological contexts will clarify the role of in reprogramming. Similarly, future work on how the Ythdfs achieve specificity yet function coherently to interpret the mark is required. Finally, understanding how methylation is connected to other regulatory pathways will be fundamental to comprehend how the activity of multiple posttranscriptional regulators is coordinated. Addressing these questions will provide pivotal information regarding the function and universality of RNA modifications in shaping gene expression changes during essential developmental transitions.

Chapter 6: Methods

6.1. Methylated mRNA analysis and reporters

Reporter construction and injection

The methylated reporter was generated as follows: DNA fragments for the CDS and 3'UTR were ordered as gBlocks Gene Fragments from IDT. The CDS was designed without adenine in the sequence (with the exception of the ATG start codon, TGA stop codon, and HA tag) to limit incorporation of m^{6}A to the 3'UTR. The 3'UTR was designed with 12 copies of GGACT methylation motif. DNA fragments were PCR amplified for In-Fusion cloning. The pCS2+ vector was linearized with BamHI, and fragments were ligated with the In-Fusion HD enzyme (Takara, 639642). Adenines in the 5'UTR were converted to thymines using site directed mutagenesis with oligos 5'- TTTCTTGCTTCTTGTTCTTTTTGCTGGTTCCATGGCCCGCCTTTGTGCTGC-3' and 5' GGAACCAGCAAAAAGAACAAGAAGCAAGAAATCTATAGTGTCACCTAAAT-3' followed by DpnI digest to remove non-mutated plasmid. Plasmids were linearized with XbaI. Capped reporter mRNA was generated by IVT using the HiScribe SP6 RNA Synthesis Kit (New England BioLabs, E2070S) with the addition of 40 mM m^{7}G(5')ppp(5')G RNA cap structure analog (New England BioLabs, S1404S). For methylation containing reporters, 50 mM of N^6-methyladenosine 5'triphosphate (TriLink, N-1013-5) was added to the IVT in place of adenine. m^{6}A-IP verified the presence of m^{6}A modifications in the reporter mRNA. mRNAs were DNase treated following IVT. The poly(A) tail was added after IVT using the Poly(A) tailing kit (Invitrogen, AM1350) according to the manufacturer's instructions. Resultant mRNA was purified using the RNeasy RNA extraction kit (Qiagen, 74104). Reverse transcription followed by Sanger sequencing of the methylated reporter mRNA confirmed proper incorporation of m^{6}A only as

specified by the plasmid sequence. Zebrafish embryos were injected with 35 pg of either m^{6}A-modified or unmodified reporter mRNA. Thirty embryos were collected for each condition at different timepoints during the MZT for RNA extraction and subsequent Northern blot analysis.

RNA isolation

Total RNA was extracted from zebrafish embryos using the TRIzol reagent Invitrogen (15596-018) according to the manufacturer's protocol and eluted in RNase-free water. RNA isolated for qRT-PCR was treated with TURBO DNase (Invitrogen, AM2238) at 37°C for 20 minutes following RNA extraction and purified using phenol chloroform extraction.

Northern blot analysis

Briefly, 3 μg of total RNA was resuspended in formamide and 2x tracking dye (1mM EDTA, 60 mM triethanolamine, 60 mM tricine, 0.04% bromophenol blue, 2.5% formaldehyde) and heated at 65°C for 10 minutes to denature the RNA. Samples were separated by electrophoresis using a 1.5% agarose/1.25% formaldehyde gel in 1x Tri/Tri buffer (30 mM triethanolamine, 30 mM tricine). The gel was capillary transferred to a Nytran SPC membrane (Whatman, 10416294). RNA was crosslinked to the membrane with 254 nm UV light at 1200 mJ. Membranes were prehybridized with 5 mL of ExpressHyb hybridization solution (Clontech, 686831) for 1 hour at 68°C with constant rotation. RNA species were detected by either cDNA or oligonucleotide probes hybridized at 68°C or 42°C, respectively, overnight with 5 mL of ExpressHyb solution and 5,000,000 cpm of either the reporter or the 18S control radiolabeled probes:reporter mRNA 5'-GTCCTTTCTGCTGGTCCTTCCTGTGGGGGTGTCCTGTGTGGGGCCGTGCTTTGGGCTG CCGTGCTGTCTGCTGGCCCCCTCTGCGCTGGTCCGCTTTGCGGGGGTCGCCTGTTGGC

TGCCCGTCTCTGCGGGGGTCGTCTGTTGGGGGGGCCCTCTCTGGGCTGGCGTTTCCTCT GCTGGTCCGTCCTTGTTCGGCGTTCTCTGTT- 3' Internal 18S maternal rRNA 5'CGTTCG TTATCGGAATCAACCAGACAAATCGCTCCACCAACTACGAACGG- 3' Internal 18S somatic rRNA 5'-CCGTTCTTAGTTGGTGGAGCGATTTGTCTGGTTCATTCCGATAACGA ACGAG- 3'.

cDNA probes were radiolabeled with α-P^{32}-dATP using the Nick Translation Kit (Sigma-Aldrich, 10976776001) according to the manufacturer's protocol. Oligo probes were radiolabeled by T4 PNK end labeling (New England BioLabs, M0201S) with γ-P^{32}-ATP. Radiolabeled probes were purified using ProbeQuant G-50 Micro Columns (GE Healthcare, 28903408) and cDNA probes were heated at 95°C for 5 minutes prior to hybridization. Membranes probed by cDNA were washed three times with 2x SSC/0.05% SDS for 15 minutes and twice with 0.1x SSC/0.1% SDS for 20 minutes at 50°C. Membranes probed with oligos were washed once with 2x SSC/0.05% SDS for 10 minutes at room temperature and once with 0.1x SSC/0.1% SDS for 2 minutes at 42°C. Northern blots were quantitated using a phosphorimager (Bio-Rad Personal Molecular Imager). Levels of reporter mRNA were normalized to 18S rRNA controls.

Poly(A) tail length analysis

Datasets for poly(A) tail length were downloaded from public repositories. PAL-sequencing (Subtelny et al., 2014) was downloaded from GEO accession number GSE52809 and TAIL-sequencing data (Chang et al., 2018) was downloaded from Zenodo doi: 10.5281/zenodo.2640028. For each dataset, the average poly(A) tail length was calculated by averaging counts for the poly(A) tail reads for each gene at each timepoint. The same sets of methylated and non-methylated transcripts were used to analyze each poly(A) tail dataset.

6.2. Transcriptomic and molecular analyses of *Ythdf* mutants

In situ **hybridization**

    In situ hybridization was performed as in Thisse & Thisse, 2014. To generate antisense RNA *in situ* probes, transcript regions were amplified from zebrafish cDNA using the oligos listed in Table 6.1. The reverse-orientation oligo contained a T7 promoter overhang for probe synthesis by IVT using T7 polymerase. Probes were purified using the RNeasy RNA extraction kit (Qiagen, 74104). Each 200 μL hybridization reaction used 20 ng of DIG-labeled RNA probe. Before imaging, embryos were cleared with 2:1 benzyl benzoate:benzyl alcohol solution. For each condition, at least 20 embryos were analyzed and all displayed comparable levels of staining following equal stain time. Imaging was performed using a Zeiss Discovery V12 stereo microscope. Maternal-zygotic mutant embryos of *miR-430* were collected from an incross of homozygous *miR-430* deletion fish from Y. Liu et al., 2013. Wild-type control embryos used for *in situ* experiments were background-matched wild-type relatives of MZ*ythdf2* embryos.

qRT-PCR measure of RNA abundance

    Total RNA was extracted from 20 embryos per experimental condition and DNase treated. cDNA was synthesized from 1 μg of total RNA using reverse transcription with random hexamers and the Superscript III reverse transcriptase kit (Invitrogen, 18080093). cDNA was diluted 1:20 and 10 μl reactions for PCR reactions were prepared with 5 ml of Power SYBR Green PCR Master Mix (Applied Biosystems, 4368706), 4.5 μl of 1:100 diluted cDNA, and 0.5 μl of 10 mM forward and reverse primer mix. At least two biological and two technical replicates were performed for each sample. Relative expression was measured with ViiA 7 software v1.2.2 using the DDCT

method, with *dcun15d* as a reference control. Oligonucleotides used for qRT-PCR are listed in Table 6.1.

Immunoprecipitation and western blotting

Fifty embryos were collected, flash frozen in liquid nitrogen, and resuspended in lysis buffer (150 mM NaCl, 25 mM Tris-HCl, 1 mM EDTA, 1% Igepal CA-630, 0.1% SDS) with 1X protease inhibitor cocktail (Roche, 11873580001). Lysates were incubated at 4°C for 10 minutes, followed by centrifugation at 14000 rpm for 15 minutes at 4°C. Supernatants were added to antibody-coupled Protein A Dynabeads (Invitrogen, 10008D) (10 μl of beads and 1.5 μg of antibody, coupled according to manufacturer's protocol). Lysates and antibodies were incubated at 4°C for at least two hours, with rotation. Prior to washes, 20 μl of supernatant was removed for input control. Beads were then washed three times in lysis buffer and resuspended in sample buffer (7.5 μl of 4x NuPAGE LDS Sample Buffer (Invitrogen, NP0321PK2), 3 μl of 1 M DTT (Sigma-Aldrich, 43816), 19.5 μl of nuclease-free water). Samples were heated at 70°C for 10 minutes and separated on a 1.0 mm 4-12% Bis-Tris NuPAGE mini protein gel (Invitrogen) at 180 V for 50 minutes and wet transferred onto a nitrocellulose membrane (GE LifeSciences) at 20 V for 4 hours. Membranes were blocked in 5% milk, 1% Tween-20 in PBS for 1 hour and then incubated overnight at 4°C with constant rotation in anti- Ythdf1, Ythdf2, or Ythdf3 antibody diluted 1:1000 or in anti-Actin diluted 1:5000 in block buffer. Secondary antibody Goat Anti-rabbit IgG antibody (H+L) HRP conjugate (Millipore, AP307P) was diluted 1:10,000 in block buffer and the membrane was incubated for one hour at room temperature. Membranes were washed three times for 5-10 minutes after each antibody incubation. Membranes were developed by chemiluminescent detection using ECL Western blotting substrate (Thermo Fisher, 34095) and imaged by and X-ray

111

film (Denville Scientific, E3012). Actin was used as a loading control for input for immunoprecipitated samples.

Antibodies against Ythdf1, Ythdf2, and Ythdf3 were custom generated by YenZyme by raising antibodies in rabbit against amino acid sequences as follows: CKNLEPAPIQNRSRLDQERQ for Ythdf1, PQQTSLPTNGQPPNQSSPQ for Ythdf2, RNRGTMFNQNSGMDN for (amino acid sequences are listed from N to C terminus).

RNA-sequencing library preparation

For RNA-sequencing in *ythdf* mutants, 20 embryos per condition were collected at indicated developmental time points and snap frozen in liquid nitrogen. Embryo collections for mutants and background-matched wild-type were performed at the same time (time-matched), with synchronously developing embryos. Total RNA was subjected to either poly(A)-selection by oligo(dT) beads or to ribosomal RNA-depletion with Epicentre Ribo-Zero Gold, according to manufacturer's instructions. Strand-specific TruSeq Illumina RNA-sequencing libraries were then constructed, and samples were multiplexed and sequenced on Illumina HiSeq 2500 machines to generate 76-nucleotide single-end reads. Library preparation and mRNA sequencing was performed by the Yale Center for Genome Analysis.

RNA-sequencing analysis

The zebrafish mRNA sequencing embryonic development time course datasets were from previously published SRP189512 (Vejnar et al., 2019), SRP149556 (Beaudoin et al., 2018), and SRP072296 (Bazzini et al., 2016). MZ*dicer* fish were obtained from Giraldez et al., 2006. Re-

analysis of published MZ*ythdf2* RNA-sequencing data was performed on dataset from Zhao et al., 2017, from GEO accession number GSE79213.

Mapping reads

Raw reads were mapped using STAR (Dobin et al., 2013) version 2.7.1a to the zebrafish GRCz11 reference genome. Genomic sequence indices for STAR were built including exon-junction coordinates from Ensembl v92 (Aken et al., 2017). Gene annotations were created by concatenating all Ensembl transcript isoforms together. To calculate read counts per gene, all reads that mapped uniquely to the genome and overlapped at least ten nucleotides of the gene annotation were summed. Because the *miR-430* locus is internally repetitive, genome tracks for *miR-430* were generated by allowing up to 900 alignments per read. To calculate per gene RPKMs, the total number of RNA reads mapped to each gene were summed and normalized by gene length and the total numbers of reads mapped to the zebrafish transcriptome per million.

Differential gene expression analysis

To identify significantly differentially expressed genes between background-matched wild-type controls and MZ*ythdf2* mutants, read counts were compared using the R package DESeq2 (Love et al., 2014). Genes were excluded from the analysis if the gene count was below one for both replicates in either condition. To get DE genes, counts for all Ensembl genes were input to the *results* function with the options *pAdjustMethod = 'fdr'* and *independentFiltering = FALSE*. *P*-values reported from DESeq2 are adjusted *P*-values corrected for multiple testing.

Determination of maternal and zygotic genes

Maternal, maternal-zygotic, and zygotic genes were previously defined in Lee et al., 2013. For analyses directly comparing maternal mRNA abundance between m6A-modified and unmodified mRNAs, only strictly maternal transcripts were included. For analyses analyzing global abundance of maternal mRNAs, both exclusively maternally expressed and maternal-zygotic mRNAs were included.

Methylated and unmethylated gene definition

Datasets for m6A-methylation in zebrafish (Zhao et al., 2017) are available from GEO accession number GSE79213. Genes found to have transcript methylation were defined previously from Zhao et al., 2017, and were taken directly from the provided table of processed data. Maternal m6A-modified transcripts used for analysis here included those that were found to contain m6A-modification in both the m6A-seq and m6A-CLIP-seq from Zhao et al., 2017 at either 0 hpf or 2 hpf.

6.3. Generation of zebrafish mutants and phenotype analysis

Zebrafish maintenance and embryo production

Danio rerio (zebrafish) embryos were obtained from natural matings of adult fish of mixed wild-type backgrounds (TU-AB and TLF strains) of mixed ages. Embryos from multiple wild-type crosses were pooled, unless performing experiments on mutant and background-matched controls, in which case clutches from individual pairs were analyzed separately. Embryos were grown and staged according to published standards (Kimmel et al., 1995) and all zebrafish and embryo experiments were performed at 28°C. For experiments involving mutants and wild-type controls, fish pairs were mated at the same time to generate synchronously growing embryos.

Embryo collections of mutants and background-matched controls were then performed at the same time to ensure that all embryos were time-matched for all experiments.

Treatment of juvenile fish with EE2

17 α-ethynylestradiol (EE2) (Sigma-Aldrich, E4876) was diluted with system water to make a 100,000X stock. Approximately 40 fish were raised in a 10-liter tank with EE2 solution at a final concentration of 10 ng/L. Fish water was renewed by dripping 40 L of EE2 solution per day. Fish were treated from 22 to 60 days post fertilization and were sexed 30 days later.

Embryo treatments and injections

All injections into zebrafish embryos were performed on chorionated, one-cell stage embryos with 1 nL volumes, unless otherwise stated. To inhibit RNA Polymerase II, embryos were bathed in 5.8 mM of triptolide (Sigma-Aldrich, T3652) or injected with 0.2 ng of α-amanitin (Sigma-Aldrich, A2263) re-suspended in nuclease-free water.

To generate rescue constructs, zebrafish *ythdf1*, *ythdf2*, and *ythdf3* were PCR amplified from cDNA from 2 hpf embryos. DNA was ligated into a pHA-SP vector containing a 3x-flag sequence using EcoRI and XhoI restriction sites and In-Fusion cloning (Takara, 639642). Final constructs were confirmed by Sanger sequencing. Constructs were linearized with SalI restriction digest and purified using QIAquick PCR purification kit (Qiagen, 28104). Linearized DNA was used as a template for *in vitro* transcription (IVT) using the mMessage mMachine SP6 Transcription Kit (Invitrogen, AM1340) to generate capped reporter mRNA. Resultant mRNA was DNase treated and purified using the RNeasy RNA extraction kit (Qiagen, 74104). Zebrafish

embryos were injected with 100 pg of mRNA and expression of the flag-tagged protein was confirmed by Western blotting.

Gene editing and maternal-zygotic mutants

CRISPR-Cas9 gene editing in zebrafish was performed as described in Vejnar et al., 2016. sgRNAs targeting each gene were designed using the CRISPRscan tool (crisprscan.org) (Moreno-Mateos et al., 2015). Guides are listed in Table 6.1. For gene editing to generate *ythdf2*$^{-223/-223}$ and *ythdf3* mutants, 30 pg of each sgRNA was co-injected with 150 pg of Cas9 (plasmid pT3TS-nCas9n, Addgene #46757, (Jao et al., 2013)) capped mRNA synthesized using mMessage mMachine T3 Transcription kit (Thermo Fisher Scientific, AM1340). For mutagenesis of *ythdf1*, 20 pg of each sgRNA and 150 pg of Cas9 mRNA was co-injected with 20 pg of a single-stranded DNA template (*ythdf1* 5'- gggcagccattgctagcaaaccggccaagcctcagcaactgaaggtgaagagtaagccaggga tgcccatgtagtagtagaccaactcgcgtgacacacaggaggtgcctctggaa-3') to facilitate large deletion and insertion of a stop codon cassette (TAGATAGATAG) by homologous recombination. Mosaic F0 founders were identified by genotyping, using the oligos in Table 6.1. Fish were backcrossed twice to wild-type fish before incrossing heterozygous adults to generate homozygous mutants. Homozygous fish were then incrossed to generate maternal-zygotic mutant embryos. Homozygous *ythdf2*$^{-8/-8}$ zebrafish were generated by Zhao et al., 2017 and were obtained from the laboratory of Robert Ho. Double and triple mutants were generated by crossing fish heterozygous for each gene mutation, and then incrossing double or triple heterozygous. These fish were subject to EE2 treatment, to generate both male and female double or triple homozygous. Males and females with double homozygous genotypes were subsequently incrossed to generate maternal-zygotic embryos.

To genotype zebrafish, DNA was extracted from embryos or tissue clipped from the end of the zebrafish tail. Samples were incubated in 100 ml of 100 mM NaOH at 95°C for 20 minutes and neutralized with 40 ml of 1 M Tris, pH 7.4 (AmericanBio, AB14044). 1 µl of crude DNA extraction was used as a template for PCR using Taq polymerase and indicated genotyping oligos. For the genotyping time course of triple *ythdf* mutants, 48 embryos were removed at random from the pool of offspring every 3 days and subject to genotyping, without being returned to the pool. At 30 dpf, an additional 200 fish were also genotyped.

For experiments comparing MZ mutants to wild-type embryos, wild-type controls were generated from incrossing background-matched wild-type adults that were siblings with homozygous mutants. This was done to homogenize the genetic background between homozygous MZ mutants and wild-type controls. Background-matched wild-type embryos were used as wild-type controls for all experiments involving MZ mutants, unless otherwise noted. As an additional control, some experiments included embryos generated by crossing unrelated, wild-type fish from TU-AB stock.

Microscopy

All imaging was observed using a Zeiss Discovery V12 stereo microscope and images were captured with an AxioCam MRc digital camera (Carl Zeiss). All imaging experiments were performed at a monitored temperature of 28°C and were repeated with at least three biological samples for each condition. For live imaging time course assays, live dechorionated embryos were mounted in 0.25% low melt agarose (AmericanBio, CAS: 9012-36-6) and imaged at least every two minutes. All image analysis was performed using ImageJ (Schneider et al., 2012).

Histology

For juvenile fish aged either 27- or 34-days post fertilization, heads and tails were removed and the middle body section containing the gonads were fixed in Bouin's solution (Sigma-Aldrich, HT10132) overnight at 4°C. Fixed tissues were embedded in paraffin and sectioned at 10 mm. Hematoxylin and Eosin (H&E) staining was performed on the sections according to standard protocols. Slides were mounted in Omnimount (National Diagnostics, 17997-01) and imaged using a Zeiss Axio Imager M1 and an AxioCam MRc digital camera (Carl Zeiss).

Ythdf protein sequence alignments

Protein sequence alignment was generated using SnapGene® software (GSL Biotech, available at snapgene.com), with Clustal Omega alignment, made relative to the consensus sequence with a consensus threshold of > 50%. Phylogenetic tree was generated from the protein sequence alignment described above using Clustal W2 and neighbor-joining clustering.

Table 6.1. Oligonucleotide sequences for gene-editing, genotyping, *in situs*, and qRT-PCR.

CRISPR-cas9 guide RNAs		
ythdf1 sgRNA 1	taatacgactcactatagggtcacgcgagttggtcacgttttagagctagaa	
ythdf1 sgRNA 2	taatacgactcactataggcagggtgcctccagccatgttttagagctagaa	
ythdf2 sgRNA 1	taatacgactcactatagggcatgtaggagtcggacagttttagagctagaa	
ythdf2 sgRNA 2	taatacgactcactataggcttcaacttctttcccaggttttagagctagaa	
ythdf3 sgRNA 1	taatacgactcactatagggcgtgttgcctaaagcacgttttagagctagaa	
ythdf3 sgRNA 2	taatacgactcactataggtgcagaggagctgacagggttttagagctagaa	
mettl3 sgRNA 1	taatacgactcactatagggagatgcactggggccacgttttagagctagaa	
mettl14 sgRNA 1	taatacgactcactatagggtttggctgacaggtttggttttagagctagaa	
mettl14 sgRNA 2	taatacgactcactatagggatcgaggggggattcaggttttagagctagaa	
Genotyping zebrafish mutants		
ythdf1 pair 1	atgaccgacccatacctgtc	agcgatgatcttcagcacct
ythdf1 pair 2	aacagtcagctcaggcacatc	catcgaagatggaggttgtgt
ythdf2 Δ223	gggagcaattgtcacctg	gggagactgtccgtcaatca
ythdf2 Δ8	tgctgttccacctcaactctc	ttaccatgcgcagtttttct
ythdf3	ggacagatgagcaatggtga	caaaatcatgttgggcttcg
mettl3	gcttccacatggacacctg	ttctaaatcacaagattcaaatcca
mettl14 pair 1	atcggggtcgagagagaaat	attgaaccccatccctaacc
mettl14 pair 2	tattgccagcactttgtgga	ttggcacgttgcagactatc
***in situ* hybridization probe amplification**		
mtus1a	gactatttaggtgacactatagatgctgcttgtctagcgtttg	gacttaatacgactcactatagggcaagcactcgtccgtttaca
zgc:162879	gactatttaggtgacactatagaatatggccacctctcctgtg	gacttaatacgactcactatagggcagcaacgtcatgaggaaaa
qRT-PCR oligos		
buc	caagttactggacctcaggatc	ggcagtaggtaaattcggtctc
brca2	ttgtaaagccacgagcactg	ccgcaaggttgaaaaactgt
dcun1d5	agagtggctgaagggaatga	ccaacatggattttgcagtg
mtus1a	aaggatggagcttgctgaga	tctggctttgaggtcttcgt
mylipa	gggaggctctgctctgtatg	cgccaatggtcaggtttagt
otx1b	tacatttacgcgctcacagc	gctgacgacatttagcacga
setdb1a	cttctcaacccaaaacactgc	ctatctgaagagacgggtgaaac
tdrd1	ccctgcctttaagtgtcagc	caagcaggagaaccaactcc
ticrr	tcaccagttcggcttctttt	caactgtccggtttggagtt
uspl1	ctgtgtttgcgttgcacttt	tcaagttccagccaaaatcc
vps26a	aatggaagtgggcattgaag	tgactggtgctccatccata
zgc:162879	cgaggcaagtgctaaagagg	acagcagttgctcagggtct
ythdf1	aacggtccacgacaatgact	tgatggtctccattgctgag
ythdf2	ttcgagccttacctgaatgc	taggggcataggcgtaactg
ythdf3	gaatggcaggactgaagctc	tctctaggggcacttcctga

All oligonucleotides are listed 5'-3'. The two columns for corresponding to the genotyping, *in situ*, and qRT-PCR entries correspond to the forward (left) and reverse (right) oligos.

Bibliography

Aanes, H., Winata, C.L., Lin, C.H., Chen, J.P., Srinivasan, K.G., Lee, S.G.P., Lim, A.Y.M., Hajan, H.S., Collas, P., Bourque, G., et al. (2011). Zebrafish mRNA sequencing deciphers novelties in transcriptome dynamics during maternal to zygotic transition. Genome Res. *21*, 1328–1338.

Aanes, H., Engelsen, D., Manaf, A., Alemu, E.A., Vagbo, C.B., Martin, L., Lerdrup, M., Hansen, K., Mathavan, S., Winata, C., et al. (2019). N6-methyladenosine dynamics during early vertebrate embryogenesis. BioRxiv 528422.

Adams, J.M., and Cory, S. (1975). Modified nucleosides and bizarre 5′-termini in mouse myeloma mRNA. Nature *255*, 28–33.

Agarwala, S.D., Blitzblau, H.G., Hochwagen, A., and Fink, G.R. (2012). RNA Methylation by the MIS Complex Regulates a Cell Fate Decision in Yeast. PLoS Genet. *8*, e1002732.

Aguilo, F., Zhang, F., Sancho, A., Fidalgo, M., Di Cecilia, S., Vashisht, A., Lee, D.F., Chen, C.H., Rengasamy, M., Andino, B., et al. (2015). Coordination of m6A mRNA Methylation and Gene Transcription by ZFP217 Regulates Pluripotency and Reprogramming. Cell Stem Cell *17*, 689–704.

Aik, W., Scotti, J.S., Choi, H., Gong, L., Demetriades, M., Schofield, C.J., and McDonough, M.A. (2014). Structure of human RNA N6-methyladenine demethylase ALKBH5 provides insights into its mechanisms of nucleic acid recognition and demethylation. Nucleic Acids Res. *42*, 4741–4754.

Aken, B.L., Achuthan, P., Akanni, W., Amode, M.R., Bernsdorff, F., Bhai, J., Billis, K., Carvalho-Silva, D., Cummins, C., Clapham, P., et al. (2017). Ensembl 2017. Nucleic Acids Res. *45*, D635–D642.

Alarcón, C.R., Goodarzi, H., Lee, H., Liu, X., Tavazoie, S., and Tavazoie, S.F. (2015a). HNRNPA2B1 Is a Mediator of m6A-Dependent Nuclear RNA Processing Events. Cell *162*, 1299–1308.

Alarcón, C.R., Lee, H., Goodarzi, H., Halberg, N., and Tavazoie, S.F. (2015b). N6-methyladenosine marks primary microRNAs for processing. Nature *519*, 482–485.

An, S., Huang, W., Huang, X., Cun, Y., Cheng, W., Sun, X., Ren, Z., Chen, Y., Chen, W., and

Wang, J. (2020). Integrative network analysis identifies cell-specific trans regulators of m6A. Nucleic Acids Res. *48*, 1715–1729.

Anreiter, I., Mir, Q., Simpson, J.T., Janga, S.C., and Soller, M. (2021). New Twists in Detecting mRNA Modification Dynamics. Trends Biotechnol. *39*, 72–89.

Arguello, A.E., Deliberto, A.N., and Kleiner, R.E. (2017). RNA Chemical Proteomics Reveals the N6-Methyladenosine (m6A)-Regulated Protein-RNA Interactome. J. Am. Chem. Soc. *139*, 17249–17252.

Bailey, A.S., Batista, P.J., Gold, R.S., Grace Chen, Y., de Rooij, D.G., Chang, H.Y., and Fuller, M.T. (2017). The conserved RNA helicase YTHDC2 regulates the transition from proliferation to differentiation in the germline. Elife *6*.

Balacco, D.L., and Soller, M. (2019). The m6A Writer: Rise of a Machine for Growing Tasks. Biochemistry *58*, 363–378.

Barbieri, I., Tzelepis, K., Pandolfini, L., Shi, J., Millán-Zambrano, G., Robson, S.C., Aspris, D., Migliori, V., Bannister, A.J., Han, N., et al. (2017). Promoter-bound METTL3 maintains myeloid leukaemia by m6A-dependent translation control. Nature *552*, 126–131.

Barckmann, B., Pierson, S., Dufourt, J., Papin, C., Armenise, C., Port, F., Grentzinger, T., Chambeyron, S., Baronian, G., Desvignes, J.P., et al. (2015). Aubergine iCLIP Reveals piRNA-Dependent Decay of mRNAs Involved in Germ Cell Development in the Early Embryo. Cell Rep. *12*, 1205–1216.

Bartosovic, M., Molares, H.C., Gregorova, P., Hrossova, D., Kudla, G., and Vanacova, S. (2017). N6-methyladenosine demethylase FTO targets pre-mRNAs and regulates alternative splicing and 3′-end processing. Nucleic Acids Res. *45*, 11356–11370.

Batista, P.J., Molinie, B., Wang, J., Qu, K., Zhang, J., Li, L., Bouley, D.M., Lujan, E., Haddad, B., Daneshvar, K., et al. (2014). M6A RNA modification controls cell fate transition in mammalian embryonic stem cells. Cell Stem Cell *15*, 707–719.

Bazzini, A.A., Lee, M.T., and Giraldez, A.J. (2012). Ribosome profiling shows that miR-430 reduces translation before causing mRNA decay in Zebrafish. Science (80-.). *336*, 233–237.

Bazzini, A.A., Viso, F., Moreno-Mateos, M.A., Johnstone, T.G., Vejnar, C.E., Qin, Y., Yao, J., Khokha, M.K., and Giraldez, A.J. (2016). Codon identity regulates <scp>mRNA</scp> stability and translation efficiency during the maternal-to-zygotic transition. EMBO J. *35*, 2087–2103.

Beaudoin, J.D., Novoa, E.M., Vejnar, C.E., Yartseva, V., Takacs, C.M., Kellis, M., and Giraldez, A.J. (2018). Analyses of mRNA structure dynamics identify embryonic gene regulatory programs. Nat. Struct. Mol. Biol. *25*, 677–686.

Beemon, K., and Keith, J. (1977). Localization of N6-methyladenosine in the Rous sarcoma virus genome. J. Mol. Biol. *113*, 165–179.

Bell, J.L., Wächter, K., Mühleck, B., Pazaitis, N., Köhn, M., Lederer, M., and Hüttelmaier, S. (2013). Insulin-like growth factor 2 mRNA-binding proteins (IGF2BPs): Post-transcriptional drivers of cancer progression? Cell. Mol. Life Sci. *70*, 2657–2675.

Bertero, A., Brown, S., Madrigal, P., Osnato, A., Ortmann, D., Yiangou, L., Kadiwala, J., Hubner, N.C., De Los Mozos, I.R., Sadée, C., et al. (2018). The SMAD2/3 interactome reveals that TGFβ controls m 6 A mRNA methylation in pluripotency. Nature *555*, 256–259.

Berulava, T., Rahmann, S., Rademacher, K., Klein-Hitpass, L., and Horsthemke, B. (2015). N6-Adenosine Methylation in MiRNAs. PLoS One *10*.

Bhat, S.S., Bielewicz, D., Gulanicz, T., Bodi, Z., Yu, X., Anderson, S.J., Szewc, L., Bajczyk, M., Dolata, J., Grzelak, N., et al. (2020). mRNA adenosine methylase (MTA) deposits m6A on pri-miRNAs to modulate miRNA biogenesis in Arabidopsis thaliana. Proc. Natl. Acad. Sci. U. S. A. *117*, 21785–21795.

Bodi, Z., Button, J.D., Grierson, D., and Fray, R.G. (2010). Yeast targets for mRNA methylation. Nucleic Acids Res. *38*, 5327–5335.

Bodi, Z., Zhong, S., Mehra, S., Song, J., Graham, N., Li, H., May, S., and Fray, R.G. (2012). Adenosine methylation in Arabidopsis mRNA is associated with the 3′ end and reduced levels cause developmental defects. Front. Plant Sci. *3*.

Boël, G., Letso, R., Neely, H., Price, W.N., Wong, K.H., Su, M., Luff, J.D., Valecha, M., Everett, J.K., Acton, T.B., et al. (2016). Codon influence on protein expression in E. coli correlates with

mRNA levels. Nature *529*, 358–363.

Boissel, S., Reish, O., Proulx, K., Kawagoe-Takaki, H., Sedgwick, B., Yeo, G.S.H., Meyre, D., Golzio, C., Molinari, F., Kadhom, N., et al. (2009). Loss-of-Function Mutation in the Dioxygenase-Encoding FTO Gene Causes Severe Growth Retardation and Multiple Malformations. Am. J. Hum. Genet. *85*, 106–111.

Bokar, J.A., Shambaugh, M.E., Polayes, D., Matera, A.G., and Rottman, F.M. (1997). Purification and cDNA cloning of the AdoMet-binding subunit of the human mRNA (N6-adenosine)-methyltransferase. RNA *3*, 1233–1247.

Boo, S.H., and Kim, Y.K. (2020). The emerging role of RNA modifications in the regulation of mRNA stability. Exp. Mol. Med. *52*, 400–408.

Boylan, K.L.M., Mische, S., Li, M., Marqués, G., Morin, X., Chia, W., and Hays, T.S. (2008). Motility screen identifies Drosophila IGF-II mRNA-binding protein - Zipcode-binding protein acting in oogenesis and synaptogenesis. PLoS Genet. *4*.

Brachova, P., Alvarez, N.S., and Christenson, L.K. (2021). Loss of Cnot6l impairs inosine RNA modifications in mouse oocytes. Int. J. Mol. Sci. *22*, 1–17.

Briand, J., Sérandour, A.A., Nadaradjane, A., Bougras-Cartron, G., Heymann, D., Ory, B., Vallette, F.M., and Cartron, P.F. (2020). N6-Adenosine Methylation of miRNA-200b-3p Influences Its Functionality and Is a Theranostic Tool. Mol. Ther. - Nucleic Acids *22*, 72–83.

Buschauer, R., Matsuo, Y., Sugiyama, T., Chen, Y.H., Alhusaini, N., Sweet, T., Ikeuchi, K., Cheng, J., Matsuki, Y., Nobuta, R., et al. (2020). The Ccr4-Not complex monitors the translating ribosome for codon optimality. Science (80-.). *368*.

Bushati, N., Stark, A., Brennecke, J., and Cohen, S.M. (2008). Temporal Reciprocity of miRNAs and Their Targets during the Maternal-to-Zygotic Transition in Drosophila. Curr. Biol. *18*, 501–506.

Cai, X., Wang, X., Cao, C., Gao, Y., Zhang, S., Yang, Z., Liu, Y., Zhang, X., Zhang, W., and Ye, L. (2018). HBXIP-elevated methyltransferase METTL3 promotes the progression of breast cancer via inhibiting tumor suppressor let-7g. Cancer Lett. *415*, 11–19.

Camper, S.A., Albers, R.J., Coward, J.K., and Rottman, F.M. (1984). Effect of undermethylation on mRNA cytoplasmic appearance and half-life. Mol. Cell. Biol. *4*, 538–543.

Canaani, D., Kahana, C., Lavi, S., and Groner, Y. (1979). Identification and mapping of N6-methyladenosine containing sequences in simian virus 40 RNA. Nucleic Acids Res. *6*, 2879–2899.

Cao, Z., Zhang, L., Hong, R., Li, Y., Wang, Y., Qi, X., Ning, W., Gao, D., Xu, T., Ma, Y., et al. (2021). METTL3-mediated m6A methylation negatively modulates autophagy to support porcine blastocyst development. Biol. Reprod.

Chang, G., Shi, L., Ye, Y., Shi, H., Zeng, L., Tiwary, S., Huse, J.T., Huo, L., Ma, L., Ma, Y., et al. (2020). YTHDF3 Induces the Translation of m6A-Enriched Gene Transcripts to Promote Breast Cancer Brain Metastasis. Cancer Cell *38*, 857-871.e7.

Chang, H., Yeo, J., Kim, J. gyun, Kim, H., Lim, J., Lee, M., Kim, H.H., Ohk, J., Jeon, H.Y., Lee, H., et al. (2018). Terminal Uridylyltransferases Execute Programmed Clearance of Maternal Transcriptome in Vertebrate Embryos. Mol. Cell *70*, 72-82.e7.

Charlesworth, A., Meijer, H.A., and de Moor, C.H. (2013). Specificity factors in cytoplasmic polyadenylation. Wiley Interdiscip. Rev. RNA *4*, 437–461.

Chen, C.Y.A., and Shyu, A. Bin (2011). Mechanisms of deadenylation-dependent decay. Wiley Interdiscip. Rev. RNA *2*, 167–183.

Chen, L., Dumelie, J.G., Li, X., Cheng, M.H.K., Yang, Z., Laver, J.D., Siddiqui, N.U., Westwood, J.T., Morris, Q., Lipshitz, H.D., et al. (2014a). Global regulation of mRNA translation and stability in the early Drosophila embryo by the Smaug RNA-binding protein. Genome Biol. *15*, R4.

Chen, T., Hao, Y.J., Zhang, Y., Li, M.M., Wang, M., Han, W., Wu, Y., Lv, Y., Hao, J., Wang, L., et al. (2015). M6A RNA methylation is regulated by microRNAs and promotes reprogramming to pluripotency. Cell Stem Cell *16*, 289–301.

Chen, W., Zhang, L., Zheng, G., Fu, Y., Ji, Q., Liu, F., Chen, H., and He, C. (2014b). Crystal structure of the RNA demethylase ALKBH5 from zebrafish. FEBS Lett. *588*, 892–898.

Chen, X., Xu, M., Xu, X., Zeng, K., Liu, X., Sun, L., Pan, B., He, B., Pan, Y., Sun, H., et al. (2020a). METTL14 Suppresses CRC Progression via Regulating N6-Methyladenosine-Dependent Primary miR-375 Processing. Mol. Ther. *28*, 599–612.

Chen, X.Y., Zhang, J., and Zhu, J.S. (2019). The role of m6A RNA methylation in human cancer. Mol. Cancer *18*.

Chen, Y., Lin, Y., Shu, Y., He, J., and Gao, W. (2020b). Interaction between N 6-methyladenosine (m6A) modification and noncoding RNAs in cancer. Mol. Cancer *19*.

Cheng, J., Xu, L., Deng, L., Xue, L., Meng, Q., Wei, F., and Wang, J. (2020). RNA N6-methyladenosine modification is required for miR-98/MYCN axis-mediated inhibition of neuroblastoma progression. Sci. Rep. *10*, 1–9.

Choe, J., Lin, S., Zhang, W., Liu, Q., Wang, L., Ramirez-Moya, J., Du, P., Kim, W., Tang, S., Sliz, P., et al. (2018). mRNA circularization by METTL3–eIF3h enhances translation and promotes oncogenesis. Nature *561*, 556–560.

Choi, J., Ieong, K.W., Demirci, H., Chen, J., Petrov, A., Prabhakar, A., O'Leary, S.E., Dominissini, D., Rechavi, G., Soltis, S.M., et al. (2016). N6-methyladenosine in mRNA disrupts tRNA selection and translation-elongation dynamics. Nat. Struct. Mol. Biol. *23*, 110–115.

Church, C., Moir, L., McMurray, F., Girard, C., Banks, G.T., Teboul, L., Wells, S., Brüning, J.C., Nolan, P.M., Ashcroft, F.M., et al. (2010). Overexpression of Fto leads to increased food intake and results in obesity. Nat. Genet. *42*, 1086–1092.

Clancy, M.J., Shambaugh, M.E., Timpte, C.S., and Bokar, J.A. (2002). Induction of sporulation in Saccharomyces cerevisiae leads to the formation of N6-methyladenosine in mRNA: A potential mechanism for the activity of the IME4 gene. Nucleic Acids Res. *30*, 4509–4518.

Coots, R.A., Liu, X.M., Mao, Y., Dong, L., Zhou, J., Wan, J., Zhang, X., and Qian, S.B. (2017). m6A Facilitates eIF4F-Independent mRNA Translation. Mol. Cell *68*, 504-514.e7.

Cui, Q., Shi, H., Ye, P., Li, L., Qu, Q., Sun, G., Sun, G., Lu, Z., Huang, Y., Yang, C.G., et al. (2017). m6A RNA Methylation Regulates the Self-Renewal and Tumorigenesis of Glioblastoma Stem Cells. Cell Rep. *18*, 2622–2634.

D'Agostino, I., Merritt, C., Chen, P.L., Seydoux, G., and Subramaniam, K. (2006). Translational repression restricts expression of the C. elegans Nanos homolog NOS-2 to the embryonic germline. Dev. Biol. *292*, 244–252.

Dai, X., Wang, T., Gonzalez, G., and Wang, Y. (2018). Identification of YTH Domain-Containing Proteins as the Readers for N1-Methyladenosine in RNA. Anal. Chem. *90*, 6380–6384.

Darnell, R.R., Shengdong, K.E., and Darnell, J.E. (2018). Pre-mRNA processing includes N6 methylation of adenosine residues that are retained in mRNA exons and the fallacy of "RNA epigenetics." RNA *24*, 262–267.

Delaunay, S., and Frye, M. (2019). RNA modifications regulating cell fate in cancer. Nat. Cell Biol. *21*, 552–559.

Deng, M., Chen, B.B., Liu, Z., Cai, Y., Wan, Y., Zhang, G., Fan, Y., Zhang, Y., and Wang, F. (2020). YTHDF2 Regulates Maternal Transcriptome Degradation and Embryo Development in Goat. Front. Cell Dev. Biol. *8*, 580367.

Deng, X., Chen, K., Luo, G.Z., Weng, X., Ji, Q., Zhou, T., and He, C. (2015). Widespread occurrence of N6-methyladenosine in bacterial mRNA. Nucleic Acids Res. *43*, 6557–6567.

DeRenzo, C., and Seydoux, G. (2004). A clean start: Degradation of maternal proteins at the oocyte-to-embryo transition. Trends Cell Biol. *14*, 420–426.

Despic, V., and Neugebauer, K.M. (2018). RNA tales - how embryos read and discard messages from mom. J. Cell Sci. *131*.

Despic, V., Dejung, M., Gu, M., Krishnan, J., Zhang, J., Herzel, L., Straube, K., Gerstein, M.B., Butter, F., and Neugebauer, K.M. (2017). Dynamic RNA-protein interactions underlie the zebrafish maternal-to-zygotic transition. Genome Res. *27*, 1184–1194.

Desrosiers, R., Friderici, K., and Rottman, F. (1974). Identification of methylated nucleosides in messenger RNA from Novikoff hepatoma cells. Proc. Natl. Acad. Sci. U. S. A. *71*, 3971–3975.

Dobin, A., Davis, C.A., Schlesinger, F., Drenkow, J., Zaleski, C., Jha, S., Batut, P., Chaisson, M., and Gingeras, T.R. (2013). STAR: Ultrafast universal RNA-seq aligner. Bioinformatics *29*, 15–

21.

Dominissini, D., Moshitch-Moshkovitz, S., Schwartz, S., Salmon-Divon, M., Ungar, L., Osenberg, S., Cesarkas, K., Jacob-Hirsch, J., Amariglio, N., Kupiec, M., et al. (2012). Topology of the human and mouse m6A RNA methylomes revealed by m6A-seq. Nature *485*, 201–206.

Dong, L., Mao, Y., Zhou, A., Liu, X.M., Zhou, J., Wan, J., and Qian, S.B. (2021). Relaxed initiation pausing of ribosomes drives oncogenic translation. Sci. Adv. *7*, 6927–6944.

Du, H., Zhao, Y., He, J., Zhang, Y., Xi, H., Liu, M., Ma, J., and Wu, L. (2016). YTHDF2 destabilizes m 6 A-containing RNA through direct recruitment of the CCR4-NOT deadenylase complex. Nat. Commun. *7*, 1–11.

Du, M., Zhang, Y., Mao, Y., Mou, J., Zhao, J., Xue, Q., Wang, D., Huang, J., Gao, S., and Gao, Y. (2017). MiR-33a suppresses proliferation of NSCLC cells via targeting METTL3 mRNA. Biochem. Biophys. Res. Commun. *482*, 582–589.

Dubin, D.T., and Taylor, R.H. (1975). The methylation state of poly A-containing-messenger RNA from cultured hamster cells. Nucleic Acids Res. *2*, 1653–1668.

Dufourt, J., Bontonou, G., Chartier, A., Jahan, C., Meunier, A.C., Pierson, S., Harrison, P.F., Papin, C., Beilharz, T.H., and Simonelig, M. (2017). PiRNAs and Aubergine cooperate with Wispy poly(A) polymerase to stabilize mRNAs in the germ plasm. Nat. Commun. *8*, 1–12.

Edupuganti, R.R., Geiger, S., Lindeboom, R.G.H., Shi, H., Hsu, P.J., Lu, Z., Wang, S.Y., Baltissen, M.P.A., Jansen, P.W.T.C., Rossa, M., et al. (2017). N6-methyladenosine (m6A) recruits and repels proteins to regulate mRNA homeostasis. Nat. Struct. Mol. Biol. *24*, 870–878.

Eichhorn, S.W., Subtelny, A.O., Kronja, I., Kwasnieski, J.C., Orr-Weaver, T.L., and Bartel, D.P. (2016). mRNA poly(A)-tail changes specified by deadenylation broadly reshape translation in Drosophila oocytes and early embryos. Elife *5*.

Engel, M., Eggert, C., Kaplick, P.M., Eder, M., Röh, S., Tietze, L., Namendorf, C., Arloth, J., Weber, P., Rex-Haffner, M., et al. (2018). The Role of m6A/m-RNA Methylation in Stress Response Regulation. Neuron *99*, 389-403.e9.

Fazi, F., and Fatica, A. (2019). Interplay between N6-methyladenosine (M6A) and noncoding RNAs in cell development and cancer. Front. Cell Dev. Biol. 7, 116.

Feng, C., Liu, Y., Wang, G., Deng, Z., Zhang, Q., Wu, W., Tong, Y., Cheng, C., and Chen, Z. (2014). Crystal structures of the human RNA demethylase alkbh5 reveal basis for substrate recognition. J. Biol. Chem. 289, 11571–11583.

Fischer, J., Koch, L., Emmerling, C., Vierkotten, J., Peters, T., Brüning, J.C., and Rüther, U. (2009). Inactivation of the Fto gene protects from obesity. Nature 458, 894–898.

Fry, N.J., Law, B.A., Ilkayeva, O.R., Holley, C.L., and Mansfield, K.D. (2017). N6-methyladenosine is required for the hypoxic stabilization of specific mRNAs. RNA 23, 1444–1455.

Frye, M., Harada, B.T., Behm, M., and He, C. (2018). RNA modifications modulate gene expression during development. Science (80-.). 361, 1346–1349.

Fu, Y., and Zhuang, X. (2020). m6A-binding YTHDF proteins promote stress granule formation. Nat. Chem. Biol. 16, 955–963.

Fukusumi, Y., Naruse, C., and Asano, M. (2008). Wtap is required for differentiation of endoderm and mesoderm in the mouse embryo. Dev. Dyn. 237, 618–629.

Furuichi, Y., Shatkin, A.J., Stavnezer, E., and Bishop, J.M. (1975). Blocked, methylated 5'-terminal sequence in avian sarcoma virus RNA. Nature 257, 618–620.

Gallo, C.M., Munro, E., Rasoloson, D., Merritt, C., and Seydoux, G. (2008). Processing bodies and germ granules are distinct RNA granules that interact in C. elegans embryos. Dev. Biol. 323, 76–87.

Gao, X., Shin, Y.-H., Li, M., Wang, F., Tong, Q., and Zhang, P. (2010). The Fat Mass and Obesity Associated Gene FTO Functions in the Brain to Regulate Postnatal Growth in Mice. PLoS One 5, e14005.

Gao, Y., Pei, G., Li, D., Li, R., Shao, Y., Zhang, Q.C., and Li, P. (2019). Multivalent m6A motifs promote phase separation of YTHDF proteins. Cell Res. 29, 767–769.

Garcias Morales, D., and Reyes, J.L. (2021). A birds'-eye view of the activity and specificity of the <scp> mRNA m ^{6} A </scp> methyltransferase complex. WIREs RNA *12*.

Geng, C., and Macdonald, P.M. (2006). Imp Associates with Squid and Hrp48 and Contributes to Localized Expression of gurken in the Oocyte. Mol. Cell. Biol. *26*, 9508–9516.

Gerber, A.P., Luschnig, S., Krasnow, M.A., Brown, P.O., and Herschlag, D. (2006). Genome-wide identification of mRNAs associated with the translational regulator PUMILIO in Drosophila melanogaster. Proc. Natl. Acad. Sci. U. S. A. *103*, 4487–4492.

Gerken, T., Girard, C.A., Tung, Y.C.L., Webby, C.J., Saudek, V., Hewitson, K.S., Yeo, G.S.H., McDonough, M.A., Cunliffe, S., McNeill, L.A., et al. (2007). The obesity-associated FTO gene encodes a 2-oxoglutarate-dependent nucleic acid demethylase. Science (80-.). *318*, 1469–1472.

Geula, S., Moshitch-Moshkovitz, S., Dominissini, D., Mansour, A.A.F., Kol, N., Salmon-Divon, M., Hershkovitz, V., Peer, E., Mor, N., Manor, Y.S., et al. (2015). m6A mRNA methylation facilitates resolution of naïve pluripotency toward differentiation. Science (80-.). *347*, 1002–1006.

Giraldez, A.J., Mishima, Y., Rihel, J., Grocock, R.J., Van Dongen, S., Inoue, K., Enright, A.J., and Schier, A.F. (2006). Zebrafish MiR-430 promotes deadenylation and clearance of maternal mRNAs. Science (80-.). *312*, 75–79.

Graindorge, A., Le Tonquèze, O., Thuret, R., Pollet, N., Osborne, H.B., and Audic, Y. (2008). Identification of CUG-BP1/EDEN-BP target mRNAs in Xenopus tropicalis. Nucleic Acids Res. *36*, 1861–1870.

Granadino, B., Campuzano, S., and Sánchez, L. (1990). The Drosophila melanogaster fl(2)d gene is needed for the female-specific splicing of Sex-lethal RNA. EMBO J. *9*, 2597–2602.

Griswold, M.D. (2016). Spermatogenesis: The Commitment to Meiosis. Physiol. Rev. *96*, 1–17.

Gu, J., Zhan, Y., Zhuo, L., Zhang, Q., Li, G., Li, Q., Qi, S., Zhu, J., Lv, Q., Shen, Y., et al. (2021). Biological functions of m6A methyltransferases. Cell Biosci. *11*, 15.

Gulati, P., Cheung, M.K., Antrobus, R., Church, C.D., Harding, H.P., Tung, Y.C.L., Rimmington, D., Ma, M., Ron, D., Lehner, P.J., et al. (2013). Role for the obesity-related FTO gene in the cellular sensing of amino acids. Proc. Natl. Acad. Sci. U. S. A. *110*, 2557–2562.

Guo, J., Tang, H.W., Li, J., Perrimon, N., and Yan, D. (2018). Xio is a component of the Drosophila sex determination pathway and RNA N6-methyladenosine methyltransferase complex. Proc. Natl. Acad. Sci. U. S. A. *115*, 3674–3679.

Han, B., Yan, S., Wei, S., Xiang, J., Liu, K., Chen, Z., Bai, R., Sheng, J., Xu, Z., and Gao, X. (2020). YTHDF 1-mediated translation amplifies Wnt-driven intestinal stemness . EMBO Rep. *21*.

Han, D., Liu, J., Chen, C., Dong, L., Liu, Y., Chang, R., Huang, X., Liu, Y., Wang, J., Dougherty, U., et al. (2019a). Anti-tumour immunity controlled through mRNA m6A methylation and YTHDF1 in dendritic cells. Nature *566*, 270–274.

Han, J., Wang, J., Yang, X., Yu, H., Zhou, R., Lu, H.-C., Yuan, W.-B., Lu, J., Zhou, Z., Lu, Q., et al. (2019b). METTL3 promote tumor proliferation of bladder cancer by accelerating pri-miR221/222 maturation in m6A-dependent manner. Mol. Cancer *18*, 110.

Hansen, T.V.O., Hammer, N.A., Nielsen, J., Madsen, M., Dalbaeck, C., Wewer, U.M., Christiansen, J., and Nielsen, F.C. (2004). Dwarfism and Impaired Gut Development in Insulin-Like Growth Factor II mRNA-Binding Protein 1-Deficient Mice. Mol. Cell. Biol. *24*, 4448–4464.

Hao, J., Hu, H., Jiang, Z., Yu, X., Li, C., Chen, L., Xia, Y., Liu, D., and Wang, D. (2020). microRNA-670 modulates Igf2bp1 expression to regulate RNA methylation in parthenogenetic mouse embryonic development. Sci. Rep. *10*, 1–6.

Harper, J.E., Miceli, S.M., Roberts, R.J., and Manley, J.L. (1990). Sequence specificity of the human mRNA N6-adenosine methylase in vitro. Nucleic Acids Res. *18*, 5735–5741.

Haussmann, I.U., Bodi, Z., Sanchez-Moran, E., Mongan, N.P., Archer, N., Fray, R.G., and Soller, M. (2016). M6 A potentiates Sxl alternative pre-mRNA splicing for robust Drosophila sex determination. Nature *540*, 301–304.

He, H., Wu, W., Sun, Z., and Chai, L. (2019). MiR-4429 prevented gastric cancer progression through targeting METTL3 to inhibit m6A-caused stabilization of SEC62. Biochem. Biophys.

Res. Commun. *517*, 581–587.

Heck, A.M., and Wilusz, C.J. (2019). Small changes, big implications: The impact of m6A RNA methylation on gene expression in pluripotency and development. Biochim. Biophys. Acta - Gene Regul. Mech. *1862*.

Heck, A.M., Russo, J., Wilusz, J., Nishimura, E.O., and Wilusz, C.J. (2020). YTHDF2 destabilizes m6A-modified neural-specific RNAs to restrain differentiation in induced pluripotent stem cells. RNA *26*, 739–755.

Hilfikert, A., Amrein, H., Dübendorfer, A., Schneiter, R., and Nöthiger, R. (1995). The gene virilizer is required for female-specific splicing controlled by SxI, the master gene for sexual development in Drosophila. Development *121*, 4017–4026.

Ho, A.J., Stein, J.L., Hua, X., Lee, S., Hibar, D.P., Leow, A.D., Dinov, I.D., Toga, A.W., Saykin, A.J., Shen, L., et al. (2010). A commonly carried allele of the obesity-related FTO gene is associated with reduced brain volume in the healthy elderly. Proc. Natl. Acad. Sci. U. S. A. *107*, 8404–8409.

Hoernes, T.P., Heimdörfer, D., Köstner, D., Faserl, K., Nußbaumer, F., Plangger, R., Kreutz, C., Lindner, H., and Erlacher, M.D. (2019). Eukaryotic Translation Elongation is Modulated by Single Natural Nucleotide Derivatives in the Coding Sequences of mRNAs. Genes (Basel). *10*, 84.

Holstein, A.F., Schulze, W., and Davidoff, M. (2003). Understanding spermatogenesis is a prerequisite for treatment. Reprod. Biol. Endocrinol. *1*, 107.

Hongay, C.F., and Orr-Weaver, T.L. (2011). Drosophila inducer of MEiosis 4 (IME4) is required for Notch signaling during oogenesis. Proc. Natl. Acad. Sci. U. S. A. *108*, 14855–14860.

Horiuchi, K., Kawamura, T., Iwanari, H., Ohashi, R., Naito, M., Kodama, T., and Hamakubo, T. (2013). Identification of Wilms' tumor 1-associating protein complex and its role in alternative splicing and the cell cycle. J. Biol. Chem. *288*, 33292–33302.

Horowitz, S., Horowitz, A., and Nilsen, T.W. (1984). Mapping of N6-methyladenosine residues in bovine prolactin mRNA. Proc. Natl. Acad. Sci. U. S. A. *81*, 5667–5671.

Hou, G., Zhao, X., Li, L., Yang, Q., Liu, X., Huang, C., Lu, R., Chen, R., Wang, Y., Jiang, B., et al. (2021). OUP accepted manuscript. Nucleic Acids Res.

Hsu, P.J., Zhu, Y., Ma, H., Guo, Y., Shi, X., Liu, Y., Qi, M., Lu, Z., Shi, H., Wang, J., et al. (2017). Ythdc2 is an N6 -methyladenosine binding protein that regulates mammalian spermatogenesis. Cell Res. *27*, 1115–1127.

Hu, Y., Ouyang, Z., Sui, X., Qi, M., Li, M., He, Y., Cao, Y., Cao, Q., Lu, Q., Zhou, S., et al. (2020). Oocyte competence is maintained by m6A methyltransferase KIAA1429-mediated RNA metabolism during mouse follicular development. Cell Death Differ. 1–16.

Huang, H., Weng, H., Sun, W., Qin, X., Shi, H., Wu, H., Zhao, B.S., Mesquita, A., Liu, C., Yuan, C.L., et al. (2018). Recognition of RNA N 6 -methyladenosine by IGF2BP proteins enhances mRNA stability and translation. Nat. Cell Biol. *20*, 285–295.

Huang, H., Weng, H., Zhou, K., Wu, T., Zhao, B.S., Sun, M., Chen, Z., Deng, X., Xiao, G., Auer, F., et al. (2019a). Histone H3 trimethylation at lysine 36 guides m6A RNA modification co-transcriptionally. Nature *567*, 414–419.

Huang, J., Dong, X., Gong, Z., Qin, L.Y., Yang, S., Zhu, Y.L., Wang, X., Zhang, D., Zou, T., Yin, P., et al. (2019b). Solution structure of the RNA recognition domain of METTL3-METTL14 N 6 -methyladenosine methyltransferase. Protein Cell *10*, 272–284.

Huang, T., Guo, J., Lv, Y., Zheng, Y., Feng, T., Gao, Q., and Zeng, W. (2019c). Meclofenamic acid represses spermatogonial proliferation through modulating m6A RNA modification. J. Anim. Sci. Biotechnol. *10*, 63.

Huang, T., Chen, W., Liu, J., Gu, N., and Zhang, R. (2019d). Genome-wide identification of mRNA 5-methylcytosine in mammals. Nat. Struct. Mol. Biol. *26*, 380–388.

Huang, T., Liu, Z., Zheng, Y., Feng, T., Gao, Q., and Zeng, W. (2020). YTHDF2 promotes spermagonial adhesion through modulating MMPs decay via m6A/mRNA pathway. Cell Death Dis. *11*, 1–11.

Ivanova, I., Much, C., Di Giacomo, M., Azzi, C., Morgan, M., Moreira, P.N., Monahan, J., Carrieri, C., Enright, A.J., and O'Carroll, D. (2017). The RNA m6A Reader YTHDF2 Is Essential for the Post-transcriptional Regulation of the Maternal Transcriptome and Oocyte Competence.

Mol. Cell *67*, 1059-1067.e4.

Jain, D., Puno, M.R., Meydan, C., Lailler, N., Mason, C.E., Lima, C.D., Anderson, K. V., and Keeney, S. (2018). Ketu mutant mice uncover an essential meiotic function for the ancient RNA helicase YTHDC2. Elife *7*.

Jao, L.E., Wente, S.R., and Chen, W. (2013). Efficient multiplex biallelic zebrafish genome editing using a CRISPR nuclease system. Proc. Natl. Acad. Sci. U. S. A. *110*, 13904–13909.

Jia, G., Fu, Y., Zhao, X., Dai, Q., Zheng, G., Yang, Y., Yi, C., Lindahl, T., Pan, T., Yang, Y.G., et al. (2011). N6-Methyladenosine in nuclear RNA is a major substrate of the obesity-associated FTO. Nat. Chem. Biol. *7*, 885–887.

Jia, G.X., Lin, Z., Yan, R.G., Wang, G.W., Zhang, X.N., Li, C., Tong, M.H., and Yang, Q.E. (2020). WTAP Function in Sertoli Cells Is Essential for Sustaining the Spermatogonial Stem Cell Niche. Stem Cell Reports *15*, 968–982.

Jin, D., Guo, J., Wu, Y., Yang, L., Wang, X., Du, J., Dai, J., Chen, W., Gong, K., Miao, S., et al. (2020). M6A demethylase ALKBH5 inhibits tumor growth and metastasis by reducing YTHDFs-mediated YAP expression and inhibiting miR-107/LATS2-mediated YAP activity in NSCLC. Mol. Cancer *19*, 40.

Kan, L., Grozhik, A. V., Vedanayagam, J., Patil, D.P., Pang, N., Lim, K.S., Huang, Y.C., Joseph, B., Lin, C.J., Despic, V., et al. (2017). The m 6 A pathway facilitates sex determination in Drosophila. Nat. Commun. *8*.

Kane, D.A., Hammerschmidt, M., Mullins, M.C., Maischein, H.M., Brand, M., van Eeden, F.J., Furutani-Seiki, M., Granato, M., Haffter, P., Heisenberg, C.P., et al. (1996). The zebrafish epiboly mutants. Development *123*.

Kasowitz, S.D., Ma, J., Anderson, S.J., Leu, N.A., Xu, Y., Gregory, B.D., Schultz, R.M., and Wang, P.J. (2018). Nuclear m6A reader YTHDC1 regulates alternative polyadenylation and splicing during mouse oocyte development. PLoS Genet. *14*, e1007412.

Ke, S., Pandya-Jones, A., Saito, Y., Fak, J.J., Vågbø, C.B., Geula, S., Hanna, J.H., Black, D.L., Darnell, J.E., and Darnell, R.B. (2017). m6A mRNA modifications are deposited in nascent pre-mRNA and are not required for splicing but do specify cytoplasmic turnover. Genes Dev. *31*, 990–

1006.

Kennedy, E.M., Bogerd, H.P., Kornepati, A.V.R., Kang, D., Ghoshal, D., Marshall, J.B., Poling, B.C., Tsai, K., Gokhale, N.S., Horner, S.M., et al. (2016). Posttranscriptional m6A Editing of HIV-1 mRNAs Enhances Viral Gene Expression. Cell Host Microbe *19*, 675–685.

Kimmel, C.B., Ballard, W.W., Kimmel, S.R., Ullmann, B., and Schilling, T.F. (1995). Stages of embryonic development of the zebrafish. Dev. Dyn. *203*, 253–310.

Knuckles, P., Carl, S.H., Musheev, M., Niehrs, C., Wenger, A., and Bühler, M. (2017). RNA fate determination through cotranscriptional adenosine methylation and microprocessor binding. Nat. Struct. Mol. Biol. *24*, 561–569.

Knuckles, P., Lence, T., Haussmann, I.U., Jacob, D., Kreim, N., Carl, S.H., Masiello, I., Hares, T., Villaseñor, R., Hess, D., et al. (2018). Zc3h13/Flacc is required for adenosine methylation by bridging the mRNA-binding factor RbM15/spenito to the m6 a machinery component Wtap/Fl(2)d. Genes Dev. *32*, 415–429.

Koh, C.W.Q., Goh, Y.T., and Goh, W.S.S. (2019). Atlas of quantitative single-base-resolution N 6-methyl-adenine methylomes. Nat. Commun. *10*, 1–15.

Konno, M., Koseki, J., Asai, A., Yamagata, A., Shimamura, T., Motooka, D., Okuzaki, D., Kawamoto, K., Mizushima, T., Eguchi, H., et al. (2019). Distinct methylation levels of mature microRNAs in gastrointestinal cancers. Nat. Commun. *10*, 1–7.

Kontur, C., and Giraldez, A. (2017). RNA Methylation Clears the Way. Dev. Cell *40*, 427–428.

Kontur, C., Jeong, M., Cifuentes, D., and Giraldez, A.J. (2020). Ythdf m6A Readers Function Redundantly during Zebrafish Development. Cell Rep. *33*, 108598.

Kretschmer, J., Rao, H., Hackert, P., Sloan, K.E., Höbartner, C., and Bohnsack, M.T. (2018). The m6A reader protein YTHDC2 interacts with the small ribosomal subunit and the 5′-3′ exoribonuclease XRN1. RNA *24*, 1339–1350.

Kwon, J., Jo, Y.J., Namgoong, S., and Kim, N.H. (2019). Functional roles of hnRNPA2/B1 regulated by METTL3 in mammalian embryonic development. Sci. Rep. *9*.

Lasman, L., Krupalnik, V., Viukov, S., Mor, N., Aguilera-Castrejon, A., Schneir, D., Bayerl, J., Mizrahi, O., Peles, S., Tawil, S., et al. (2020a). Context-dependent functional compensation between Ythdf m6A reader proteins. Genes Dev.

Lasman, L., Hanna, J.H., and Novershtern, N. (2020b). Role of m6A in Embryonic Stem Cell Differentiation and in Gametogenesis. Epigenomes *4*, 5.

Laver, J.D., Li, X., Ray, D., Cook, K.B., Hahn, N.A., Nabeel-Shah, S., Kekis, M., Luo, H., Marsolais, A.J., Fung, K.Y.Y., et al. (2015). Brain tumor is a sequence-specific RNA-binding protein that directs maternal mRNA clearance during the Drosophila maternal-to-zygotic transition. Genome Biol. *16*, 94.

Lee, M.T., Bonneau, A.R., Takacs, C.M., Bazzini, A.A., Divito, K.R., Fleming, E.S., and Giraldez, A.J. (2013). Nanog, Pou5f1 and SoxB1 activate zygotic gene expression during the maternal-to-zygotic transition. Nature *503*, 360–364.

Lee, M.T., Bonneau, A.R., and Giraldez, A.J. (2014). Zygotic Genome Activation During the Maternal-to-Zygotic Transition. Annu. Rev. Cell Dev. Biol. *30*, 581–613.

Lee, Y., Choe, J., Park, O.H., and Kim, Y.K. (2020). Molecular Mechanisms Driving mRNA Degradation by m6A Modification. Trends Genet. *36*, 177–188.

Lence, T., Akhtar, J., Bayer, M., Schmid, K., Spindler, L., Ho, C.H., Kreim, N., Andrade-Navarro, M.A., Poeck, B., Helm, M., et al. (2016). M6A modulates neuronal functions and sex determination in Drosophila. Nature *540*, 242–247.

Lence, T., Paolantoni, C., Worpenberg, L., and Roignant, J.Y. (2019). Mechanistic insights into m 6 A RNA enzymes. Biochim. Biophys. Acta - Gene Regul. Mech. *1862*, 222–229.

Li, A., Chen, Y.S., Ping, X.L., Yang, X., Xiao, W., Yang, Y., Sun, H.Y., Zhu, Q., Baidya, P., Wang, X., et al. (2017a). Cytoplasmic m 6 A reader YTHDF3 promotes mRNA translation. Cell Res. *27*, 444–447.

Li, F., Zhao, D., Wu, J., and Shi, Y. (2014). Structure of the YTH domain of human YTHDF2 in complex with an m6A mononucleotide reveals an aromatic cage for m6A recognition. Cell Res.

24, 1490–1492.

Li, H.B., Tong, J., Zhu, S., Batista, P.J., Duffy, E.E., Zhao, J., Bailis, W., Cao, G., Kroehling, L., Chen, Y., et al. (2017b). M 6 A mRNA methylation controls T cell homeostasis by targeting the IL-7/STAT5/SOCS pathways. Nature *548*, 338–342.

Li, J., Wu, L., Pei, M., and Zhang, Y. (2020). YTHDF2, a protein repressed by miR-145, regulates proliferation, apoptosis, and migration in ovarian cancer cells. J. Ovarian Res. *13*.

Li, L., Zang, L., Zhang, F., Chen, J., Shen, H., Shu, L., Liang, F., Feng, C., Chen, D., Tao, H., et al. (2017c). Fat mass and obesity-associated (FTO) protein regulates adult neurogenesis. Hum. Mol. Genet. *26*, 2398–2411.

Li, M., Zhao, X., Wang, W., Shi, H., Pan, Q., Lu, Z., Perez, S.P., Suganthan, R., He, C., Bjørås, M., et al. (2018). Ythdf2-mediated m6A mRNA clearance modulates neural development in mice. Genome Biol. *19*.

Li, Y., Bedi, R.K., Wiedmer, L., Sun, X., Huang, D., and Caflisch, A. (2021). Atomistic and Thermodynamic Analysis of N6-Methyladenosine (m ^{6} A) Recognition by the Reader Domain of YTHDC1. J. Chem. Theory Comput. acs.jctc.0c01136.

Li, Z., Weng, H., Su, R., Weng, X., Zuo, Z., Li, C., Huang, H., Nachtergaele, S., Dong, L., Hu, C., et al. (2017d). FTO Plays an Oncogenic Role in Acute Myeloid Leukemia as a N6-Methyladenosine RNA Demethylase. Cancer Cell *31*, 127–141.

Liang, W., Lin, Z., Du, C., Qiu, D., and Zhang, Q. (2020). mRNA modification orchestrates cancer stem cell fate decisions. Mol. Cancer *19*, 38.

Lin, S., Choe, J., Du, P., Triboulet, R., and Gregory, R.I. (2016). The m6A Methyltransferase METTL3 Promotes Translation in Human Cancer Cells. Mol. Cell *62*, 335–345.

Lin, X., Chai, G., Wu, Y., Li, J., Chen, F., Liu, J., Luo, G., Tauler, J., Du, J., Lin, S., et al. (2019). RNA m 6 A methylation regulates the epithelial mesenchymal transition of cancer cells and translation of Snail. Nat. Commun. *10*.

Lin, Z., Hsu, P.J., Xing, X., Fang, J., Lu, Z., Zou, Q., Zhang, K.J., Zhang, X., Zhou, Y., Zhang, T.,

et al. (2017). Mettl3-/Mettl14-mediated mRNA N 6-methyladenosine modulates murine spermatogenesis. Cell Res. *27*, 1216–1230.

Lindell, T.J., Weinberg, F., Morris, P.W., Roeder, R.G., and Rutter, W.J. (1970). Specific inhibition of nuclear RNA polymerase II by α-amanitin. Science (80-.). *170*, 447–449.

Linder, B., and Jaffrey, S.R. (2019). Discovering and mapping the modified nucleotides that comprise the epitranscriptome of mrna. Cold Spring Harb. Perspect. Biol. *11*, a032201.

Linder, B., Grozhik, A. V., Olarerin-George, A.O., Meydan, C., Mason, C.E., and Jaffrey, S.R. (2015). Single-nucleotide-resolution mapping of m6A and m6Am throughout the transcriptome. Nat. Methods *12*, 767–772.

Liu, H. Bin, Muhammad, T., Guo, Y., Li, M.J., Sha, Q.Q., Zhang, C.X., Liu, H., Zhao, S.G., Zhao, H., Zhang, H., et al. (2019). RNA-Binding Protein IGF2BP2/IMP2 is a Critical Maternal Activator in Early Zygotic Genome Activation. Adv. Sci. *6*.

Liu, J., Yue, Y., Han, D., Wang, X., Fu, Y., Zhang, L., Jia, G., Yu, M., Lu, Z., Deng, X., et al. (2014). A METTL3-METTL14 complex mediates mammalian nuclear RNA N6-adenosine methylation. Nat. Chem. Biol. *10*, 93–95.
Liu, J., Yue, Y., Liu, J., Cui, X., Cao, J., Luo, G., Zhang, Z., Cheng, T., Gao, M., Shu, X., et al. (2018a). VIRMA mediates preferential m6A mRNA methylation in 3′UTR and near stop codon and associates with alternative polyadenylation. Cell Discov. *4*, 10.

Liu, J., Eckert, M.A., Harada, B.T., Liu, S.M., Lu, Z., Yu, K., Tienda, S.M., Chryplewicz, A., Zhu, A.C., Yang, Y., et al. (2018b). m 6 A mRNA methylation regulates AKT activity to promote the proliferation and tumorigenicity of endometrial cancer. Nat. Cell Biol. *20*, 1074–1083.

Liu, J., Li, K., Cai, J., Zhang, M., Zhang, X., Xiong, X., Meng, H., Xu, X., Huang, Z., Peng, J., et al. (2020a). Landscape and Regulation of m6A and m6Am Methylome across Human and Mouse Tissues. Mol. Cell *77*, 426-440.e6.

Liu, J., Gao, M., Xu, S., Chen, Y., Wu, K., Liu, H., Wang, J., Yang, X., Wang, J., Liu, W., et al. (2020b). YTHDF2/3 Are Required for Somatic Reprogramming through Different RNA Deadenylation Pathways. Cell Rep. *32*, 108120.

Liu, N., Dai, Q., Zheng, G., He, C., Parisien, M., and Pan, T. (2015). N6 -methyladenosine-

dependent RNA structural switches regulate RNA-protein interactions. Nature *518*, 560–564.

Liu, N., Zhou, K.I., Parisien, M., Dai, Q., Diatchenko, L., and Pan, T. (2017). N6-methyladenosine alters RNA structure to regulate binding of a low-complexity protein. Nucleic Acids Res. *45*, 6051–6063.

Liu, T., Wei, Q., Jin, J., Luo, Q., Liu, Y., Yang, Y., Cheng, C., Li, L., Pi, J., Si, Y., et al. (2020c). The m6A reader YTHDF1 promotes ovarian cancer progression via augmenting EIF3C translation. Nucleic Acids Res. *48*, 3816–3831.

Liu, Y., Luo, D., Zhao, H., Zhu, Z., Hu, W., and Cheng, C.H.K. (2013). Inheritable and Precise Large Genomic Deletions of Non-Coding RNA Genes in Zebrafish Using TALENs. PLoS One *8*, e76387.

Liu, Z., Zhang, J., and Yeager, M. (2018c). Most m6A RNA Modifications in Protein-Coding Regions Are Evolutionary Unconserved and Likely Nonfunctional. Mol. Biol. Evol. *35*, 666–675.

Livneh, I., Moshitch-Moshkovitz, S., Amariglio, N., Rechavi, G., and Dominissini, D. (2020). The m6A epitranscriptome: transcriptome plasticity in brain development and function. Nat. Rev. Neurosci. *21*, 36–51.

Louloupi, A., Ntini, E., Conrad, T., and Ørom, U.A.V. (2018). Transient N-6-Methyladenosine Transcriptome Sequencing Reveals a Regulatory Role of m6A in Splicing Efficiency. Cell Rep. *23*, 3429–3437.

Love, M.I., Huber, W., and Anders, S. (2014). Moderated estimation of fold change and dispersion for RNA-seq data with DESeq2. Genome Biol. *15*, 550.

Lu, W., Tirumuru, N., Gelais, C.S., Koneru, P.C., Liu, C., Kvaratskhelia, M., He, C., and Wu, L. (2018). N 6 -Methyladenosine– binding proteins suppress HIV-1 infectivity and viral production. J. Biol. Chem. *293*, 12992–13005.

Lund, E., Liu, M., Hartley, R.S., Sheets, M.D., and Dahlberg, J.E. (2009). Deadenylation of maternal mRNAs mediated by miR-427 in Xenopus laevis embryos. RNA *15*, 2351–2363.

Luo, S., and Tong, L. (2014). Molecular basis for the recognition of methylated adenines in RNA

by the eukaryotic YTH domain. Proc. Natl. Acad. Sci. U. S. A. *111*, 13834–13839.

Luo, J.H., Wang, Y., Wang, M., Zhang, L.Y., Peng, H.R., Zhou, Y.Y., Jia, G.F., and He, Y. (2020a). Natural variation in RNA m6a methylation and its relationship with translational status. Plant Physiol. *182*, 332–344.

Luo, Y., Na, Z., and Slavoff, S.A. (2018). P-Bodies: Composition, Properties, and Functions. Biochemistry *57*, 2424–2431.

Luo, Y., Schofield, J.A., Simon, M.D., and Slavoff, S.A. (2020b). Global Profiling of Cellular Substrates of Human Dcp2. Biochemistry *59*, 4176–4188.

Ma, C., Chang, M., Lv, H., Zhang, Z.W., Zhang, W., He, X., Wu, G., Zhao, S., Zhang, Y., Wang, D., et al. (2018). RNA m6A methylation participates in regulation of postnatal development of the mouse cerebellum. Genome Biol. *19*.

Ma, J.Z., Yang, F., Zhou, C.C., Liu, F., Yuan, J.H., Wang, F., Wang, T.T., Xu, Q.G., Zhou, W.P., and Sun, S.H. (2017). METTL14 suppresses the metastatic potential of hepatocellular carcinoma by modulating N6-methyladenosine-dependent primary MicroRNA processing. Hepatology *65*, 529–543.

Makino, S., Mishima, Y., Inoue, K., and Inada, T. (2015). Roles of mRNA fate modulators Dhh1 and Pat1 in TNRC6-dependent gene silencing recapitulated in yeast. J. Biol. Chem. *290*, 8331–8347.

Mao, Y., Dong, L., Liu, X.M., Guo, J., Ma, H., Shen, B., and Qian, S.B. (2019). m6A in mRNA coding regions promotes translation via the RNA helicase-containing YTHDC2. Nat. Commun. *10*, 1–11.

Marlow, F.L. (2018). Recent advances in understanding oogenesis: Interactions with the cytoskeleton, microtubule organization, and meiotic spindle assembly in oocytes [version 1; referees: 2 approved]. F1000Research *7*, 468.

Mathavan, S., Lee, S.G.P., Mak, A., Miller, L.D., Murthy, K.R.K., Govindarajan, K.R., Tong, Y., Wu, Y.L., Lam, S.H., Yang, H., et al. (2005). Transcriptome analysis of zebrafish embryogenesis using microarrays. PLoS Genet. *1*, 0260–0276.

Mauer, J., and Jaffrey, S.R. (2018). FTO, m ^{6} A $_m$, and the hypothesis of reversible epitranscriptomic mRNA modifications. FEBS Lett. *592*, 2012–2022.

Mauer, J., Luo, X., Blanjoie, A., Jiao, X., Grozhik, A. V., Patil, D.P., Linder, B., Pickering, B.F., Vasseur, J.J., Chen, Q., et al. (2017). Reversible methylation of m6 Am in the 5′ cap controls mRNA stability. Nature *541*, 371–375.

Mauer, J., Sindelar, M., Despic, V., Guez, T., Hawley, B.R., Vasseur, J.J., Rentmeister, A., Gross, S.S., Pellizzoni, L., Debart, F., et al. (2019). FTO controls reversible m 6 Am RNA methylation during snRNA biogenesis. Nat. Chem. Biol. *15*, 340–347.

McIntyre, A.B.R., Gokhale, N.S., Cerchietti, L., Jaffrey, S.R., Horner, S.M., and Mason, C.E. (2020). Limits in the detection of m6A changes using MeRIP/m6A-seq. Sci. Rep. *10*, 1–15.

Medina-Muñoz, S.G., Kushawah, G., Castellano, L.A., Diez, M., DeVore, M.L., Salazar, M.J.B., and Bazzini, A.A. (2021). Crosstalk between codon optimality and cis-regulatory elements dictates mRNA stability. Genome Biol. *22*, 14.

Meng, T.G., Lu, X., Guo, L., Hou, G.M., Ma, X.S., Li, Q.N., Huang, L., Fan, L.H., Zhao, Z.H., Ou, X.H., et al. (2019). Mettl14 is required for mouse postimplantation development by facilitating epiblast maturation. FASEB J. *33*, 1179–1187.

Merkestein, M., Laber, S., McMurray, F., Andrew, D., Sachse, G., Sanderson, J., Li, M., Usher, S., Sellayah, D., Ashcroft, F.M., et al. (2015). FTO influences adipogenesis by regulating mitotic clonal expansion. Nat. Commun. *6*, 1–9.

Meyer, K.D. (2019). m 6 A-mediated translation regulation. Biochim. Biophys. Acta - Gene Regul. Mech. *1862*, 301–309.

Meyer, K.D., Saletore, Y., Zumbo, P., Elemento, O., Mason, C.E., and Jaffrey, S.R. (2012). Comprehensive analysis of mRNA methylation reveals enrichment in 3′ UTRs and near stop codons. Cell *149*, 1635–1646.

Meyer, K.D., Patil, D.P., Zhou, J., Zinoviev, A., Skabkin, M.A., Elemento, O., Pestova, T. V., Qian, S.B., and Jaffrey, S.R. (2015). 5′ UTR m6A Promotes Cap-Independent Translation. Cell *163*, 999–1010.

Miao, L., Yuan, Y., Cheng, F., Fang, J., Zhou, F., Ma, W., Jiang, Y., Huang, X., Wang, Y., Shan, L., et al. (2017). Translation repression by maternal RNA binding protein Zar1 is essential for early oogenesis in zebrafish. Dev. *144*, 128–138.

Miao, W., Li, L., Zhao, Y., Dai, X., Chen, X., and Wang, Y. (2019). HSP90 inhibitors stimulate DNAJB4 protein expression through a mechanism involving N 6-methyladenosine. Nat. Commun. *10*, 1–12.

Min, K.W., Zealy, R.W., Davila, S., Fomin, M., Cummings, J.C., Makowsky, D., Mcdowell, C.H., Thigpen, H., Hafner, M., Kwon, S.H., et al. (2018). Profiling of m6A RNA modifications identified an age-associated regulation of AGO2 mRNA stability. Aging Cell *17*.

Mishima, Y., and Tomari, Y. (2016). Codon Usage and 3' UTR Length Determine Maternal mRNA Stability in Zebrafish. Mol. Cell *61*, 874–885.

Mishima, Y., and Tomari, Y. (2017). Pervasive yet nonuniform contributions of Dcp2 and Cnot7 to maternal mRNA clearance in zebrafish. Genes to Cells *22*, 670–678.

Moindrot, B., Cerase, A., Coker, H., Masui, O., Grijzenhout, A., Pintacuda, G., Schermelleh, L., Nesterova, T.B., and Brockdorff, N. (2015). A Pooled shRNA Screen Identifies Rbm15, Spen, and Wtap as Factors Required for Xist RNA-Mediated Silencing. Cell Rep. *12*, 562–572.

Moraes, K.C.M., Wilusz, C.J., and Wilusz, J. (2006). CUG-BP binds to RNA substrates and recruits PARN deadenylase. RNA *12*, 1084–1091.

Moreno-Mateos, M.A., Vejnar, C.E., Beaudoin, J.D., Fernandez, J.P., Mis, E.K., Khokha, M.K., and Giraldez, A.J. (2015). CRISPRscan: Designing highly efficient sgRNAs for CRISPR-Cas9 targeting in vivo. Nat. Methods *12*, 982–988.

Morgan, M., Much, C., DiGiacomo, M., Azzi, C., Ivanova, I., Vitsios, D.M., Pistolic, J., Collier, P., Moreira, P.N., Benes, V., et al. (2017). MRNA 3′ uridylation and poly(A) tail length sculpt the mammalian maternal transcriptome. Nature *548*, 347–351.

Müller, S., Glaß, M., Singh, A.K., Haase, J., Bley, N., Fuchs, T., Lederer, M., Dahl, A., Huang, H., Chen, J., et al. (2019). IGF2BP1 promotes SRF-dependent transcription in cancer in a m 6 A-

and miRNA-dependent manner. Nucleic Acids Res. *47*, 375–390.

Munro, T.P., Kwon, S., Schnapp, B.J., and St Johnston, D. (2006). A repeated IMP-binding motif controls oskar mRNA translation and anchoring independently of Drosophila melanogaster IMP. J. Cell Biol. *172*, 577–588.

Nagabhushana, A., and Mishra, R.K. (2016). Finding clues to the riddle of sex determination in zebrafish. J. Biosci. *41*, 145–155.

Newton, F.G., Harris, R.E., Sutcliffe, C., and Ashe, H.L. (2015). Coordinate post-transcriptional repression of Dpp-dependent transcription factors attenuates signal range during development. Dev. *142*, 3362–3373.

Nichols, J.L. (1979). N6-methyladenosine in maize poly(A)-containing RNA. Plant Sci. Lett. *15*, 357–361.

Nielsen, J., Christiansen, J., Lykke-Andersen, J., Johnsen, A.H., Wewer, U.M., and Nielsen, F.C. (1999). A Family of Insulin-Like Growth Factor II mRNA-Binding Proteins Represses Translation in Late Development. Mol. Cell. Biol. *19*, 1262–1270.

Ontiveros, R.J., Shen, H., Stoute, J., Yanas, A., Cui, Y., Zhang, Y., and Liu, K.F. (2020). Coordination of mRNA and tRNA methylations by TRMT10A. Proc. Natl. Acad. Sci. *117*, 201913448.

Örn, S., Holbech, H., Madsen, T.H., Norrgren, L., and Petersen, G.I. (2003). Gonad development and vitellogenin production in zebrafish (Danio rerio) exposed to ethinylestradiol and methyltestosterone. Aquat. Toxicol. *65*, 397–411.

Ortega, A., Niksic, M., Bachi, A., Wilm, M., Sánchez, L., Hastie, N., and Valcárcel, J. (2003). Biochemical function of female-lethal (2)D/Wilms' tumor suppressor-1-associated proteins in alternative pre-mRNA splicing. J. Biol. Chem. *278*, 3040–3047.

Paillard, L., Omilli, F., Legagneux, V., Bassez, T., Maniey, D., and Osborne, H.B. (1998). EDEN and EDEN-BP, a cis element and an associated factor that mediate sequence-specific mRNA deadenylation in Xenopus embryos. EMBO J. *17*, 278–287.

Pan, H., O'Brien, M.J., Wigglesworth, K., Eppig, J.J., and Schultz, R.M. (2005). Transcript profiling during mouse oocyte development and the effect of gonadotropin priming and development in vitro. Dev. Biol. *286*, 493–506.

Pandey, R.R., Delfino, E., Homolka, D., Roithova, A., Chen, K.M., Li, L., Franco, G., Vågbø, C.B., Taillebourg, E., Fauvarque, M.O., et al. (2020). The Mammalian Cap-Specific m6Am RNA Methyltransferase PCIF1 Regulates Transcript Levels in Mouse Tissues. Cell Rep. *32*, 108038.

Panneerdoss, S., Eedunuri, V.K., Yadav, P., Timilsina, S., Rajamanickam, S., Viswanadhapalli, S., Abdelfattah, N., Onyeagucha, B.C., Cui, X., Lai, Z., et al. (2018). Cross-talk among writers, readers, and erasers of m6A regulates cancer growth and progression. Sci. Adv. *4*.

Paris, J., Morgan, M., Campos, J., Spencer, G.J., Shmakova, A., Ivanova, I., Mapperley, C., Lawson, H., Wotherspoon, D.A., Sepulveda, C., et al. (2019). Targeting the RNA m6A Reader YTHDF2 Selectively Compromises Cancer Stem Cells in Acute Myeloid Leukemia. Cell Stem Cell *25*, 137-148.e6.

Park, O.H., Ha, H., Lee, Y., Boo, S.H., Kwon, D.H., Song, H.K., and Kim, Y.K. (2019). Endoribonucleolytic Cleavage of m6A-Containing RNAs by RNase P/MRP Complex. Mol. Cell *74*, 494-507.e8.

Patil, D.P., Chen, C.K., Pickering, B.F., Chow, A., Jackson, C., Guttman, M., and Jaffrey, S.R. (2016). M6 A RNA methylation promotes XIST-mediated transcriptional repression. Nature *537*, 369–373.

Patil, D.P., Pickering, B.F., and Jaffrey, S.R. (2018). Reading m6A in the Transcriptome: m6A-Binding Proteins. Trends Cell Biol. *28*, 113–127.

Peng, W., Li, J., Chen, R., Gu, Q., Yang, P., Qian, W., Ji, D., Wang, Q., Zhang, Z., Tang, J., et al. (2019). Upregulated METTL3 promotes metastasis of colorectal Cancer via miR-1246/SPRED2/MAPK signaling pathway. J. Exp. Clin. Cancer Res. *38*.

Penn, J.K.M., Graham, P., Deshpande, G., Calhoun, G., Chaouki, A.S., Salz, H.K., and Schedl, P. (2008). Functioning of the drosophila Wilms'-tumor-1-associated protein homolog, Fl(2)d, in sex-lethal-dependent alternative splicing. Genetics *178*, 737–748.

Perry, R.P., and Kelley, D.E. (1974). Existence of methylated messenger RNA in mouse L cells.

Cell *1*, 37–42.

Perry, R.P., Kelley, D.E., Friderici, K., and Rottman, F. (1975). The methylated constituents of L cell messenger RNA: Evidence for an unusual cluster at the 5′ terminus. Cell *4*, 387–394.

Ping, X.L., Sun, B.F., Wang, L., Xiao, W., Yang, X., Wang, W.J., Adhikari, S., Shi, Y., Lv, Y., Chen, Y.S., et al. (2014). Mammalian WTAP is a regulatory subunit of the RNA N6-methyladenosine methyltransferase. Cell Res. *24*, 177–189.

Presnyak, V., Alhusaini, N., Chen, Y.H., Martin, S., Morris, N., Kline, N., Olson, S., Weinberg, D., Baker, K.E., Graveley, B.R., et al. (2015). Codon optimality is a major determinant of mRNA stability. Cell *160*, 1111–1124.

Qi, S.T., Ma, J.Y., Wang, Z.B., Guo, L., Hou, Y., and Sun, Q.Y. (2016). N6 -methyladenosine sequencing highlights the involvement of mRNA methylation in oocyte meiotic maturation and embryo development by regulating translation in xenopus laevis. J. Biol. Chem. *291*, 23020–23026.

Rabani, M., Raychowdhury, R., Jovanovic, M., Rooney, M., Stumpo, D.J., Pauli, A., Hacohen, N., Schier, A.F., Blackshear, P.J., Friedman, N., et al. (2014). High-resolution sequencing and modeling identifies distinct dynamic RNA regulatory strategies. Cell *159*, 1698–1710.

Rabani, M., Pieper, L., Chew, G.L., and Schier, A.F. (2017). A Massively Parallel Reporter Assay of 3′ UTR Sequences Identifies In Vivo Rules for mRNA Degradation. Mol. Cell *68*, 1083-1094.e5.

Radhakrishnan, A., Chen, Y.H., Martin, S., Alhusaini, N., Green, R., and Coller, J. (2016). The DEAD-Box Protein Dhh1p Couples mRNA Decay and Translation by Monitoring Codon Optimality. Cell *167*, 122-132.e9.

Raffel, G.D., Chu, G.C., Jesneck, J.L., Cullen, D.E., Bronson, R.T., Bernard, O.A., and Gilliland, D.G. (2009). Ott1 (Rbm15) Is Essential for Placental Vascular Branching Morphogenesis and Embryonic Development of the Heart and Spleen. Mol. Cell. Biol. *29*, 333–341.

Rajecka, V., Skalicky, T., and Vanacova, S. (2019). The role of RNA adenosine demethylases in the control of gene expression. Biochim. Biophys. Acta - Gene Regul. Mech. *1862*, 343–355.

Ren, F., Lin, Q., Gong, G., Du, X., Dan, H., Qin, W., Miao, R., Xiong, Y., Xiao, R., Li, X., et al. (2020). Igf2bp3 maintains maternal RNA stability and ensures early embryo development in zebrafish. Commun. Biol. *3*, 94.

Ries, R.J., Zaccara, S., Klein, P., Olarerin-George, A., Namkoong, S., Pickering, B.F., Patil, D.P., Kwak, H., Lee, J.H., and Jaffrey, S.R. (2019). m6A enhances the phase separation potential of mRNA. Nature *571*, 424–428.

Robbens, S., Rouzé, P., Cock, J.M., Spring, J., Worden, A.Z., and Van De Peer, Y. (2008). The FTO gene, implicated in human obesity, is found only in vertebrates and marine algae. J. Mol. Evol. *66*, 80–84.

Roost, C., Lynch, S.R., Batista, P.J., Qu, K., Chang, H.Y., and Kool, E.T. (2015). Structure and thermodynamics of N6-methyladenosine in RNA: A spring-loaded base modification. J. Am. Chem. Soc. *137*, 2107–2115.

Rouget, C., Papin, C., Boureux, A., Meunier, A.C., Franco, B., Robine, N., Lai, E.C., Pelisson, A., and Simonelig, M. (2010). Maternal mRNA deadenylation and decay by the piRNA pathway in the early Drosophila embryo. Nature *467*, 1128–1132.

Roundtree, I.A., Evans, M.E., Pan, T., and He, C. (2017a). Dynamic RNA Modifications in Gene Expression Regulation. Cell *169*, 1187–1200.

Roundtree, I.A., Luo, G.Z., Zhang, Z., Wang, X., Zhou, T., Cui, Y., Sha, J., Huang, X., Guerrero, L., Xie, P., et al. (2017b). YTHDC1 mediates nuclear export of N6-methyladenosine methylated mRNAs. Elife *6*.

Růžička, K., Zhang, M., Campilho, A., Bodi, Z., Kashif, M., Saleh, M., Eeckhout, D., El-Showk, S., Li, H., Zhong, S., et al. (2017). Identification of factors required for m6A mRNA methylation in Arabidopsis reveals a role for the conserved E3 ubiquitin ligase HAKAI. New Phytol. *215*, 157–172.

Sánchez, F., and Smitz, J. (2012). Molecular control of oogenesis. Biochim. Biophys. Acta - Mol. Basis Dis. *1822*, 1896–1912.

Santos, D., Luzio, A., and Coimbra, A.M. (2017). Zebrafish sex differentiation and gonad

development: A review on the impact of environmental factors. Aquat. Toxicol. *191*, 141–163.

Schneider, C.A., Rasband, W.S., and Eliceiri, K.W. (2012). NIH Image to ImageJ: 25 years of image analysis. Nat. Methods *9*, 671–675.

Schöller, E., Weichmann, F., Treiber, T., Ringle, S., Treiber, N., Flatley, A., Feederle, R., Bruckmann, A., and Meister, G. (2018). Interactions, localization, and phosphorylation of the m6A generating METTL3–METTL14–WTAP complex. RNA *24*, 499–512.

Schubert, C.M., Lin, R., De Vries, C.J., Plasterk, R.H.A., and Priess, J.R. (2000). MEX-5 and MEX-6 function to establish soma/germline asymmetry in early C. elegans embryos. Mol. Cell *5*, 671–682.

Schwartz, S., Agarwala, S.D., Mumbach, M.R., Jovanovic, M., Mertins, P., Shishkin, A., Tabach, Y., Mikkelsen, T.S., Satija, R., Ruvkun, G., et al. (2013). High-Resolution mapping reveals a conserved, widespread, dynamic mRNA methylation program in yeast meiosis. Cell *155*, 1409–1421.

Schwartz, S., Mumbach, M.R., Jovanovic, M., Wang, T., Maciag, K., Bushkin, G.G., Mertins, P., Ter-Ovanesyan, D., Habib, N., Cacchiarelli, D., et al. (2014). Perturbation of m6A writers reveals two distinct classes of mRNA methylation at internal and 5' sites. Cell Rep. *8*, 284–296.

Semotok, J.L., Cooperstock, R.L., Pinder, B.D., Vari, H.K., Lipshitz, H.D., and Smibert, C.A. (2005). Smaug recruits the CCR4/POP2/NOT deadenylase complex to trigger maternal transcript localization in the early Drosophila embryo. Curr. Biol. *15*, 284–294.

Seo, K.W., and Kleiner, R.E. (2020). YTHDF2 Recognition of N1-Methyladenosine (m1A)-Modified RNA Is Associated with Transcript Destabilization. ACS Chem. Biol. *15*, 132–139.

Sharpe, J.J., and Cooper, T.A. (2017). Unexpected consequences: Exon skipping caused by CRISPR-generated mutations. Genome Biol. *18*.

Shen, C., Sheng, Y., Zhu, A.C., Robinson, S., Jiang, X., Dong, L., Chen, H., Su, R., Yin, Z., Li, W., et al. (2020). RNA Demethylase ALKBH5 Selectively Promotes Tumorigenesis and Cancer Stem Cell Self-Renewal in Acute Myeloid Leukemia. Cell Stem Cell *27*, 64-80.e9.

Shen, L., Liang, Z., Gu, X., Chen, Y., Teo, Z.W.N., Hou, X., Cai, W.M., Dedon, P.C., Liu, L., and Yu, H. (2016). N6-Methyladenosine RNA Modification Regulates Shoot Stem Cell Fate in Arabidopsis. Dev. Cell *38*, 186–200.

Shen, S., Faouzi, S., Bastide, A., Martineau, S., Malka-Mahieu, H., Fu, Y., Sun, X., Mateus, C., Routier, E., Roy, S., et al. (2019). An epitranscriptomic mechanism underlies selective mRNA translation remodelling in melanoma persister cells. Nat. Commun. *10*, 1–14.

Shi, H., Wang, X., Lu, Z., Zhao, B.S., Ma, H., Hsu, P.J., Liu, C., and He, C. (2017). YTHDF3 facilitates translation and decay of N 6-methyladenosine-modified RNA. Cell Res. *27*, 315–328.

Shi, H., Wei, J., and He, C. (2019). Where, When, and How: Context-Dependent Functions of RNA Methylation Writers, Readers, and Erasers. Mol. Cell *74*, 640–650.

Shu, H., Donnard, E., Liu, B., Jung, S., Wang, R., and Richter, J.D. (2020). FMRP links optimal codons to mRNA stability in neurons. Proc. Natl. Acad. Sci. U. S. A. *117*, 30400–30411.

Simen Zhao, B., Nachtergaele, S., and Roundtree, I.A. (2018). Our views of dynamic N 6-methyladenosine RNA methylation.

Śledź, P., and Jinek, M. (2016). Structural insights into the molecular mechanism of the m6A writer complex. Elife *5*.

Slobodin, B., Han, R., Calderone, V., Vrielink, J.A.F.O., Loayza-Puch, F., Elkon, R., and Agami, R. (2017). Transcription Impacts the Efficiency of mRNA Translation via Co-transcriptional N6-adenosine Methylation. Cell *169*, 326-337.e12.

Sommer, S., Lavi, U., and Darnell, J.E. (1978). The absolute frequency of labeled N-6-methyladenosine in HeLa cell messenger RNA decreases with label time. J. Mol. Biol. *124*, 487–499.

Song, H., Wang, Y., Wang, R., Zhang, X., Liu, Y., Jia, G., and Chen, P.R. (2020a). SFPQ Is an FTO-Binding Protein that Facilitates the Demethylation Substrate Preference. Cell Chem. Biol. *27*, 283-291.e6.

Song, T., Yang, Y., Jiang, S., and Peng, J. (2020b). Novel Insights into Adipogenesis from the

Perspective of Transcriptional and RNA N6-Methyladenosine-Mediated Post-Transcriptional Regulation. Adv. Sci. *7*, 2001563.

Sorci, M., Ianniello, Z., Cruciani, S., Larivera, S., Ginistrelli, L.C., Capuano, E., Marchioni, M., Fazi, F., and Fatica, A. (2018). METTL3 regulates WTAP protein homeostasis. Cell Death Dis. *9*.

Stitzel, M.L., and Seydoux, G. (2007). Regulation of the oocyte-to-zygote transition. Science (80-.). *316*, 407–408.

Stoeckius, M., Grün, D., Kirchner, M., Ayoub, S., Torti, F., Piano, F., Herzog, M., Selbach, M., and Rajewsky, N. (2014). Global characterization of the oocyte-to-embryo transition in <scp>C</scp> *aenorhabditis elegans* uncovers a novel m <scp>RNA</scp> clearance mechanism. EMBO J. *33*, 1751–1766.

Su, R., Dong, L., Li, C., Nachtergaele, S., Wunderlich, M., Qing, Y., Deng, X., Wang, Y., Weng, X., Hu, C., et al. (2018). R-2HG Exhibits Anti-tumor Activity by Targeting FTO/m6A/MYC/CEBPA Signaling. Cell *172*, 90-105.e23.

Subtelny, A.O., Eichhorn, S.W., Chen, G.R., Sive, H., and Bartel, D.P. (2014). Poly(A)-tail profiling reveals an embryonic switch in translational control. Nature *508*, 66–71.

Sui, X., Hu, Y., Ren, C., Cao, Q., Zhou, S., Cao, Y., Li, M., Shu, W., and Huo, R. (2020). METTL3-mediated m6A is required for murine oocyte maturation and maternal-to-zygotic transition. Cell Cycle *19*, 391–404.

Sun, J., Yan, L., Shen, W., and Meng, A. (2018). Maternal ybx1 safeguards zebrafish oocyte maturation and maternal-to-zygotic transition by repressing global translation. Dev. *145*.

Sun, L., Fazal, F.M., Li, P., Broughton, J.P., Lee, B., Tang, L., Huang, W., Kool, E.T., Chang, H.Y., and Zhang, Q.C. (2019). RNA structure maps across mammalian cellular compartments. Nat. Struct. Mol. Biol. *26*, 322–330.

Tadros, W., and Lipshitz, H.D. (2009). The maternal-to-zygotic transition: A play in two acts. Development *136*, 3033–3042.

Tadros, W., Goldman, A.L., Babak, T., Menzies, F., Vardy, L., Orr-Weaver, T., Hughes, T.R.,

Westwood, J.T., Smibert, C.A., and Lipshitz, H.D. (2007). SMAUG Is a Major Regulator of Maternal mRNA Destabilization in Drosophila and Its Translation Is Activated by the PAN GU Kinase. Dev. Cell *12*, 143–155.

Tanabe, A., Tanikawa, K., Tsunetomi, M., Takai, K., Ikeda, H., Konno, J., Torigoe, T., Maeda, H., Kutomi, G., Okita, K., et al. (2016). RNA helicase YTHDC2 promotes cancer metastasis via the enhancement of the efficiency by which HIF-1α mRNA is translated. Cancer Lett. *376*, 34–42.

Tang, C., Klukovich, R., Peng, H., Wang, Z., Yu, T., Zhang, Y., Zheng, H., Klungland, A., and Yan, W. (2017). ALKBH5-dependent m6A demethylation controls splicing and stability of long 3'-UTR mRNAs in male germ cells. Proc. Natl. Acad. Sci. U. S. A. *115*, E325–E333.

Tang, C., Xie, Y., Yu, T., Liu, N., Wang, Z., Woolsey, R.J., Tang, Y., Zhang, X., Qin, W., Zhang, Y., et al. (2020). m6A-dependent biogenesis of circular RNAs in male germ cells. Cell Res. *30*, 211–228.

Temme, C., Zhang, L., Kremmer, E., Ihling, C., Chartier, A., Sinz, A., Simonelig, M., and Wahle, E. (2010). Subunits of the Drosophila CCR4-NOT complex and their roles in mRNA deadenylation. RNA *16*, 1356–1370.

Thalhammer, A., Bencokova, Z., Poole, R., Loenarz, C., Adam, J., O'Flaherty, L., Schödel, J., Mole, D., Giaslakiotis, K., Schofield, C.J., et al. (2011). Human AlkB Homologue 5 Is a Nuclear 2-Oxoglutarate Dependent Oxygenase and a Direct Target of Hypoxia-Inducible Factor 1α (HIF-1α). PLoS One *6*, e16210.

Theler, D., Dominguez, C., Blatter, M., Boudet, J., and Allain, F.H.T. (2014). Solution structure of the YTH domain in complex with N6-methyladenosine RNA: A reader of methylated RNA. Nucleic Acids Res. *42*, 13911–13919.

Thisse, B., and Thisse, C. (2014). In situ hybridization on whole-mount zebrafish embryos and young larvae. Methods Mol. Biol. *1211*, 53–67.

Thomsen, S., Anders, S., Janga, S.C., Huber, W., and Alonso, C.R. (2010). Genome-wide analysis of mRNA decay patterns during early Drosophila development. Genome Biol. *11*, R93.

Tirumuru, N., Zhao, B.S., Lu, W., Lu, Z., He, C., and Wu, L. (2016). N6-methyladenosine of HIV-1 RNA regulates viral infection and HIV-1 Gag protein expression. Elife *5*.

Toh, J.D.W., Crossley, S.W.M., Bruemmer, K.J., Ge, E.J., He, D., Iovan, D.A., and Chang, C.J. (2020). Distinct RNA N-demethylation pathways catalyzed by nonheme iron ALKBH5 and FTO enzymes enable regulation of formaldehyde release rates. Proc. Natl. Acad. Sci. U. S. A. *117*, 25284–25292.

Tung, Y.C.L., Gulati, P., Liu, C.H., Rimmington, D., Dennis, R., Ma, M., Saudek, V., O'Rahilly, S., Coll, A.P., and Yeo, G.S.H. (2015). FTO is necessary for the induction of leptin resistance by high-fat feeding. Mol. Metab. *4*, 287–298.

Ulitsky, I., Shkumatava, A., Jan, C.H., Subtelny, A.O., Koppstein, D., Bell, G.W., Sive, H., and Bartel, D.P. (2012). Extensive alternative polyadenylation during zebrafish development. Genome Res. *22*, 2054–2066.

Vastenhouw, N.L., Cao, W.X., and Lipshitz, H.D. (2019). The maternal-to-zygotic transition revisited. Development *146*.

Vejnar, C.E., Moreno-Mateos, M.A., Cifuentes, D., Bazzini, A.A., and Giraldez, A.J. (2016). Optimized CRISPR-Cas9 system for genome editing in zebrafish. Cold Spring Harb. Protoc. *2016*, 856–870.

Vejnar, C.E., Messih, M.A., Takacs, C.M., Yartseva, V., Oikonomou, P., Christiano, R., Stoeckius, M., Lau, S., Lee, M.T., Beaudoin, J.D., et al. (2019). Genome wide analysis of 3′ UTR sequence elements and proteins regulating mRNA stability during maternal-to-zygotic transition in zebrafish. Genome Res. *29*, 1100–1114.

Vissers, C., Sinha, A., Ming, G. li, and Song, H. (2020). The epitranscriptome in stem cell biology and neural development. Neurobiol. Dis. *146*, 105139.

Voeltz, G.K., and Steitz, J.A. (1998). AUUUA Sequences Direct mRNA Deadenylation Uncoupled from Decay during Xenopus Early Development . Mol. Cell. Biol. *18*, 7537–7545.

Vong, Y.H., Sivashanmugam, L., Zaucker, A., Jones, A., and Sampath, K. (2020). The RNA-binding protein Igf2bp3 is critical for embryonic and germline development in zebrafish. BioRxiv 2020.06.23.167163.

Vu, L.P., Cheng, Y., and Kharas, M.G. (2019). The biology of m 6 a RNA methylation in normal and malignant hematopoiesis. Cancer Discov. *9*, 25–33.

Wagner, D.S., Dosch, R., Mintzer, K.A., Wiemelt, A.P., and Mullins, M.C. (2004). Maternal control of development at the midblastula transition and beyond: Mutants from the zebrafish II. Dev. Cell *6*, 781–790.

Wahle, E., and Winkler, G.S. (2013). RNA decay machines: Deadenylation by the Ccr4-Not and Pan2-Pan3 complexes. Biochim. Biophys. Acta - Gene Regul. Mech. *1829*, 561–570.

Wang, J., Wang, J., Gu, Q., Ma, Y., Yang, Y., Zhu, J., and Zhang, Q. (2020a). The biological function of m6A demethylase ALKBH5 and its role in human disease. Cancer Cell Int. *20*, 347.

Wang, J., Wang, L., Diao, J., Shi, Y.G., Shi, Y., Ma, H., and Shen, H. (2020b). Binding to m6A RNA promotes YTHDF2-mediated phase separation. Protein Cell *11*, 304–307.

Wang, P., Doxtader, K.A., and Nam, Y. (2016a). Structural Basis for Cooperative Function of Mettl3 and Mettl14 Methyltransferases. Mol. Cell *63*, 306–317.

Wang, X., Lu, Z., Gomez, A., Hon, G.C., Yue, Y., Han, D., Fu, Y., Parisien, M., Dai, Q., Jia, G., et al. (2014a). N 6-methyladenosine-dependent regulation of messenger RNA stability. Nature *505*, 117–120.

Wang, X., Zhu, L., Chen, J., and Wang, Y. (2015a). MRNA m6A methylation downregulates adipogenesis in porcine adipocytes. Biochem. Biophys. Res. Commun. *459*, 201–207.

Wang, X., Zhao, B.S., Roundtree, I.A., Lu, Z., Han, D., Ma, H., Weng, X., Chen, K., Shi, H., and He, C. (2015b). N6-methyladenosine modulates messenger RNA translation efficiency. Cell *161*, 1388–1399.

Wang, X., Feng, J., Xue, Y., Guan, Z., Zhang, D., Liu, Z., Gong, Z., Wang, Q., Huang, J., Tang, C., et al. (2016b). Structural basis of N6-adenosine methylation by the METTL3-METTL14 complex. Nature *534*, 575–578.

Wang, Y., Li, Y., Toth, J.I., Petroski, M.D., Zhang, Z., and Zhao, J.C. (2014b). N6 - methyladenosine modification destabilizes developmental regulators in embryonic stem cells. Nat.

Cell Biol. *16*, 191–198.

Wang, Y., Li, Y., Yue, M., Wang, J., Kumar, S., Wechsler-Reya, R.J., Zhang, Z., Ogawa, Y., Kellis, M., Duester, G., et al. (2018). N 6-methyladenosine RNA modification regulates embryonic neural stem cell self-renewal through histone modifications. Nat. Neurosci. *21*, 195–206.

Wang, Z., Pan, Z., Adhikari, S., Harada, B.T., Shen, L., Yuan, W., Abeywardana, T., Al-Hadid, Q., Stark, J.M., He, C., et al. (2021). m ^{6} A deposition is regulated by PRMT1-mediated arginine methylation of METTL14 in its disordered C-terminal region. EMBO J.

Wei, C.M., Gershowitz, A., and Moss, B. (1975). N6, O2'-dimethyladenosine a novel methylated ribonucleoside next to the 5' terminal of animal cell and virus mRNAs. Nature *257*, 251–253.

Wei, C.M., Gershowitz, A., and Moss, B. (1976). 5′-Terminal and Internal Methylated Nucleotide Sequences in Hela Cell mRNA. Biochemistry *15*, 397–401.

Wei, J., Liu, F., Lu, Z., Fei, Q., Ai, Y., He, P.C., Shi, H., Cui, X., Su, R., Klungland, A., et al. (2018). Differential m 6 A, m 6 A m , and m 1 A Demethylation Mediated by FTO in the Cell Nucleus and Cytoplasm. Mol. Cell *71*, 973-985.e5.

Weidmann, C.A., Raynard, N.A., Blewett, N.H., Van Etten, J., and Goldstrohm, A.C. (2014). The RNA binding domain of Pumilio antagonizes poly-adenosine binding protein and accelerates deadenylation. RNA *20*, 1298–1319.

Wen, J., Lv, R., Ma, H., Shen, H., He, C., Wang, J., Jiao, F., Liu, H., Yang, P., Tan, L., et al. (2018). Zc3h13 Regulates Nuclear RNA m6A Methylation and Mouse Embryonic Stem Cell Self-Renewal. Mol. Cell *69*, 1028-1038.e6.

Weng, H., Huang, H., and Chen, J. (2019). RNA N 6-Methyladenosine Modification in Normal and Malignant Hematopoiesis. In Advances in Experimental Medicine and Biology, (Springer New York LLC), pp. 75–93.

Weng, Y.L., Wang, X., An, R., Cassin, J., Vissers, C., Liu, Y., Liu, Y., Xu, T., Wang, X., Wong, S.Z.H., et al. (2018). Epitranscriptomic m6A Regulation of Axon Regeneration in the Adult Mammalian Nervous System. Neuron *97*, 313-325.e6.

Winata, C.L., Łapiński, M., Pryszcz, L., Vaz, C., Ismail, M.H. Bin, Nama, S., Hajan, H.S., Lee, S.G.P., Korzh, V., Sampath, P., et al. (2018). Cytoplasmic polyadenylation-mediated translational control of maternal mRNAs directs maternal-to-zygotic transition. Dev. *145*.

Wojtas, M.N., Pandey, R.R., Mendel, M., Homolka, D., Sachidanandam, R., and Pillai, R.S. (2017). Regulation of m6A Transcripts by the 3′→5′ RNA Helicase YTHDC2 Is Essential for a Successful Meiotic Program in the Mammalian Germline. Mol. Cell *68*, 374-387.e12.

Worpenberg, L., Paolantoni, C., Longhi, S., Mulorz, M.M., Lence, T., Wessels, H., Dassi, E., Aiello, G., Sutandy, F.X.R., Scheibe, M., et al. (2021). Ythdf is a N6-methyladenosine reader that modulates Fmr1 target mRNA selection and restricts axonal growth in *Drosophila*. EMBO J. e104975.

Wu, R., and Wang, X. (2021). Epigenetic regulation of adipose tissue expansion and adipogenesis by N^6 -methyladenosine. Obes. Rev. *22*, e13124.

Wu, B., Su, S., Patil, D.P., Liu, H., Gan, J., Jaffrey, S.R., and Ma, J. (2018). Molecular basis for the specific and multivariant recognitions of RNA substrates by human hnRNP A2/B1. Nat. Commun. *9*, 1–12.

Wu, G., Suo, C., Yang, Y., Shen, S., Sun, L., Li, S., Zhou, Y., Yang, D., Wang, Y., Cai, Y., et al. (2021). MYC promotes cancer progression by modulating m ^{6} A modifications to suppress target gene translation. EMBO Rep. e51519.

Wu, Q., Medina, S.G., Kushawah, G., Devore, M.L., Castellano, L.A., Hand, J.M., Wright, M., and Bazzini, A.A. (2019a). Translation affects mRNA stability in a codon-dependent manner in human cells. Elife *8*.

Wu, R., Li, A., Sun, B., Sun, J.G., Zhang, J., Zhang, T., Chen, Y., Xiao, Y., Gao, Y., Zhang, Q., et al. (2019b). A novel m6A reader Prrc2a controls oligodendroglial specification and myelination. Cell Res. *29*, 23–41.

Wu, R., Liu, Y., Zhao, Y., Bi, Z., Yao, Y., Liu, Q., Wang, F., Wang, Y., and Wang, X. (2019c). m6A methylation controls pluripotency of porcine induced pluripotent stem cells by targeting SOCS3/JAK2/STAT3 pathway in a YTHDF1/YTHDF2-orchestrated manner. Cell Death Dis. *10*, 171.

Xia, H., Zhong, C., Wu, X., Chen, J., Tao, B., Xia, X., Shi, M., Zhu, Z., Trudeau, V.L., and Hu, W. (2018). Mettl3 mutation disrupts gamete maturation and reduces fertility in zebrafish. Genetics *208*, 729–743.

Xia, T., Li, X., Wang, X., Zhu, Y., Zhang, H., Cheng, W., Chen, M., Ye, Y., Li, Y., Zhang, A., et al. (2021). N(6)-methyladenosine-binding protein YTHDF1 suppresses EBV replication and promotes EBV RNA decay. EMBO Rep.

Xiang, Y., Laurent, B., Hsu, C.H., Nachtergaele, S., Lu, Z., Sheng, W., Xu, C., Chen, H., Ouyang, J., Wang, S., et al. (2017). RNA m6 A methylation regulates the ultraviolet-induced DNA damage response. Nature *543*, 573–576.

Xiao, W., Adhikari, S., Dahal, U., Chen, Y.S., Hao, Y.J., Sun, B.F., Sun, H.Y., Li, A., Ping, X.L., Lai, W.Y., et al. (2016). Nuclear m6A Reader YTHDC1 Regulates mRNA Splicing. Mol. Cell *61*, 507–519.

Xu, C., Liu, K., Tempel, W., Demetriades, M., Aik, W.S., Schofield, C.J., and Min, J. (2014a). Structures of human ALKBH5 demethylase reveal a unique binding mode for specific single-stranded N6-methyladenosine RNA demethylation. J. Biol. Chem. *289*, 17299–17311.

Xu, C., Wang, X., Liu, K., Roundtree, I.A., Tempel, W., Li, Y., Lu, Z., He, C., and Min, J. (2014b). Structural basis for selective binding of m6A RNA by the YTHDC1 YTH domain. Nat. Chem. Biol. *10*, 927–929.

Xu, C., Liu, K., Ahmed, H., Loppnau, P., Schapira, M., and Min, J. (2015). Structural basis for the discriminative recognition of N6-Methyladenosine RNA by the human YT521-B homology domain family of proteins. J. Biol. Chem. *290*, 24902–24913.

Xu, K., Yang, Y., Feng, G.H., Sun, B.F., Chen, J.Q., Li, Y.F., Chen, Y.S., Zhang, X.X., Wang, C.X., Jiang, L.Y., et al. (2017). Mettl3-mediated m 6 A regulates spermatogonial differentiation and meiosis initiation. Cell Res. *27*, 1100–1114.

Yan, D., and Perrimon, N. (2015). Spenito is required for sex determination in Drosophila melanogaster. Proc. Natl. Acad. Sci. U. S. A. *112*, 11606–11611.

Yang, Y., Huang, W., Huang, J.T., Shen, F., Xiong, J., Yuan, E.F., Qin, S.S., Zhang, M., Feng, Y.Q., Yuan, B.F., et al. (2016). Increased N6-methyladenosine in Human Sperm RNA as a Risk

Factor for Asthenozoospermia. Sci. Rep. *6*.

Yang, Y., Fan, X., Mao, M., Song, X., Wu, P., Zhang, Y., Jin, Y., Yang, Y., Chen, L.L., Wang, Y., et al. (2017a). Extensive translation of circular RNAs driven by N 6 -methyladenosine. Cell Res. *27*, 626–641.

Yang, Y., Wang, L., Han, X., Yang, W.L., Zhang, M., Ma, H.L., Sun, B.F., Li, A., Xia, J., Chen, J., et al. (2019). RNA 5-Methylcytosine Facilitates the Maternal-to-Zygotic Transition by Preventing Maternal mRNA Decay. Mol. Cell *75*, 1188-1202.e11.

Yang, Z., Li, J., Feng, G., Gao, S., Wang, Y., Zhang, S., Liu, Y., Ye, L., Li, Y., and Zhang, X. (2017b). MicroRNA-145 Modulates N6-methyladenosine levels by targeting the 3'-untranslated mRNA Region of the N6-Methyladenosine Binding YTH domain family 2 protein. J. Biol. Chem. *292*, 3614–3623.

Yao, Y., Bi, Z., Wu, R., Zhao, Y., Liu, Y., Liu, Q., Wang, Y., and Wang, X. (2019). METTL3 inhibits BMSC adipogenic differentiation by targeting the JAK1/STAT5/C/EBPβ pathway *via* an m [6] A-YTHDF2–dependent manner. FASEB J. *33*, 7529–7544.

Yartseva, V., and Giraldez, A.J. (2015). The Maternal-to-Zygotic Transition During Vertebrate Development: A Model for Reprogramming. In Current Topics in Developmental Biology, (Academic Press Inc.), pp. 191–232.

Yoon, K.J., Ringeling, F.R., Vissers, C., Jacob, F., Pokrass, M., Jimenez-Cyrus, D., Su, Y., Kim, N.S., Zhu, Y., Zheng, L., et al. (2017). Temporal Control of Mammalian Cortical Neurogenesis by m6A Methylation. Cell *171*, 877-889.e17.

Yu, C., Ji, S.Y., Sha, Q.Q., Dang, Y., Zhou, J.J., Zhang, Y.L., Liu, Y., Wang, Z.W., Hu, B., Sun, Q.Y., et al. (2016). BTG4 is a meiotic cell cycle-coupled maternal-zygotic-transition licensing factor in oocytes. Nat. Struct. Mol. Biol. *23*, 387–394.

Yu, J., Chen, M., Huang, H., Zhu, J., Song, H., Zhu, J., Park, J., and Ji, S.J. (2018). Dynamic m6A modification regulates local translation of mRNA in axons. Nucleic Acids Res. *46*, 1412–1423.

Zaccara, S., and Jaffrey, S.R. (2020). A Unified Model for the Function of YTHDF Proteins in Regulating m6A-Modified mRNA. Cell.

Zaccara, S., Ries, R.J., and Jaffrey, S.R. (2019). Reading, writing and erasing mRNA methylation. Nat. Rev. Mol. Cell Biol. *20*, 608–624.

Zhang, C., Samanta, D., Lu, H., Bullen, J.W., Zhang, H., Chen, I., He, X., and Semenza, G.L. (2016). Hypoxia induces the breast cancer stem cell phenotype by HIF-dependent and ALKBH5-mediated m6A-demethylation of NANOG mRNA. Proc. Natl. Acad. Sci. U. S. A. *113*, E2047–E2056.

Zhang, C., Chen, Y., Sun, B., Wang, L., Yang, Y., Ma, D., Lv, J., Heng, J., Ding, Y., Xue, Y., et al. (2017a). M6A modulates haematopoietic stem and progenitor cell specification. Nature *549*, 273–276.

Zhang, F., Kang, Y., Wang, M., Li, Y., Xu, T., Yang, W., Song, H., Wu, H., Shu, Q., and Jin, P. (2018). Fragile X mental retardation protein modulates the stability of its m6A-marked messenger RNA targets. Hum. Mol. Genet. *27*, 3936–3950.

Zhang, H., Shi, X., Huang, T., Zhao, X., Chen, W., Gu, N., and Zhang, R. (2020a). Dynamic landscape and evolution of m6A methylation in human. Nucleic Acids Res. *48*, 6251–6264.

Zhang, J., Bai, R., Li, M., Ye, H., Wu, C., Wang, C., Li, S., Tan, L., Mai, D., Li, G., et al. (2019a). Excessive miR-25-3p maturation via N 6 -methyladenosine stimulated by cigarette smoke promotes pancreatic cancer progression. Nat. Commun. *10*.

Zhang, M., Zhang, Y., Ma, J., Guo, F., Cao, Q., Zhang, Y., Zhou, B., Chai, J., Zhao, W., and Zhao, R. (2015). The Demethylase Activity of FTO (Fat Mass and Obesity Associated Protein) Is Required for Preadipocyte Differentiation. PLoS One *10*, e0133788.

Zhang, M., Zhai, Y., Zhang, S., Dai, X., and Li, Z. (2020b). Roles of N6-Methyladenosine (m6A) in Stem Cell Fate Decisions and Early Embryonic Development in Mammals. Front. Cell Dev. Biol. *8*, 782.

Zhang, S., Zhao, B.S., Zhou, A., Lin, K., Zheng, S., Lu, Z., Chen, Y., Sulman, E.P., Xie, K., Bögler, O., et al. (2017b). m6A Demethylase ALKBH5 Maintains Tumorigenicity of Glioblastoma Stem-like Cells by Sustaining FOXM1 Expression and Cell Proliferation Program. Cancer Cell *31*, 591-606.e6.

Zhang, X., Wei, L.H., Wang, Y., Xiao, Y., Liu, J., Zhang, W., Yan, N., Amu, G., Tang, X., Zhang, L., et al. (2019b). Structural insights into FTO's catalytic mechanism for the demethylation of multiple RNA substrates. Proc. Natl. Acad. Sci. U. S. A. *116*, 2919–2924.

Zhang, Y., Wang, X., Zhang, X., Wang, J., Ma, Y., Zhang, L., and Cao, X. (2019c). RNA-binding protein YTHDF3 suppresses interferon-dependent antiviral responses by promoting FOXO3 translation. Proc. Natl. Acad. Sci. U. S. A. *116*, 976–981.

Zhang, Z., Luo, K., Zou, Z., Qiu, M., Tian, J., Sieh, L., Shi, H., Zou, Y., Wang, G., Morrison, J., et al. (2020c). Genetic analyses support the contribution of mRNA N 6-methyladenosine (m6A) modification to human disease heritability. Nat. Genet. *52*, 939–949.

Zhao, B.S., Roundtree, I.A., and He, C. (2016). Post-transcriptional gene regulation by mRNA modifications. Nat. Rev. Mol. Cell Biol. *18*, 31–42.

Zhao, B.S., Wang, X., Beadell, A. V., Lu, Z., Shi, H., Kuuspalu, A., Ho, R.K., and He, C. (2017). M6 A-dependent maternal mRNA clearance facilitates zebrafish maternal-to-zygotic transition. Nature *542*, 475–478.

Zhao, X., Yang, Y., Sun, B.F., Shi, Y., Yang, X., Xiao, W., Hao, Y.J., Ping, X.L., Chen, Y.S., Wang, W.J., et al. (2014). FTO-dependent demethylation of N6-methyladenosine regulates mRNA splicing and is required for adipogenesis. Cell Res. *24*, 1403–1419.

Zhao, X., Tian, G.G., Fang, Q., Pei, X., Wang, Z., and Wu, J. (2021). Comparison of RNA m6A and DNA methylation profiles between mouse female germline stem cells and STO cells. Mol. Ther. - Nucleic Acids *23*, 431–439.

Zheng, D., Ezzeddine, N., Chen, C.Y.A., Zhu, W., He, X., and Shyu, A. Bin (2008). Deadenylation is prerequisite for P-body formation and mRNA decay in mammalian cells. J. Cell Biol. *182*, 89–101.

Zheng, G., Dahl, J.A., Niu, Y., Fedorcsak, P., Huang, C.M., Li, C.J., Vågbø, C.B., Shi, Y., Wang, W.L., Song, S.H., et al. (2013). ALKBH5 Is a Mammalian RNA Demethylase that Impacts RNA Metabolism and Mouse Fertility. Mol. Cell *49*, 18–29.

Zheng, Q., Gan, H., Yang, F., Yao, Y., Hao, F., Hong, L., and Jin, L. (2020). Cytoplasmic m1A reader YTHDF3 inhibits trophoblast invasion by downregulation of m1A-methylated IGF1R. Cell

Discov. *6*, 12.

Zhong, S., Li, H., Bodi, Z., Button, J., Vespa, L., Herzog, M., and Fray, R.G. (2008). MTA is an Arabidopsis messenger RNA adenosine methylase and interacts with a homolog of a sex-specific splicing factor. Plant Cell *20*, 1278–1288.

Zhou, J., Wan, J., Gao, X., Zhang, X., Jaffrey, S.R., and Qian, S.B. (2015). Dynamic m6 A mRNA methylation directs translational control of heat shock response. Nature *526*, 591–594.

Zhou, J., Wan, J., Shu, X.E., Mao, Y., Liu, X.M., Yuan, X., Zhang, X., Hess, M.E., Brüning, J.C., and Qian, S.B. (2018). N6-Methyladenosine Guides mRNA Alternative Translation during Integrated Stress Response. Mol. Cell *69*, 636-647.e7.

Zhu, T., Roundtree, I.A., Wang, P., Wang, X., Wang, L., Sun, C., Tian, Y., Li, J., He, C., and Xu, Y. (2014). Crystal structure of the YTH domain of YTHDF2 reveals mechanism for recognition of N6-methyladenosine. Cell Res. *24*, 1493–1496.

Zhuang, M., Li, X., Zhu, J., Zhang, J., Niu, F., Liang, F., Chen, M., Li, D., Han, P., and Ji, S.J. (2019). The m6A reader YTHDF1 regulates axon guidance through translational control of Robo3.1 expression. Nucleic Acids Res. *47*, 4765–4777.

Zou, S., Toh, J.D.W., Wong, K.H.Q., Gao, Y.G., Hong, W., and Woon, E.C.Y. (2016). N 6 - Methyladenosine: A conformational marker that regulates the substrate specificity of human demethylases FTO and ALKBH5. Sci. Rep. *6*, 1–12.